Aus dem Institut für Medizinische Genetik
der Medizinischen Fakultät Charité – Universitätsmedizin Berlin

DISSERTATION

Investigation of the genetical basis of autosomal recessive Cutis Laxa

zur Erlangung des akademischen Grades
Doctor medicinae (Dr. med.)

vorgelegt der Medizinischen Fakultät
Charité – Universitätsmedizin Berlin
von

Aikaterini Dimopoulou
aus Thessaloniki

Gutachter/in: 1. Prof. Dr. med. S. Mundlos

2. Prof. Dr. med. Dr. h. c. T. Krieg

3. Prof. Dr. med. B. Zabel

Datum der Promotion: 19 November 2010

For my family and
for all my good friends…..

Contents

Index of figures

Abbreviations

ADCL	Autosomal dominant cutis laxa
ARCL	Autosomal recessive cutis laxa
ATP	Adenosine triphosphate
ATP6V0A2	ATPase, H+ transporting, lysosomal V0 subunit a2
BSA	Bovine Serum Albumin
CDG	Congenital Disorder of Glycosylation
CL	Cutis Laxa
DNA	Deoxyribonucleic acid
DBS	de Barsy syndrome
EGF	Epidermal growth factor
ELN	elastin (gene)
EM	electron microscopy
ER	endoplasmic reticulum
EST	expressing sequence tag
GAPDH	Glycerinaldehyde-3-phosphate-Dehydrogenase
GO	Gerodermia Osteodysplastica
GORAB	golgin, RAB6-interacting
HAF	Human Adult Fibroblasts
HDR	homology-dependent recombination repair

HGPS	Hutchinson-Gilford Progeria Syndrome
IUGR	Intrauterine Growth Retardation
LOX	lysyl oxidase
Mb	megabase
MNK	Menkes Disease
MRI	magnetic resonance imaging
mRNA	messenger RNA
NAD(P)H	Nicotinamide adenine dinucleotide phosphate
NADH	Nicotinamide adenine dinucleotide
NMD	nonsense mediated decay
OHS	occipital-horn syndrome
MIM	Mendelian Inheritance of Man
P5C	Δ1-pyrroline-5-carboxylate
P5CS	Δ1-pyrroline-5-carboxylate synthetase
PCR	Polymerase Chain Reaction
POX	proline oxidase
PS	progeroid syndromes
PYCR1/P5CR	Pyrroline-5-carboxylate reductase
PYCR2	pyrroline-5-carboxylate reductase family, member 2
PYCRL	pyrroline-5-carboxylate reductase-like
qPCR	Quantitative Polymerase Chain Reaction
RNA	Ribonucleic acid
ROS	reactive oxygen species
s.d	standard deviation
SNP	Single nucleotide polymorphism
TGF	Transforming growth factor beta
TRF	terminal restriction fragment
T-SCE	telomere sister-chromatid exchange
UV	Ultra-Violet
V-ATPase	Vacuolar ATPases
WNR	Werner syndrome
WSS	Wrinkly Skin Syndrome
WT	Wildtype

Co-operation:

The genotype and linkage analysis on the five consanguineous families was performed by Prof. Dr. rer. nat. Peter Nürnberg, Dr. Gudrun Nürnberg and Dr. rer. nat. Birgit Budde from the Cologne Center for Genomics, Universität zu Köln, Germany.

The ultrastructural analysis was performed by the EM facility of the Anatomy Department of the Charité University of Berlin. The amino acid measurements were performed in the Institute for Laboratory medicine- Clinical Chemistry and Pathobiochemistry of the Charité University of Berlin.

Selbständigkeitserklärung

„Ich, Aikaterini Dimopoulou, erkläre, dass ich die vorgelegte Dissertation mit dem Thema: Investigation of the genetical basis of autosomal recessive cutis laxa, selbst verfasst und keine anderen als die angegebenen Quellen und Hilfsmittel benutzt, ohne die (unzulässige) Hilfe Dritter verfasst und auch in Teilen keine Kopien anderer Arbeiten dargestellt habe."

Datum Unterschrift

1 Introduction

1.1 Lax skin - definition

Skin is the largest organ of the human body and its main role is to maintain a safe barrier between the inner organs and the out environment. Skin anomalies and diseases are probably the first ever described and observed by humans, mainly because of their obvious presentation, as in the case of atopic, pigmentary or infectious skin diseases. The up to date knowledge about skin physiology has offered new insights into its contribution to the preservation of human health and gave rise to an holistic notion of its role.
The first signs of chronological ageing are evident in skin, manifesting as lack of elasticity, laxity or pigmentary changes. Skin is directly exposed to environmental factors such as sun radiation, which is considered responsible in certain degree for the eventual loss of its physiological properties and the acceleration of its ageing process.

1.2 Skin structure

1.2.1 Skin layers

The skin serves as a protective barrier between the body's internal organs and the environment. Skin is a complex organ composed of many cell types and structures. It is divided into three main layers: epidermis, dermis and subcutaneous tissue (fig1.1). The epidermis is composed mainly of differentiating keratinocytes, which are the most numerous cell type of the skin and which ultimately form the skin's external protective barrier to the environment. The epidermis also comprises pigment-producing melanocytes and antigen-presenting Langerhans cells. The basement membrane separates the epidermis from the dermis. The dermis comprises primarily extracellular matrix proteins, which are produced by fibroblasts. Type I collagen is the most abundant protein of the skin connective tissue. This tissue also contains other types of collagen (III, V, VII), elastin, proteoglycans, fibronectin and extracellular matrix proteins (1). Newly synthesized type I pro-collagen is secreted into the dermal extracellular space where it undergoes enzymatic processing, which results in the formation of collagen bundles responsible for the strength and resilience of the skin (1). The dermis is also subdivided into two parts, the papillary dermis, and the reticular layer. The main role of papillary dermis is to supply nutrients to the

epidermis and to regulate temperature. Both of these functions are accomplished by a thin but extensive vascular system. The reticular layer is much denser than the papillary dermis; it strengthens the skin, providing structure and elasticity. As a foundation, it supports other components of the skin, such as hair follicles, sweat glands, and sebaceous glands. Subcutaneous tissue consists of adipose (fat) cells, which support the connective tissue framework (2).

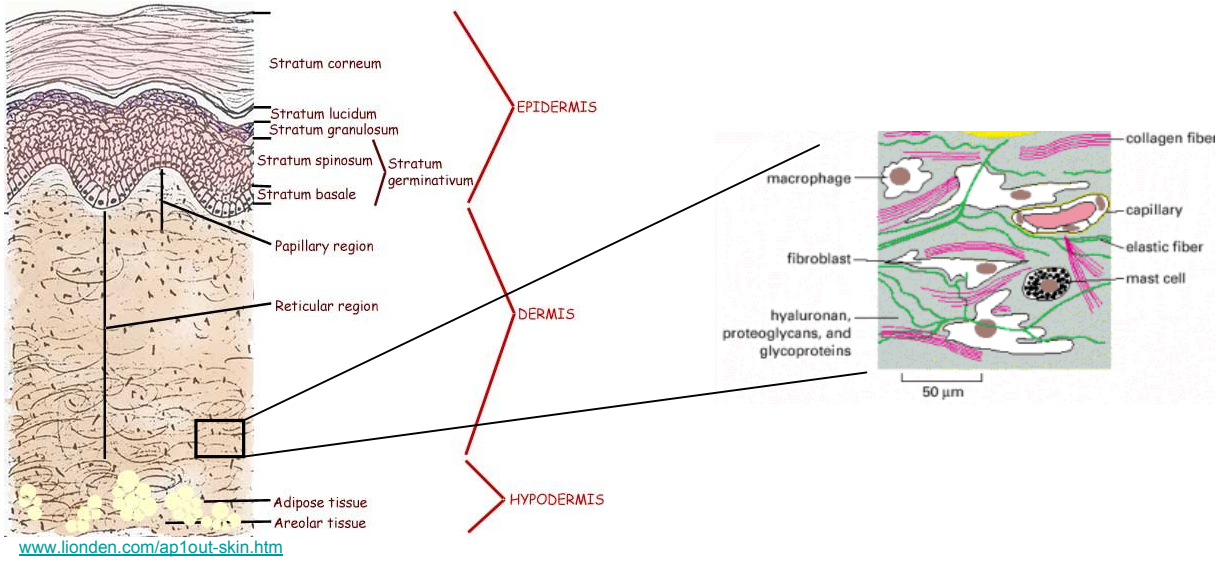

Fig. 1.1 The skin structure: The three main layers of skin and the cell composition of the dermis.

1.2.2 The elastic fibre

Elastic fibres are essential extracellular matrix macromolecules that provide the connective tissue in blood vessels, lung and skin with the critical properties of elasticity and resilience (fig1.2)(3). They are composed of two morphologically and chemically distinct components–elastin and microfibrils. Approximately 90% of the elastic fibre is constituted by elastin that forms the internal core. It is a crosslinked polymer of the monomeric secreted tropoelastin (4). The second component is visualized as small, 10–15-nm ‘‘microfibrils’’ that localize to the periphery of the fibre in adult tissues. While elastin arises from a single gene, the composition of microfibrils is more complex. The major structural element of microfibrils is contributed by the fibrillins (5). Based on ultrastructural studies, microfibrils are thought to provide a scaffold that enables elastin molecular alignment and subsequent cross-linking, which is catalyzed by members of the lysyl oxidase (LOX) gene family (6).

In *vivo* elastic fibre formation requires the coordination of a number of important processes. These include the control of intracellular transcription and translation of tropoelastin, intracellular processing of the protein, secretion of the protein into the extracellular space, delivery of tropoelastin monomers to sites of elastogenesis, alignment of the monomers with previously accreted tropoelastin through associating microfibrillar proteins, and finally, the conversion to the insoluble elastin polymer through the crosslinking action of lysyl oxidase (6,7).

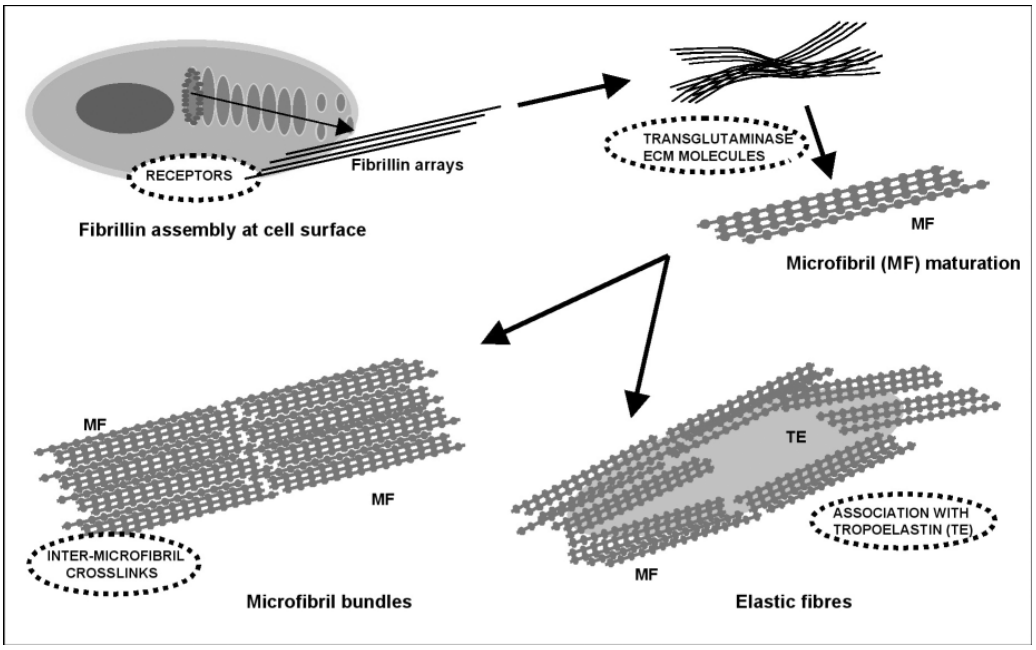

Fig. 1.2 Microfibril and elastic fibre formation (3).

Elastogenesis occurs primarily during late fetal and early neonatal periods. Elastin is synthesized and secreted from several cell types including smooth muscle cells, fibroblasts, endothelial cells and mesothelial cells (8) with tissue-specific induction of elastin expression during development (9). After elastin has been deposited, its synthesis ceases and very little turnover of elastin is seen during adult life, unless the elastic fibres are subject to injury. The reduced turnover potential of the elastic fibres allows the irreversible alterations of its properties with time, ultimately leading to an aged appearance of the skin.

The biology of elastic fibres is complex because of their multiple components, tightly regulated developmental pattern of deposition, multi-step hierarchical assembly, unique elastomeric properties and influence on cell phenotype. Furthermore, elastic fibres are involved in signaling processes, most notably in TGF-β signaling, which at the same time regulates elastogenesis. However, their molecular complexity is at last being unravelled by progress in identifying interac-

tions between component molecules, ultrastructural analyses and studies of informative mouse models (3).

1.3 Chronological ageing

Ageing is defined as the time-related deterioration of the physiological functions necessary for survival and reproduction. It affects almost all tissues leading to progressive loss of vision, loss of hearing acuity, arteriosclerosis, bone loss, deterioration of cognitive abilities-dementia, sarcopenia, heart failure and skin alterations (10).

1.3.1 Ageing of skin

Several factors can influence the ageing process in skin: genetic disposition, environmental exposure, hormonal and metabolic changes. The visible effect of these factors is the progressive alterations of the skin's appearance, which also represent the accumulative changes in its structure and function. Exogenous or extrinsic ageing affects mostly sun-exposed body areas (photoageing), while characteristic changes of endogenously aged skin are mainly visible in skin areas that are sun-protected (11).

Chronologically aged skin becomes thinner, relatively flattened, dry and unblemished, with some loss of elasticity and age-related loss of architectural regularity (1). Changes in intrinsically aged skin manifest as a result of a gradual atrophy of the epidermis which may undergo thinning by 10–50% between the age of 30 and 80 years. The number of epidermal cells decreases by 10% per decade and they divide more slowly making the skin less able to repair itself effectively. A distinct flattening of the dermo– epidermal junction occurs resulting in a decrease in surface contact area by approximately 35%. In sun-protected skin there is a general atrophy of the extracellular matrix, accompanied by a decrease in cellularity, especially of fibroblasts. In addition, the dermis is characterized by reduced levels and disintegration of collagen and elastic fibres from a decreased rate of synthesis, increased rate of degradation, or both (12). Reduced levels of collagen and elastin, with impaired organization are primarily due to decreased protein synthesis affecting types I and III collagen in the dermis, with an increased breakdown of extracellular matrix proteins (1). In the subcutaneous layer, the fat cells get smaller with age. This leads to more noticeable wrinkles and sagging, as the fat cells cannot "fill in" the damage from the other layers.

On the other hand, sun-exposed skin typically shows a thickened epidermis, which can be explained as a consequence of a chronic wound-like condition and a chronic attempt to repair (11). The dermo–epidermal junction is also a target for UV-induced skin changes. Fibrillin appears significantly truncated and depleted in the upper dermis in comparison to sun-protected skin, and there is a marked loss of fibrillin positive structures in sun-exposed skin (13). Similarly, expression of type VII collagen, which forms the anchoring fibrils at the dermo–epidermal junction, in keratinocytes is reduced in sun-exposed skin areas, confirming data that show the number of anchoring fibrils is significantly reduced in photoaged skin. Reduced content of collagen VII may contribute to wrinkles by weakening the bond between dermis and epidermis (14). Sun-exposed aged skin is also characterized by the accumulation of abnormal elastic tissue in the mid and deep dermis (elastosis). This abnormal elastic tissue replaces the normal matrix composed mainly of collagen and is almost always separated from the epidermis by a border zone of what appears to be normal collagen with or without elastic fibres (11). The vascular walls of post-capillary venules and of arterial and venous capillaries are thickened by the peripheral addition of a layer of basement membrane-like material. The veil cells, which are intimately related to these layers, often have dilated cisternae of rough endoplasmic reticulum containing electron-dense material (15).

1.4 Molecular causes of ageing

The general ageing phenotype is characteristic for each species. There are several levels at which ageing can be studied including cellular, biochemical, and genetic approaches. Many different theories exist each partially explaining a part of the ageing phenomena, there is no consensus yet on what causes ageing.

1.4.1 Oxidative damage

The free radical theory of ageing was proposed in the 1950s by Denham Harman (16). The original free radical theory of ageing supported that the molecular basis of ageing was derived from a lifetime accumulation of oxidative damage to cells resulting from excess reactive oxygen species (ROS) produced as a consequence of aerobic metabolism (1). The primary reactive oxygen species (ROS) generated by mitochondria is $O_2^{\cdot -}$, as a result of monoelectronic reduction of O_2. The

mitochondrial electron transport chain continuously reduces the bulk of O2 consumed to water but a small quantity of superoxide anion ($O_2^{\cdot -}$), is also generated. $O_2^{\cdot -}$, a reasonably reactive ROS (17), is transformed into more stable H_2O_2 by superoxide dismutase (SOD) in mitochondria. H_2O_2 generated in mitochondria has many possible fates. Because H_2O_2 is relatively stable and membrane-permeative (18) it can diffuse within the cell and be removed by cytosolic antioxidant systems such as catalase, glutathione peroxidase, and thioredoxin peroxidase (19). Mitochondrially generated H_2O_2 can also act as a signaling molecule in the cytosol, affecting multiple networks that control, for example, cell cycle, stress response, energy metabolism, and redox balance (17).

Over the past two decades, it has become apparent that many ROS, such as peroxides, which are not free radicals, also play a role in oxidative damage to cells. Therefore, the Free Radical Theory of Ageing was modified to the Oxidative Stress Theory of Ageing. A number of studies have shown an age-related increase in oxidative damage to a variety of molecules (lipid, protein, and DNA). Two main pathways have been proposed as being responsible for the impact of ROS on ageing and these are the pathways that affect the net amount of ROS in the whole organism or strategic tissues within the organism and those that repair or turnover structures that have been damaged by these ROS (fig1.3). The balance between these two pathways — the production and the scavenging of ROS — determines the absolute level of oxidative stress and subsequently the damage sustained by the cellular molecules (20).

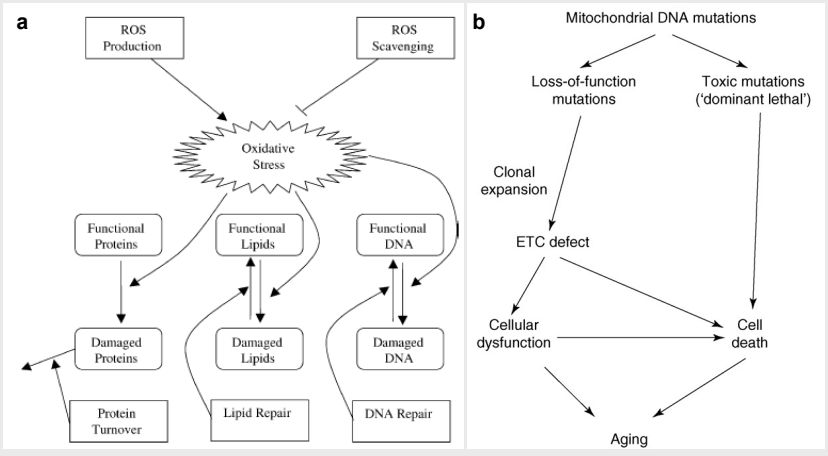

Fig. 1.3 Oxidative damage (a) A summary of the biochemical pathways involved in the free radical/oxidative stress theory of aging (20). (b) mtDNA mutations and the aging process: a summary of hypotheses (27).

Evidence for this theory includes the observation that *Drosophila* that overexpress enzymes that destroy ROS (catalase, which degrades peroxide, and superoxide dismutase) live 30–40% longer than do controls (21, 22).

1.4.2 Role of mitochondria in ageing

Mitochondria are the intracellular organelles responsible for most of the energy produced through the process of oxidative phosphorylation (OXPHOS). Mitochondria contain their own DNA (mtDNA), which is a 16,569-bp genome that replicates independently of the nuclear genome, allowing replication during high energy demands. Mitochondria are both producers and targets of oxidative stress, thus forming the basis for the mitochondrial theory of ageing. As mtDNA is located near the inner mitochondrial membrane where ROS are produced through OXPHOS they are the major targets for oxidative damage leading to the production of mtDNA mutations. This vulnerability of mtDNA to oxidative damage is exacerbated by the lack of protective histones and less efficient DNA repair systems when compared with nDNA (23). It is hypothesized that the accumulation of mutated mtDNA molecules leads to a defective OXPHOS system, leading to enhanced ROS production and in turn to accumulation of further mtDNA mutations (fig1.3), in the so called “vicious cycle”(24).
Although the accumulation of mtDNA mutations has been proposed to have a role in ageing (25,26), the levels of such mutated mtDNA in aged mammalian tissues were estimated to be low, and their causal role in ageing processes has been questioned.

1.4.3 Cellular senescence and telomeres

Diploid cells show a limited proliferation potential. After a limited number of divisions, they come into a state of replication senescence. This number of divisions, known as the Hayflick limit, has been postulated to determine the maximum lifespan of an organism (28). Telomeres have been implicated to play a critical role in determining this limit. Telomeres are repeated DNA sequences at the ends of chromosomes. They are not replicated by DNA polymerase, and they are found to shorten at each cell division unless maintained by telomerase. Telomerase adds the telomere onto the chromosome at each cell division. Telomeres shorten from 10-15 kb (germ line) to 3-5 kb after 50-60 doublings (average lengths of TRFs). Cellular senescence is triggered

when cells acquire one or a few critically short telomeres. In several premature ageing conditions, tissues of a particular chronological age contain cells much closer to their programmed cell division limit than those from similarly aged normal individuals (29). The progressive loss of telomeric DNA in human somatic (stem) cells is believed to act as a tumor suppressor mechanism that limits clonal proliferation, prevents clonal dominance, and ensures a polyclonal composition of (stem) cells in large, long-lived multicellular organisms (30). The cellular senescence theory of ageing has limitations because organs, such as the brain, which consist mostly of non-dividing cells, still age (31).

1.4.4 Caloric restriction

Diet is a key environmental factor affecting the incidence of many chronic diseases. Antioxidant substances in diet enhance the DNA, lipid and protein protection by increasing the scavenging of free radicals. Calorie restriction extends lifespan in yeast, Drosophila, worms, rodents and probably primates (32). Current knowledge of nutrition suggests that regular and sufficient consumption of fruit and vegetables, whole grain products, grain sprouts, pulses, plant oils and oil seeds together with healthy life style protect against degenerative diseases (33,34). Calorie restriction in adult men and women causes beneficial metabolic, hormonal, and functional changes, but the precise amount of calorie intake or body fat mass associated with optimal health and maximum longevity in humans is not known. Despite extensive work demonstrating the effectiveness of calorie restriction, the mechanism by which it extends lifespan is unclear. One hypothesis is that it slows metabolism and hence the production of ROS (35). Excessive adiposity on the other hand is associated with insulin resistance, dyslipidemia, low-grade inflammation, and changes in levels of growth factor and other hormones that play a role in the development of diabetes, atherosclerosis, and some types of cancer (36).

1.4.5 Genetic influence on ageing

Experimental evidence from model organisms has indicated that subtle variation in genes can dramatically influence lifespan. The key genes and molecular pathways that have been identified so far encode for metabolism, maintenance and repair mechanisms that minimize age-related accumulation of permanent damage (37). The role of genetically programmed ageing is controver-

sial and signs of a primary role for genetic programming include observations that the lifespan of a given species is relatively fixed and that human ageing has a hereditary component. Indeed, up to 25% of the variation in human lifespan is heritable (38) the rest is due to environmental factors, accidents and injuries.

The human progeroid syndromes (PSs) show features of ageing in a premature manner. The identification of the genes involved in PSs can provide important clues to understanding the molecular mechanisms underlying normal human ageing, as many of them were found to be monogenetic and to share common phenotypic and molecular features. Notably, none of the syndromes recapitulated all of the features that are observed in normal ageing, and they were therefore termed segmental, as opposed to global, progeroid syndromes (39).

Werner's syndrome is a good example of the so called "segmental progeroid syndromes", being characterised by normal development until puberty, when signs of premature ageing such as greying of the hair and skeletal changes occur much earlier than normal (40). Mutations in WNR (RECQL2; MIM 604611) gene, which encodes a RecQ helicase protein (41), were found to cause this interesting phenotype (42). The human RecQ helicase family consists of 5 proteins, of which only WRN possesses a 3' to 5' exonuclease activity and 3' to 5' helicase activity (43). The main function of the protein is homology-dependent recombination repair (HDR). HDR can be used to repair DNA damage while suppressing gene loss or rearrangement (44). WRN also has an important role in the maintenance of telomere length and the suppression of telomere sister-chromatid exchanges (T-SCEs)(45).

The Hutchinson-Gilford Progeria Syndrome (HGPS) is the most severe of the progeroid syndromes, as affected individuals have a mean lifespan of 13 years. HGPS patients generally appear normal at birth, but soon develop several features that are associated with ageing, such as alopecia, atherosclerosis, rapid loss of joint mobility, osteolysis, severe lipodystrophy, scleroderma and varied skin hyperpigmentation (46). The gene responsible for HGPS was identified in 2003, when it was found that most cases of the disease are associated with a single nucleotide substitution that leads to aberrant splicing of LMNA (LAMIN A/C; MIM 150330), giving rise to a truncated product named progerin (47). A-type lamins belong to the family of intermediate filament proteins that, along with the B-type lamins, are the main constituents of the nuclear lamina in most differentiated cells. The ability of lamins to multimerize into filaments lends both rigidity and elasticity to the nuclear lamina (48). These disorders share some common characteristics in their pathogenesis. In Werner's syndrome, the forthcoming DNA damages cannot be properly repaired because of the defect in a significant DNA-repair helicase which leads to

general genetic instability, down-regulation of p53, impaired apoptosis and ultimately to premature ageing and cancer (49). On the other hand, in HGPS DNA damages and accentuated mechanical stress due to improper lamina structure lead to up-regulation of p53 and activation of cell senescence and apoptosis. DNA repair foci are delayed, and a global genomic instability is observed as well as phenotypic features of premature ageing, but no cancer (49).

1.5 Cutis laxa - definition

Cutis laxa is a disorder of the connective tissue, which forms the body's supportive framework. Connective tissue provides structure and strength to the muscles, joints, organs, and skin. The term "cutis laxa" is Latin for loose or lax skin, and this condition is characterized by skin that is sagging and inelastic. The skin often hangs in loose folds, causing the face and other parts of the body to have a progeroid appearance. Extremely wrinkled skin may be particularly noticeable on the neck and in the armpits and groin. Cutis laxa can also affect connective tissue in other parts of the body, including the heart, blood vessels, joints, intestines, and lungs.

1.5.1 Cutis laxa phenotypes

The inherited form of cutis laxa is rather uncommon. Some 200 families have been reported in literature until now. The majority of the various subtypes of cutis laxa syndromes affect connective tissue development through structural gene defects. Cutis laxa is a heterogeneous group of disorders with variable phenotypes and inheritance patterns. It is categorized according to the phenotype and mode of inheritance. Autosomal dominant, X-linked recessive and autosomal recessive forms have been described.

1.5.2 X-linked recessive cutis laxa-occipital horn syndrome (OHS) (MIM 304150)

X-linked recessive cutis laxa, also known as occipital-horn syndrome, is the milder form of Menke’s Disease (MIM 309400). It is characterised by normal or borderline intelligence and survival until adulthood. The main clinical features of OHS are connective tissue disorders, such as occipital exostosis (occipital horns), osteoporosis, laxity of the skin and joints, and bladder diverticula (fig1.4)(50,51). OHS features the gradual development of distinctive calcifications within the tendons that attach the sternocleidomastoid and trapezius muscles to the occiput from

which the syndromic name was derived (52). Decreased levels of serum ceruloplasmin is the main biochemical finding in this disorder.

The gene ATP7A (MIM 300011), mutations in which were found to be responsible for both allelic disorders, has been mapped to Xq13.31,2 and encodes a transmembrane Cu^{++} transporting ATPase. Cu^{++} is an essential cofactor of lysyl oxidases, a family of enzymes necessary for cross-linking fibrillar collagens and elastin (53). Studies in cultured cells localized the ATP7A protein to the trans-Golgi network (TGN). At this location, ATP7A is predicted to supply copper to the copper-dependent enzymes as they migrate through the secretory pathway. However, under conditions of elevated extracellular copper, the ATP7A protein undergoes a rapid relocalization to the plasma membrane where it functions in the efflux of copper from cells (54-56).

The molecular basis for typical OHS most often involves exon skipping with reduction of correct mRNA processing compared with normal (57). Six of eight typical OHS mutations reported, as well as the molecular defect in the mouse model of OHS, involve such aberrant splicing. In two other patients with typical OHS, a deletion in the promoter region and a frameshift mutation in the final exon were associated with the phenotype (58).

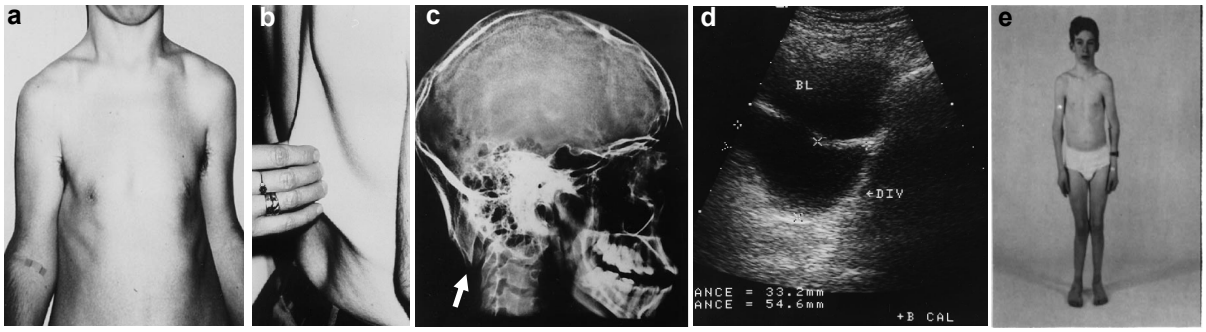

Fig. 1.4 X-linked cutis laxa, a,b) 18-year-old boy with OHS, demonstrating pale skin, cutis laxa, muscle atrophy and chest deformity,c) Bilateral occipital exostoses (occipital horns),d) Transverse US showing a 4 ´ 5-cm bladder diverticulum, (57) e) elbow dislocations and pes planus in a boy with OHS (52).

1.5.3 Autosomal dominant cutis laxa (ADCL, MIM 123700)

Autosomal dominant CL is usually a mild cutaneous disease sometimes accompanied by gastrointestinal diverticula, hernias, or genital prolapse (59). This disorder can be complicated through pulmonary artery stenosis, aortic, and arterial dilatation and tortuosity, Raynaud's phenomenon (60), bronchiectasis (59), and emphysema (61) (fig1.5). The disease is caused by mutations in the elastin gene ELN (MIM 130160) (60), or the gene encoding fibulin-5 (FBLN5; MIM

604580), which can cause either autosomal dominant or autosomal recessive cutis laxa (62). Haploinsufficiency for elastin often causes supravalvular aortic stenosis (SVAS), but not CL. Patients with Williams syndrome, who have large deletions encompassing the whole of the elastin gene, frequently suffer from SVAS, as do patients heterozygous for disruptions, deletions or point mutations in the elastin gene. In contrast with these loss-of-function mutations, the mutation first described in a cutis laxa patient is a single base deletion and is predicted to produce a stable but abnormal tropoelastin (60). This was also shown to result from a partial tandem duplication in ELN in patients with autosomal dominant CL and severe chronic obstructive pulmonary disease (COPD) (63). ELN mutations can also lead to autosomal recessive cutis laxa (64). Markova and colleagues (2003) reported a heterozygous 22-kb tandem duplication in fibulin-5 gene, encompassing the sequence from intron 4 to exon 9, which results in a mutant 0.5kb longer transcript suggesting a heterogeneous genetic background for autosomal dominant CL (62).

Fig. 1.5 Autosomal dominant cutis laxa, a)Patient with ADCL; age 10 months, showing redundant folds of skin on face, arms and trunk (60), (b) Patient's phenotype with ADCL at 3 months of age showing lax folds on the face with sagging cheeks, hanging corners of the mouth, sunken nasal bridge, broad nasal tip, retrognathia, (c) note prominent abdomen, folds of skin at the inguinal region and legs, right sided hernia inguinalis, umbilical hernia, (d) proband at 15 months of age: coarse face with bitemporal narrowness, sunken nasal bridge, flat broad nose, periorbital fullness, full cheeks with loose hanging skin (65).

1.5.4 Autosomal recessive cutis laxa (ARCL)

Autosomal recessive cutis laxa (ARCL) describes a group of syndromal disorders that are often associated with a progeroid appearance, lax and wrinkled skin, osteopenia and mental retardation (66). There are three types of autosomal recessive cutis laxa known so far and gerodermia osteo-

dysplastica, which is also categorized in this group because of its phenotypic similarities. Type I is the most severe among them, whereas types II and III overlap significantly as a number of patients diagnosed as having type III were molecurly finally found to have type II cutis laxa.

1.5.4.1 Ultrastructural alterations of skin in autosomal recessive cutis laxa.

All subtypes of autosomal recessive cutis laxa are characterised by a common ultrastructural change in the skin. Electron microscopy of skin biopsies obtained from patients showing one of the formerly described autosomal recessive phenotypes reveal a variable degree of fragmentation of the elastic fibres, whereas the collagen structure appears to remain intact (fig 1.6).

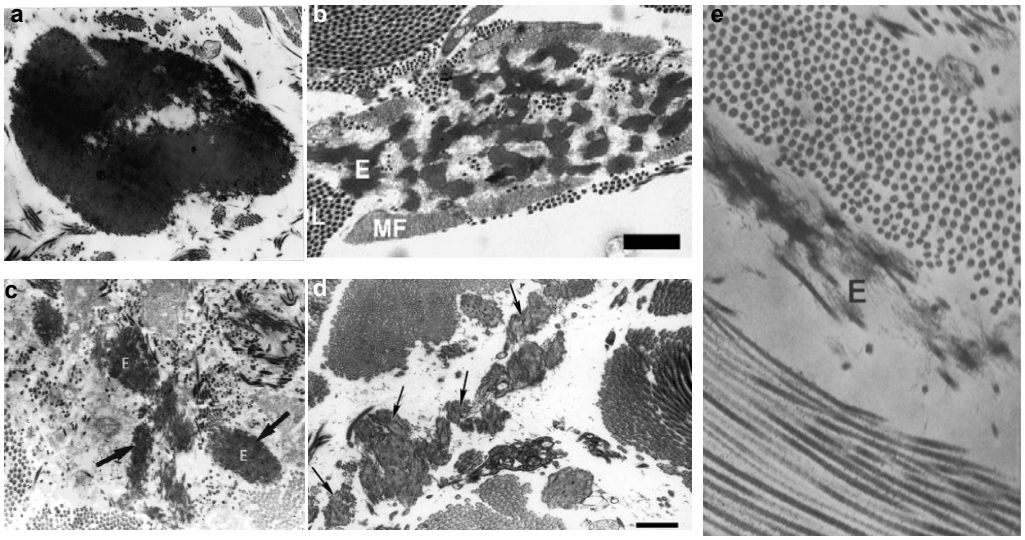

Fig. 1.6 Ultrastructural alterations of skin in autosomal recessive cutis laxa.(a) Electron micrographs (×14 400) of elastin fibre in the papillary dermis of healthy controls (b) 7-month-old ARCLI patient with a homozygous fibulin-5 mutation elastic fibres in the dermis consist of globules of elastin (E) with adjacent bundles of microfibrils (MF) Magnification bar, 1.0 mm (72) (c) Remarkable fragmentation of altered elastic fibres in WSS patient (E). Note the predominance of the microfibrillar component (arrows). (Magnification 10,000×.) (68)(d)Electron micrograph shows a fragmented elastic fibre in a GO patient (arrows). Bar = 1 lm (67). (e)rudimentary, fragmented elastic fibres (E)in skin biopsy of a de Barsy patient(at the age of 10 days)(x20000) (69).

1.5.4.2 Autosomal recessive cutis laxa type I (MIM 219100)

Type I autosomal recessive cutis laxa is characterized by pulmonary emphysema, umbilical and inguinal hernias, gastrointestinal and vesicourinary tract diverticula and the poorest prognosis

among ARCL phenotypes (fig1.7). It was found to primarily result from homozygous mutations in fibulin-5 (*FBLN5*; MIM 604580) (70). Further studies revealed that mutations in the gene encoding for EGF-containing fibulin-like extracellular matrix protein 2 gene (*EFEMP2*; MIM 604633.0001) (former fibulin-4 (FBLN4) can lead to the same phenotype (71). Hu and colleagues (2006) suggested that mutations in fibulin-5 result in misfolding and decreased secretion (72). Homozygous and compound heterozygous mutations in *EFEMP2* have been found in patients with a more severe, lethal phenotype accompanied by contractures, arachnodactyly, pulmonary artery occlusion and aortic aneurysm (73, 74).

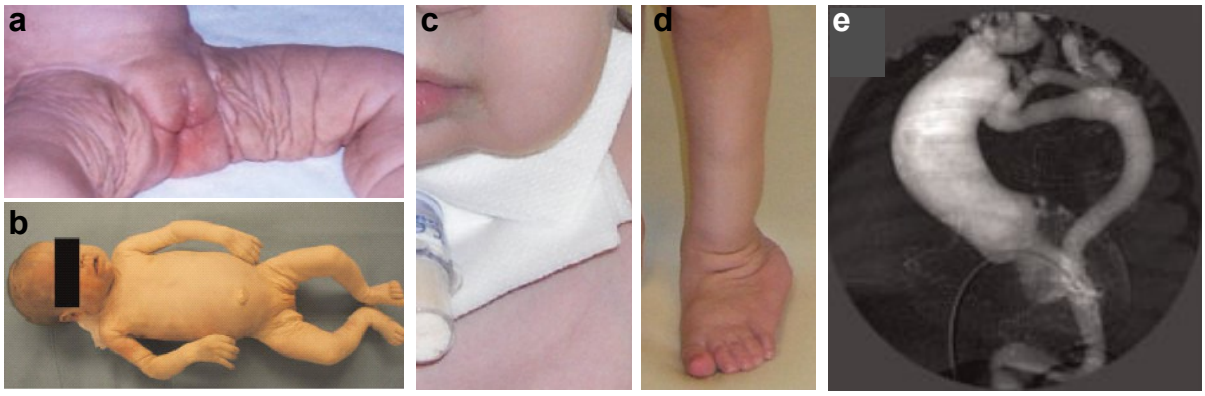

Fig. 1.7 Autosomal recessive cutis laxa type I, a) 6 months old patient with redundant skin folds in extremities (70) (b) Postmortem photograph of the propositus showing mild cutis laxa and apparent arachnodactyly (73). (c,d) Clinical photographs of the patient show sagging cheeks and tracheal tube as well as redundant skin in the extremities (71) e) Cardiac catheterization showed dilated ascending aorta, tortuous pulmonary artery and descending aorta (73).

1.5.4.3 Autosomal recessive cutis laxa type II (MIM 219200)

Debré in 1937 was the first to report a case of cutis laxa combined with osseous deformities (75). Gazit (1973) reported 3 cases with prominent wrinkled skin of the hands and feet and was the first to introduce the wrinkly skin syndrome as a separate clinical entity (76). Zlotogora (1999) proposed that ARCL with developmental delay and wrinkly skin syndrome could represent the same disorder (77).

The main clinical features of autosomal recessive cutis laxa type II, also known as Debré type, and its allelic disorder of wrinkly skin syndrome, are severe skin wrinkling, delayed closure of the anterior fontanel, downslanting palpebral fissures, a varying degree of developmental delay and a general connective tissue weakness (fig1.8). The skin anomalies appear to diminish with age, whereas the mild abnormal fat distribution around the buttock and the hips seen at birth be-

comes more severe. Cobblestone brain malformations have also been observed in patients with type II ARCL (78). In some cases a severe neurodegenerative phenotype with seizures and dementia was observed. Furthermore, patients were found to display a combined defect of N- and O-glycosylation of serum proteins (CDG-II) (fig1.9b) (79).

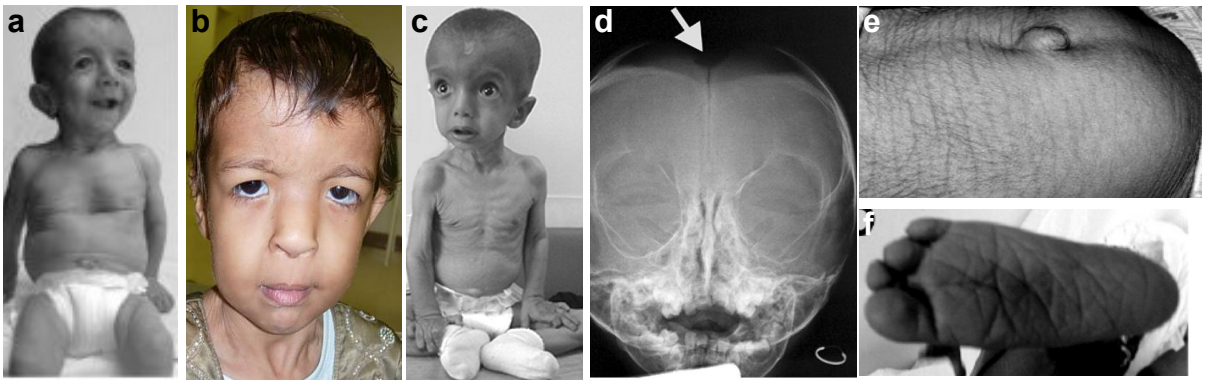

Fig. 1.8 Autosomal recessive cutis laxa type II. a) Affected 9-month-old girl with typical facial dysmorphism and depression in the frontal calvaria due to a large open fontanelle. Note skin wrinkling at neck and abdomen (79) (b) affected at the age of 2 years with skin wrinkles at the neck and down slanting palpebral fissures (c) affected at the age of 18 months with cachexic appearance, midline depression of the skull over unossified anterior fontanelle, down slanting palpebral fissures, sagging cheeks, and skin wrinkling (80), (d) large unossified fontanelle in 16-months affected (80), (e) wrinkly skin on abdomen at three years of age (80), (e) foot of an affected showing deep creases (80).

Loss-of-function mutations in *ATP6V0A2* (MIM 311716), encoding the a2 subunit of the V-type H+-ATPase, were recently identified in several families with autosomal recessive cutis laxa type II or wrinkly skin syndrome (79).

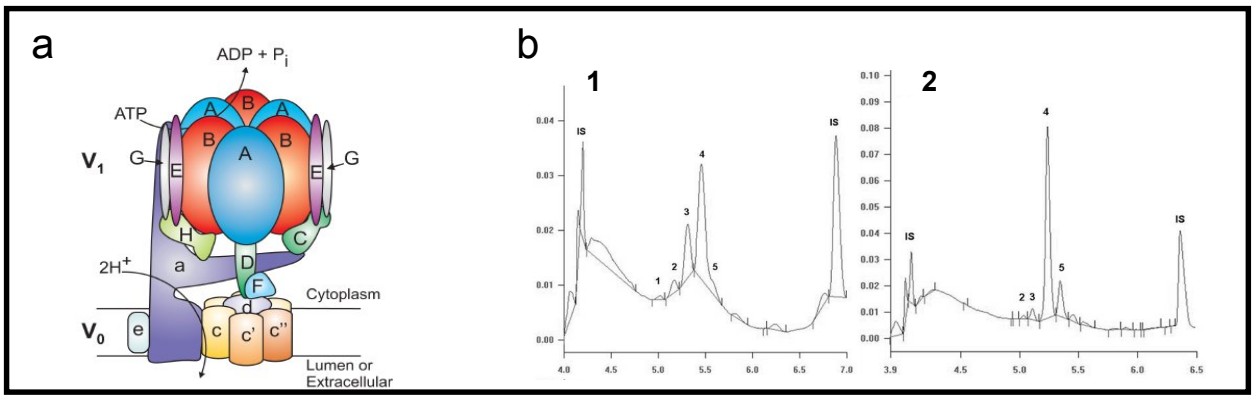

Fig. 1.9 (a)Structural model of the V-ATPase. The V-ATPase is composed of a peripheral domain (81) (V1) responsible for ATP hydrolysis and an integral domain (V0) that carries out proton transport. V1 and V0 are connected by both a central stalk (composed of subunits D and F in V1 and subunit d in V0) and peripheral stalks (composed of subunits C, E, G, H, and the N-terminal domain of subunit a). ATP hydrolysis in V1 drives rotation of the central stalk that, in turn, drives rotation of the ring of proteolipids (c, c′, and c″) past subunit a in V0. It is the movement of the proteolipid subunits past subunit a that drives proton transport across the membrane (82). (b)Sialotransferrin patterns. (1) Transferrin glycosylation pattern in ARCLII (type 2 pattern: decreased 4-sialo- and 5-sialotransferrin and

increased 3-, 2-, and 1- sialotransferrin) determined by capillary zone electrophoresis (CZE), (2) normal pattern found in control serum (80).

Vacuolar H+-ATPases are ATP-dependent proton pumps composed of two multi-subunit domains, V1 and V0, containing eight (A through H, total of 640 kDa) and five different subunits (a, c, c″, d and e in mammals, total of 260 kDa), respectively (fig1.9a). V-ATPases serve a number of functions in normal physiology mainly by regulating the pH of different intracellular compartments and the extracellular space (83). The fact that ARCL patients have a glycosylation defect indicates that the a2 subunit is necessary for the normal function of the Golgi apparatus. While the structure of the Golgi compartment in patient fibroblasts shows only mild changes, a more pronounced abnormality was seen after exposure of these cells to brefeldin A (BFA), which disturbs vesicle trafficking between the Golgi compartment and the ER. The rapid BFA-induced fusion of the Golgi with the ER was strongly delayed in ARCL fibroblasts (79).

1.5.4.4 Cutis laxa, corneal clouding and mental retardation-De Barsy Syndrome (MIM 219150)

De Barsy syndrome is a rare, autosomal recessive syndrome characterised by a progeria-like appearance with distinctive facial features and cutis laxa (fig1.10)(84). Ophthalmological, orthopaedic and neurological abnormalities are also typically present (85). The syndrome was first described by de Barsy *et al.* (1968) in a proband with cutis laxa, defective development of elastic fibres in the skin, corneal clouding, hypotonia and delayed psychomotor development (86). Since that time approximately 27 further cases have been reported worldwide (85).

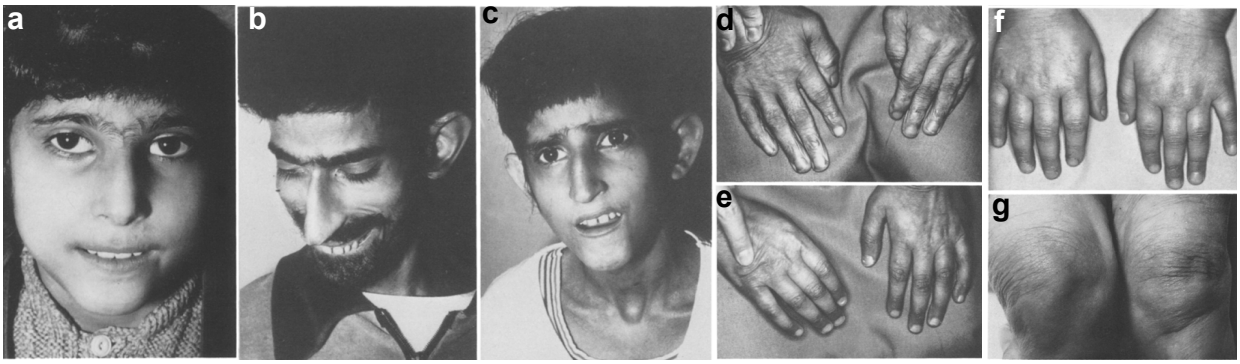

Fig. 1.10 De Barsy syndrome (a-c) three affected siblings. Note the progeroid facies, lax and dry skin, synophrys, slightly hooked nose, frontal bossing, (d-g) the hands of the same patients with wrinkled, hyperelastic, atrophic skin on the extensor surfaces of the joints (84).

1.5.4.5 Gerodermia osteodysplastica (MIM 231070)

Gerodermia osteodysplastica, is a rare autosomal recessive disorder characterized by lax, wrinkled skin, joint laxity and a typical face with a prematurely aged appearance. Skeletal signs include osteoporosis leading to frequent fractures, malar and mandibular hypoplasia and a variable degree of growth retardation (fig1.11)(80,87).

Bamatter *et al.* (1950) described for the first time this disorder in five members of a Swiss family. Twenty five additional cases have been reported in the literature (88).

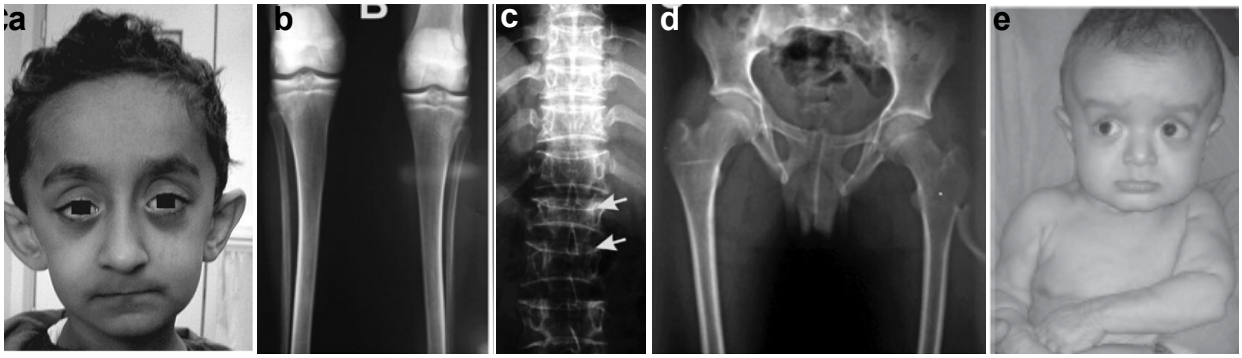

Fig. 1.11 Gerodermia osteodysplastica (a) large ears, maxilla hypoplasia and droopy face in a 6-year old patient (b-d) 12-year old affected, severe osteoporosis of lumbar spine, bowing of tibiae, and osteoporotic femoral necks, (80) (e) 9-month-old individual with gerodermia osteodysplastica, typical facial appearance with sagging cheeks and the pronounced wrinkling at the chest and dorsum of the hands (87).

Hennies et al. (2008) reported that GO is caused by loss of function mutations in *GORAB* (MIM 607983), a gene encoding a Golgi-localising protein which is highly expressed in skin and osteoblasts (87). A specific interaction of GORAB with the small G protein Rab6 together with the presence of coiled-coil domains indicates that GORAB is a golgin, the first ever found to cause a human phenotype. These results suggest a potential association between abnormalities of the secretory pathway and age-related changes in connective tissues (87).

Table 1. The forms of autosomal recessive cutis laxa

Type	MIM	Clinical features apart from cutis laxa	Gene	Ref
ARCL I	219100	supravalvular aortic stenosis, vascular tortuosity, aortic aneurysm, recurrent respiratory infections, emphysema, hernias, bladder diverticula	FBLN5 EFEMP2	70, 71
ARCL II	219200	Intrauterine growth retardation (IUGR), Failure to thrive, downslanting palpebral fissures, large anterior fontanel, delayed closure of the fontanel Congenital hip dislocation	ATP6V0A2	79
GO	231070	wrinkled skin, sagging cheeks, malar hypoplasia, joint laxity, osteoporosis	GORAB	87
De Barsy	219150	Short stature, cataract or corneal clouding, mental retardation, inguinal hernia, hip dislocation	unknown	84, 85

2 Aim of the study

Cutis laxa is a phenotypic feature of a great number of genetic diseases, as isolated cutis laxa or part of a syndrome, accompanied most of the times with general disorders of the connective tissue. The classification and nomenclature of the different phenotypes undergoes ongoing changes due to the progressive elucidation of the respective underlying genetical defect.

Two of these cutis laxa phenotypes have been the subject of research of our scientific team for the last few years, autosomal recessive cutis laxa type II (ARCLII) or wrinkly skin syndrome (WSS) and gerodermia osteodysplastica (GO). These overlapping phenotypes were clearly divided after our identification of their genetical basis (79, 87). Characteristically, ARCLII shows an abnormal glycosylation pattern (CDG II) which could only be seen in serum of patients with *ATP6V0A2* mutations (66,79). On the other hand, patients bearing mutations in *GORAB* gene showed a much more severe bone phenotype with osteoporosis and increased fracture risk (66, 80, 87). Skeletal anomalies were found to be milder in ARCLII patients, presenting as delayed closure of the frontal fontanelle, congenital hip dislocation and osteopenia.

Nevertheless, in our large patient cohort there were still probands initially diagnosed as GO, WSS/ARCLII and de Barsy syndrome that did not bear mutations in any of the known genes. This led to the conclusion that most probably mutations in further gene(s) can lead to the same phenotype.

The aim of the study was to identify the responsible genetical defect in the families negative for the autosomal recessive cutis laxa genes and without any inner organ involvement, which would indicate a possible fibulin-5 or -4 defect.

Significant information has already been obtained through the association of cutis laxa phenotypes with the two new genes *ATP6V0A2* and *GORAB*. The study of their cellular behaviour has indicated an important link lying in Golgi apparatus, as GORAB protein was proved to be a golgin (87) and the a2 subunit of the vacuolar ATP-ases was found to play a role in the maintenance of Golgi function (79). This knowledge is, of course, only the first step of a cascade of different events that ultimately lead to this specific phenotype. The identification of further responsible genes and the qualities of the respectively encoded proteins would be a great contribution to defining a plausible and well characterised pathomechanism of the cutis laxa phenotypes.

3 Materials and methods

3.1 Materials

3.1.1 Molecular biology

Table 3.1. Equipment-molecular biology

Device	Manufacturer	Description
ABI 3730 Capillary Sequencer	Applied Biosystems	48 Capillary Array
BioZyme Cycler (DNA Engine DYAD)	MJ Research	2x 96 Cell Peltier Element Thermoblock
FlexCycler	Analytikjena (Biozym Scientific GmbH)	2x 48 Cell Peltier Element Heizblock
Lab centrifuge	Eppendorf	Centrifuge 5415 D
Centrifuge	Eppendorf	Centrifuge 5810
7500 Real Time PCR Machine	Applied Biosystems	7500 Real Time PCR Machine

Table3.2. Chemicals and reagents-molecular biology

Reagents/Chemicals	Composition/Concentration	Manufacturer
2-Propanol	Reinst	J.T. Baker
Agarose	Agarose SERVA for DNA Elektrophoresis (500g)	SERVA
Chloroform	Reinst	J.T. Baker
dNTPs	dATP 100 mM dTTP 100 mM dGTP 100 mM dCTP 100 mM	BIOLINE
Ethanol	Absolut Ethanol	J.T. Baker
GeneRuler™ 1 kb DNA Ladder	---	Fermentas
HPLC H_2O	---	J.T. Baker
NH_4 Reaktionbuffer [10x]	NH_4-Reaktionbuffer incl. $MgCl_2$ (15 mM Mg^{2+}) pH 8,8	Invitek
Loading Dye [6x] for gel-electrophoresis	---	Fermentas
Big Dye Terminator Reaktionbuffer [5x]	---	Applied Biosystems
Big Dye Terminator	Version 3.1 (v3.1)	Applied Biosystems
SYBR® Green	PCR Mastermix	Applied Biosystems
Trizol®	---	Invitrogen

Table 3.3. Enzymes-molecular biology

Enzymes	Composition/Concentration	Manufacturer
Exonuclease I (Exo1)	2000 units[20000 U/ml]	New England BioLabs
Shrimp Alkaline Phosphatase (SAP)	1 units/µl	usb®
Taq DNA-Polymerase	1000 Units [5 U/µl]	Invitek

Table 3.4. Kits-molecular biology

Kit	Manufacturer
Invisorb Spin DNA Extraction Kit (250)	Invitek
RevertAid™ H Minus First Strand cDNA Synthesis Kit	Fermentas

Table 3.5. Markers used for fine mapping

Marker	Primer	Sequence	Expected Product size[bp]
D17S751	Left	TTATTCACTGCATGCAAGCATCTC	125
	Right	CTCACCATAGCTTGTTTCCCAAG	
D17S802	Left	GCCACCTGCCCCTCAA	168-188
	Right	CTGCCAGCAGAGGCCA	
D17S1847	Left	GATCACCAGGAACACCC	144-164
	Right	TCTTCAGAGCTTGCCAG	
D17S761	Left	GTGTGGCTGGTCTTGGCCTCCT	154
	Right	CTCCTGCCTCCCCTTCCTGATC	
D17S928	Left	TAAAACGGCTACAACACATACA	135-165
	Right	ATTTCCCCACTGGCTG	
D17S784	Left	GAGTCTCCTAAATGCTGGGG	226-238
	Right	AGCTCCTGCACAGTTCTTAAATA	

Table 3.6. Oligonucleotids used for the genomic sequence analysis of *PYCR1*-gene

Exon	Primer	Sequence	Product size[bp]
1	Left	GAACCTCCACCCCTCCAG	512
	Right	CTCCCCATTCCCAGGAAG	

Exon	Primer	Sequence	Product size[bp]
2	Left	AGCCAAAGCTAGCCATGAAG CAGGTCCCAA-	596
	Right	GAGCAATCAG	
3-4	Left	CAGCATTCTCTGTGCCATTC	830
	Right	TTCTCCTCCTTCCCTTCTGG	
5-6	Left	GGTGGAAGAGGACCTGATTG ATCTGCT-	752
	Right	GAGTGCGTGAATG	
7	Left	TGGTGATGCTGAGCTGATTC TTCTCACACGG-	815
	Right	GAAGGAGAG	

Table 3.7.1 Human oligonucleotids used for the expression analysis in fibroblasts

Gene	Primer	Sequence	Product size [bp]
GAPDH	Left	TGCACCACCAACTGCTTAGC	87
	Right	GGCATGGACTGTGGTCATGAG	
PYCR1	Left	ATGAGCGTGGGCTTCATC	103
	Right	GGGAGCTAGCCATTATCTTGTG	
PYCR2	Left	TCGGCTCACAAGATAATAGCC	107
	Right	TTCACCGTCTCCTTGTTGC	
P5CS	Left	GGCTGATGGCCTTGTATGAG	85
	Right	TCATGGAAATCCAAATTGGTC	

Table 3.7.2 Mouse oligonucleotids used for the expression analysis in different tissues

Gene	Primer	Sequence	Product size [bp]
Gapdh	Left	GGGAAGCCCATCACCATCTT	61
	Right	CGGCCTCACCCCATTTG	
Pycr1	Left	AGACATGGACCAAGCTACGG	107
	Right	TCACAGCCAGGAAGAGCAC	
Pycr2	Left	GTCGGCTCACAAGATAATAGCC	99
	Right	TCCTTATTGCTTCGGGTCAG	
Pycrl	Left	GTCTCAGTGGCAGTGGTGTG	116
	Right	CAGGGTCTGAGCAGCAATG	
P5cs	Left	GCATTCTTCACCTCCTGACC	100
	Right	CGGCAGAGATCCTCAACTTC	

3.1.2 Cell-culture

Table 3.8. Equipment/materials-cellculture

Equipment/Materials	Manufacturer	Description
Incubator	FormaScientific	CO_2 Water Jacketed Incubator
Coverslips	Menzel-Gläser	Coverslips ∅ 12 mm
Microscope	Zeiss	Axiovert25 (Biokular)
(Hemo)cytometer	MARIENFELD	depth 0,100 mm surface 0,0025 mm^2
tissue culture hood	Luft-und Reinraumtechnik GmbH	BDK-S 1500
Plate of 6 cells	SARSTEDT	
T_{25}-Flask	SARSTEDT	25 cm^2 culture surface
T_{75}-Flask	SARSTEDT	75 cm^2 culture surface
Vacuum pump	KifLab	Laboport
Water-bath	GFL	---
Centrifuge	Heareus	Megafuge 2.0R

Table 3.9. Celllines-cellculture

Cell line	Origin/extraction	Tissue/Status
HAF UK	Control Cells/skinbiopsy	Skinfibroblasts
HAF FB 2145	Control Cells/skinbiopsy	Skinfibroblasts
HAF SM	Patient cells/skinbiopsy	Skinfibroblasts: ARCL2 PYCR1 Mutation:
HAF JH	Patient cells/skinbiopsy	Skinfibroblasts: ARCL2 PYCR1 Mutation
HAF EG	Patient cells/skinbiopsy	Skinfibroblasts: ARCL2 PYCR1 Mutation
HAF FB 1844	Patient cells/skinbiopsy	Skinfibroblasts: ARCL2 PYCR1 Mutation

Table 3.10. Chemicals and reagents-cellculture

Reagents/Chemicals	Composition/Concentration	Manufacturer
0.9% Natriumchloride	0.9% NaCl in HPLC H_2O	---

Reagents/Chemicals	Composition/Concentration	Manufacturer
1 % v/v Ultraglutamin 1	200 mM Ultraglutamine in 0.85% NaCl Dilution	LONZA
1 % Penicillin/Streptomycin		LONZA
10 % v/v FCS	---	LONZA
DMEM	10 % v/v FCS 1 % v/v Ultraglutamin 1	LONZA
PBS (sterile)	without Ca^{2+}, Mg^{2+} Ion low Endotoxin	BIOCHROM AG
BrDU	10µM	Roche
L-Proline	-----	Sigma-Aldrich
Trypan Blau	Trypan Blau Dilution 0.4%	SIGMA

Table 3.11. Buffer/Solusions- Immunofluorescence

Buffer/Solutions/Materials	Composition/Concentration
Cell fixation solution	4 % w/v PFA in 1 x PBS
Cell permeabilisation solution	0.4 % w/v Triton-X-100 and 3 % BSA w/v in 1x PBS
Antibodies	Table 3.12, 3.13
Antibody-dilutions	3 % BSA w/v in 1x PBS
Blocking solution	3 % BSA w/v in 1x PBS
DAPI	1 mg/ml in DMF (Molecular Probes)
Mounting medium	Fluoromount G (SouthernBiotech)

Table 3.12 Primary Antibodies- Immunofluorescence

Antibody (Manufacturer)	Antibody-Origin	Manufacturer	Dilution
PYCR1	rabbit	ProteinTech group, Inc.	1:600
a-Adaptin	mouse	BD transduction laboratories	1:400
ERGIC53	mouse	Alixis	1:400
TGN46	sheep	AbD Serotec	1.2000
P5CS/ALDH18A1	mouse	Abnova	1:300
Mitophillin	mouse	MitoSciences	1:500
Cytochrome C	mouse	BD transduction laboratories	1:300

Table 3.13 Secondary antibodies- Immunofluorescence

Antibody (Manufacturer)	Antibody-Origin	Manufacturer	Dilution
a-rabbit Alex Fluo® IgG 488	donkey	Molecular Probes	1:2000
a-mouse Alex Fluo® IgG 555	donkey	Molecular Probes	1:2000
a-sheep Alex Fluo® IgG 555	donkey	Invitek	1:2000

3.1.3 Protein-chemical Methods

Table 3.14. Buffer and solutions-protein extraction methods

Buffer/Solutions	Composition/Concentration
1x PBS	NaCl 137 mM KCl 2,7 mM Na_2HPO_4 8 mM KH_2PO_4 2mM
10x TBS	1.37 M NaCl, 27 mM KCl 250 mM Tris dissolved in H_20 and adjusted with HCl to pH 7.4

Buffer/Solutions	Composition/Concentration
Cell-lysis Buffer	50 mM NaF 30 mM $NaPP_i$ 5 mM EDTA 1 Tablet Complete (Roche) in 50 ml Puffer in 1x TBS

Table 3.15. Kit/Device/Materials-protein concentration measurement

Kit/Device/Materials	Manufacturer
BCA Protein Kit	Pierce
Standard concentration line 0 µg/ml - 1000 µg/ml BSA	Diluted from 2µg/ml stock solution
96-wells Photometer	BioRAD

Table 3.16. Buffer and solutions-SDS-PAGE

Buffer/Solutions	Composition/Concentration
10 x SDS-Runbuffer	250 mM Tris 2 M Glycine 1 % w/v SDS dissolved in distilled H_2O
5 x SDS Sample Buffer	250 mM Tris 10 % w/v SDS 0.5 % w/v Bromphenolblue 50 % w/v Glycerine dissolved in distilled H_2O
APS from Merck	10 % w/v APS
Protein-Molecularweight-Marker	Precision Plus Protein Standards BIORAD
Rotiphorese Gel 30	30 % Acrylamide
Stocking gel-Buffer SDS-PAGE	0.5 M Tris 0.4 % w/v SDS dissolved in H_20 pH = 6.8 (adjusted with HCl)
TEMED from Serva	TEMED
Separating gel-Buffer SDS-PAGE	1.5 M Tris 0.4 % w/v SDS dissolved in H_20 pH = 8.8 (adjusted with HCl)

Table 13.17. Buffer, solutions and materials-Western Blot

Buffer/Solutions	**Composition/Concentration**
Blocking solution (Blocking milk)	5 % w/v fat-free milk powder 0.2 % v/v NP40 1x TBS soluted in destilled H_2O
Developing solution	GBX developer and replenisher (Kodak)
Fixation solution	GBX developer and replenisher (Kodak)
10 % v/v NP40	NP 40 Substitute Fluka diluted with 1x TBS
ECL Kit	Enhanced Chemoluminescence Kit (Amersham)
Films	BioMax MR Imaging Film (Kodak)
Gelkammer/Blotkammer	BioRad Mini-Protean 3 System
Transfer membranes	Nitrocellular Mini-Gel Membrane (BIORAD)
Ponceau-solution	0.5 % Ponceau S (w/v) 0.1 % acetic acid (v/v) Dissolved in destilled H_2O
[10x] Transfer buffer	250 mM Tris 2 M glycine dissolved in destilled H_2O pH = 8.3 (adjusted with HCl)
Wash buffer	10 ml 10 % v/v NP40 Solution 100 ml 10x TBS diluted in 890 ml destilled H_20

Table 3.18. Primary antibodies-Western blot-

Antibody (Manufacturer)	Antibody-Origin	M.W. of target protein	Manufacturer	Dilution
PYCR1	rabbit	37kDa	ProteinTech group, Inc.	1:800
Actin	rabbit	40kDa	SIGMA	1:500

Table 3.19. Secondary antibodies-Western blot

Antibody (Manufacturer)	Antibody-Source	Manufacturer	Dilution
Anti-rabbit HRP	goat	Cell Signaling	1:2000

3.2 Methods

3.2.1 Molecular biology

3.2.1.1 Patients-DNA samples

DNA samples were obtained from 22 families after participants gave their informed consent and after approval by the local ethics commission (Ethikkommission der Charité).

Family	Origin	Number of affected	Initial Diagnosis
J.I.	Iraq	1	WSS
T.P.	Palestine	1	WSS
S.P.	Palestine	3	GO/WSS
I.K.	Kuwait	2	GO/WSS
F.S.	Kuwait	1	GO/WSS
S.I.	Jordan	4	WSS
D.I.	Italy	1	GO
S.O.	Oman	1	GO
G.O.	Oman	3	GO
H.B.	Bahrain	2	GO

Family	Origin	Number of affected	Initial Diagnosis
M.A.	Austria	1	GO
M.Q.	Qatar	1	GO
H.U.	United States	1	GO
N.A.	Australia	1	GO
A.S.	Syria	1	GO
D.T.	Turkey	1	DBS
M.F.	Italy	1	DBS
S.T.	Turkey	2	DBS
E.U.	United States	1	DBS
J.A.	Australia	3	DBS
K.T.	Turkey	1	DBS
I.T.	Turkey	1	DBS

Table 3.20 Cohort of the study, WSS = Wrinkly Skin Syndrome,GO = Gerodermia Osteodysplastica, DBS = De Barsy Syndrome

3.2.1.2 Concentration measurements of nucleic acids

The NanoPhotometer (IMPLEN) was used in order to determine the concentration of the nucleic acids needed for the study. The concentration of 1 µl of DNA/RNA was measured through its absorption at 260nm. The quality of the nucleic acids was then determined through their absorption at 280nm.

3.2.1.3 RNA extraction – cDNA reverse transcription

RNA extraction was necessary for performing the expression analysis of *PYCR1* in human fibroblasts and in mouse tissues. Human fibroblasts were cultivated until confluence was reached. RNA was released through a Trizol® (Invitrogen) mediated cell lysis and was subsequently prepared by a standard RNA-extraction protocol. The extracted RNA was then transcribed into cDNA (RevertAid H kit; Fermentas).

3.2.1.4 Polymerase chain reaction (PCR) /reverse transriptions PCR (RT-PCR)

Polymerase chain reaction (PCR) was performed in order to amplify the polymorph tandem repeat markers and the 7 exons of the PYCR1-gene. The forward and reverse primers used are shown in tables 5 and 6.

Table 3.21 Standard protocol of PCR- Standard cycler conditions

Reagents	**Vol.[µl]**	**Final concentration**
Taq-Polymerase	0,20	0,4 U
dNTPs	0,25	2,5 mM
F-Primer	0,50	5,0 mM
R-Primer	0,50	5,0 mM
10x NH_4-Puffer	2,50	1x
HPLC H_2O	20,05	---
DNA	1,00	~30 ng

Temperature [°C]	**Time [min]**	**Cycles**
95	03:00	
95	00:30	3x
61	00:45	
72	01:30	
95	00:30	3x
59	00:45	
72	01:30	
95	00:30	3x
57	00:45	
72	01:30	
95	00:30	32x
55	00:45	
72	01:30	
72	10:00	
16	for ever	

3.2.1.5 Genotyping and linkage analysis

We performed genome-wide linkage analysis in ten families using the Affymetrix GeneChip® Human Mapping 250K Arrays (Affymetrix, Santa Clara, CA). Genotypes were produced by the GeneChip® DNA Analysis Software (GDAS v2.0, Affymetrix). We verified sample genders by counting heterozygous SNPs on the X chromosome. Relationship errors were evaluated with the help of the Graphical Relationship Representation program. The PedCheck program was applied to detect Mendelian errors and data for SNPs with such errors were removed from the data set. Non-Mendelian errors were identified by using the MERLIN program and unlikely genotypes for related samples were deleted. Nonparametric linkage analysis using all genotypes of a chromosome simultaneously was carried out with MERLIN. Parametric linkage analysis was performed by a modified version of the GENEHUNTER 2.1 program through stepwise use of a sliding window with sets of 110 or 200 SNPs. Haplotypes were reconstructed with GENEHUNTER 2.1 and presented graphically with HaploPainter .

3.2.1.6 Sequencing analysis according to Sanger's method (dideoxy sequencing or chain termination)

The fragments which were amplified through PCR were then subjected to sequence analysis with the aim to unveil possible mutations in *PYCR1*-gene. The primers chosen for this analysis are the same with the ones that have been used for the amplification of the gene fragments (table 6). The PCR-products were purified by a standard protocol with the help of the enzymes Shrimp Alkaline Phosphatase (SAP) and Exonuclease 1 (EXO1).

Table 3.21 PCR-products Purification

Reagents	Volume [µl]
SAP	0,300
Exo 1	0,075
H_2O	1,625
PCR Produkt	8,000

The samples were incubated in thermocycler at 37°C for 30 min, followed by the heat-inactivation of the enzymes at 72°C for 15 min.

Table 3.22 Sequencing reaction

Reagents	Volumes [µl]	Final concentration
BigDye Terminator v3.1	0,5	---
Primer F oder R	0,3	3 mM

Reagents	Volumes [µl]	Final concentration
Big Dye Terminator reaction-buffer [5x]	2,0	1x
HPLC H_2O	5,2	---
SAP/Exo 1 PCR Product	2,0	---

Cycler Conditions

Temperature [°C]	Time [min]	Cycles
96	00:10	30x
50	00:05	
60	04:00	
16	for ever	

The products were run on a 3730 DNA Analyzer (Applied Biosystems, Foster City, CA)

3.2.1.7 Mutation analysis

Positional candidate genes were obtained from the GenBank and Ensembl databases (http://www.ncbi.nlm.nih.gov/mapview/, http://www.ensembl.org). Genes were analyzed by direct sequencing of DNA with primers flanking each exon. Primer sequences were based on the reference sequences of each gene. The evaluation of the analysis results was performed with the Seqman from DNAstar software package.

3.2.1.8 Quantitative PCR (qPCR)

The gene expression analysis was performed by the SybrGreen method. The determination of the expression levels was the result of a relative quantification, relative to one endogene control and one calibrator. The chosen oligonucleotids bind to the cDNA of the *PYCR1, PYCR2, PYCRL* and *P5CS* genes as well as of the endogene control (Tables 7.1,7.2), while the specific binding of their sequence on the desired genomic sites was examined before use by means of BLAST. The primers of each fragment were designed in such a way that the forward primer binds at the end of one exon and the reverse primer at the beginning of the following exon and that each frag-

ment would be approximately as big as 100bp. In this way the amplification status can be comparable.

The quantitation of the expression levels of each sample took place in relation/comparison with an endogene control, which is typically one of the house-keeping genes. These genes, as far as they have the same cellular origin as the examined samples, are expected to be similarly expressed. In this work *GAPDH* (glycerinaldehyde-3-phosphate-dehydrogenase) was used as the endogene control for the assay. Negative controls were also used in order to exclude contamination of the samples.

Table 3.23 Reaction and cycle conditions

Reagent	**Vol.[µl]**
SybrGreen	9
F-Primer (20 µM)	0,75
R-Primer (20 µM)	0,75
cDNA	7,5

Temperature [°C]	**Time [min]**	**Cycles**
50	02:00	1x
95	10:00	1x
95	00:15	40x
60	01:00	

The results were evaluated using a formal protocol. The determination of the Ct-value was made by the software (7500 System SDS Software) of Applied Biosystems. The relative quantification values (RQ) were calculated using the following equations:

$$AvgCt = \frac{(Ct_{r1}+Ct_{r2}+Ct_{r3})}{3}$$

$$Avg\Delta Ct = AvgCt_{target\ gene} - AvgCt_{end.\ ctrl.}$$

$$\Delta\Delta Ct = Avg\Delta Ct_{target\ gene\ sample} - Avg\Delta Ct_{target\ gene\ calibrator}$$

$$RQ = 2^{-(\Delta\Delta Ctcorrected)}$$

3.2.2 Cell culture

Six cell lines of human fibroblasts were used in this study, two as controls (WT for *PYCR1*) and four obtained from cutis laxa patients through skin biopsy (table 3.9)
The human skin fibroblasts were cultivated in DMEM (Lonza) supplemented with 10% fetal calf serum (FCS) (Lonza), 1% Ultraglutamine (Lonza) and 1% penecillin/streptomycin (Lonza) at 5% CO2 and 37°C.

3.2.2.1 Protein extraction

The primary skin fibroblasts of passages 4-8 were cultivated until confluence in 6-well plates. For the protein extraction they were first washed 3 times with phosphate-buffered saline (PBS) and then subjected to lysis (protein lysis buffer). The concentration of the total lysates from the samples was determined by using the Pierce BCA Kit according to the attached protocol. The concentration was measured in 10µl of each sample, in which 200 µl of the reaction mix (50[A]:1[B]) was added. The samples were incubated for 30 min at 37 °C. The absorption of each sample at 570nm was measured with the 96-well photometer (Biorad). The values were subsequently compared with those of samples with known concentration and the final concentration was determined through a linear equation.

3.2.3 Protein expression studies

3.2.3.1 SDS-PAGE

In this study, SDS-PAGE was used to evaluate the level of the PYCR1 protein in the fibroblasts of the cutis laxa patients and the controls, as well as for the determination of its levels in different mouse tissues. 18µl of each sample, under reducing conditions, was loaded on a 10% polyacrylamide gel. The gel ran in SDS-Runbuffer at 60 V for ~ 4 h.

3.2.3.2 Western blot analysis

The complete run of the gel was followed by its transfer onto a nitrocellular membrane in transferbuffer overnight at 30 V. The proteins transferred were transiently visualised by means of Panceau solution in order to confirm the success of the transfer and also to mark the reference protein sizes. The membrane was then incubated for at least one hour in blocking solution. The

primer antibodies were applied to the membrane diluted in blocking solution and were incubated overnight at 4 °C. In order to discard the primary antibodies the membrane was washed 5 times in wash buffer. The incubation of the secondary antibodies was held in blocking solution for 1.5 h at 4 °C. The final incubation of the membrane with ECL solution for 10 min at 4 °C took place after the membrane was washed again 5 times. The films were applied to the membrane, with exposure time ranging between 30 sec and 10 min, and then developed and fixed in respective solutions.

3.2.4 Immunofluorescence analysis

3.2.4.1 Immunostainings

For immunofluorescence studies, cells were seeded on ∅ 12 mm glass coverslips and cultivated until 50% confluence. They were then washed in phosphate-buffered saline (PBS) three times. Cells were fixed in 4% (wt/vol) paraformaldehyde in 1xPBS for 10min and permeabilized with 0.4% (vol/vol) Triton-X100 in 3% BSA in 1xPBS for 10min at 4°C. Specific primary antibodies against the target proteins were incubated overnight in 3% BSA at 4°C. For visualization, different secondary antibodies were applied for 1.5 h in 3% BSA at RT. DNA was stained with DAPI diluted in PBS for 5 min and cells were mounted in Fluoromount (Scientific Services). Images were collected by using an LSM 510 meta (Carl Zeiss, Göttingen, Germany) with a x63 Plan Apochromat oil immersion objective.

3.2.4.2 Mitochondrial morphology

Morphology of the mitochondrial network was investigated as previously described in Duvezin-Caubet S., et al. (2006). Fifty-percent-confluent fibroblasts were loaded with 100 nM Mito Tracker Red CM-H2XRos (Invitrogen). Cells were incubated with 500 mM H_2O_2 for 5 min and then fixed in 4% (wt/vol) paraformaldehyde in PBS for 10 min at 4 1C. DNA was stained by DAPI and cells were mounted in Fluoromount (Scientific Services). Pictures of every sample were collected randomly using a BX60 Olympus microscope.

3.2.4.3 Ultrastructural analysis

All specimens were fixed for at least 2 h at 19–22 1C in 3% glutaraldehyde solution in 0.1 M cacodylate buffer, pH 7.4, cut into pieces of B1 mm3, washed in buffer, postfixed for 1 h at 4 1C in 1% osmium tetroxide, rinsed in water, dehydrated through graded ethanol solutions, transferred into propylene oxide, and embedded in epoxy resin (glycidether 100). Semithin and ultra thin sections were cut with an ultramicrotome (Reichert Ultracut E). Ultrathin sections were treated with uranyl acetate and lead citrate, and examined with an electron microscope (Philips EM 400).

3.2.4.4 Proliferation assay

For the assessment of the proliferation rate, $2{,}5x10^4$ cells were seeded on ∅ 12 mm glass coverslips. The cells were incubated for 8 hours in medium containing 10µM Bromdesoxyuridin (BrdU) (Roche). Cells were fixed in 4% (wt/vol) paraformaldehyde in 1xPBS for 10min after 24, 48 and 72 hours and then incubated in 3N HCL for 10 min in RT. They were permeabilized with 0.1% (vol/vol) Triton-X100 in 3% BSA in 1xPBS for 30min at 4°C. Specific antibody against BrdU (G3G4) 1:500 was incubated for 1 hour in RT. For visualization an anti-mouse IgG Alexa Fluor 488 (Invitrogen, Molecular Probes) conjugate was applied. DNA was stained with DAPI and cells were mounted in Fluoromount (Scientific Services). The experiment was also performed in medium with 10% dialysed FCS and in medium supplemented with 5mM L- Proline (Sigma-Aldrich).

3.2.4.5 Apoptosis assay

For apoptosis measurement after hydrogen peroxide (neoLab) treatment, cells were incubated with 200 mM H_2O_2 for one hour without FCS as described. Subsequently medium with 0.4% FCS was added and cells were incubated at normal conditions for an additional 24 h. Cells were fixed in 4% (wt/ vol) paraformaldehyde in PBS for 10 min and permeabilized with 0.1% (vol/ vol) Triton-X100 in 3% BSA in PBS for 2 min on ice. For apoptosis determination the TUNEL assay (Roche) was performed according to manufacturer specifications. Cells were fixed in 4% (wt/vol) paraformaldehyde in PBS for 10 min at 4 1C. DNA was stained with DAPI and cells were mounted in Fluoromount (Scientific Services). Pictures were collected randomly. Each experiment was performed three times. More than 2,000 cells were analyzed per assay.

3.2.5 Statistical analysis

All error bars represent s.d. The significance of pairwise comparisons was determined by Student's t-test. Correction for multiple testing was done according by the Bonferroni method.

3.2.6 Software

1) Bio Edit
2) DNA Star software package
3) 7500 System SDS Software of Applied Biosystems

3.2.7 Internet sites

In this study numerous programmes have been used. Pubmed and OMIM were the main sources in order to obtain the already published information about the phenotype and the protein of interest.

1) Gene Information: http://www.ncbi.nlm.nih.gov/sites/entrez?db=gene
http://www.ensembl.org/index.html
2) Primer Design: http://frodo.wi.mit.edu/
3) Exon Primer: http://ihg.gsf.de/ihg/ExonPrimer.html
4) Protein information: http://www.expasy.org/,
http://www.rcsb.org

4 Results

4.1 Mapping and sequence analysis

Two of the autosomal recessive cutis laxa phenotypes have been the subject of research of our scientific team, autosomal recessive cutis laxa type II (ARCLII) or wrinkly skin syndrome (WSS) and gerodermia osteodysplastica (GO). Mutations in *ATP6V0A2* gene, encoding for the a2 subunit of the V-ATPases, were found by our group to cause ARCLII (79), whereas mutations in *GORAB* gene were recently associated with the gerodermia osteodysplastica phenotype (87). We were able to identify several families as well as sporadic cases, who bore mutations in neither *ATP6V0A2* nor in *GORAB* gene. Type I autosomal recessive cutis laxa was clinically excluded due to lack of inner organ involvement.

The main characteristic of autosomal recessive diseases is that they tend to segregate among consanguineous families, because of the increased rate of genetic similarity between members of the same family. As homozygous mutations are typically the cause of autosomal recessive disorders, our first goal was to detect the homozygous regions along the genome in the affected families. For that reason we conducted homozygosity mapping using the Affymetrix GeneChip® Human Mapping 250K Arrays (s. 3.2.1.5) in ten consanguineous families from our cohort. The analysis revealed an overlapping homozygous candidate region, common for the five of our families, with the highest LOD score on chromosome 17q25 (fig.4.1).

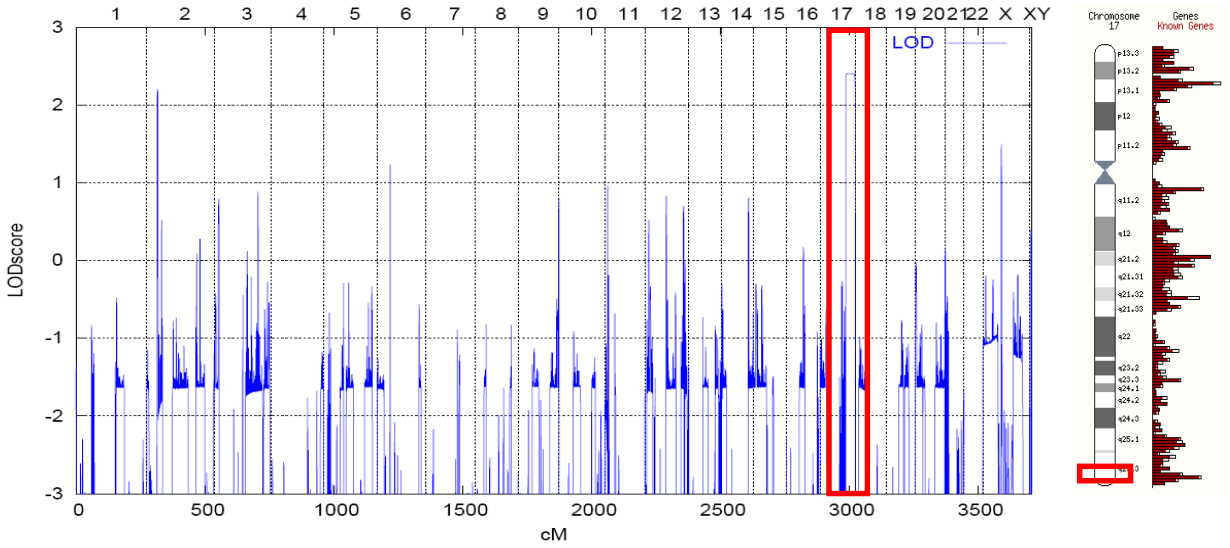

Fig. 4.1 Homozygosity mapping in ten consanguineous families of the cutis laxa cohort gave rise to a single region with the highest LOD score on chr.17q25, as indicated by the red box.

In order to define with more accuracy the borders of the homozygous region and at the same time to indicate the genes fully included we performed further analysis. We used flanking markers for the 3' strand and 5' strand ends of our original region and two more lying in the middle in order to confirm the homozygocity of the region found. We were able to determine the actual borders and to slightly shorten the found loci. Fine mapping of our primary region confirmed the chip results, which gave rise to the minimal interval of 2.8 Mb between markers rs8065431 and rs1046896 (fig 4.2).

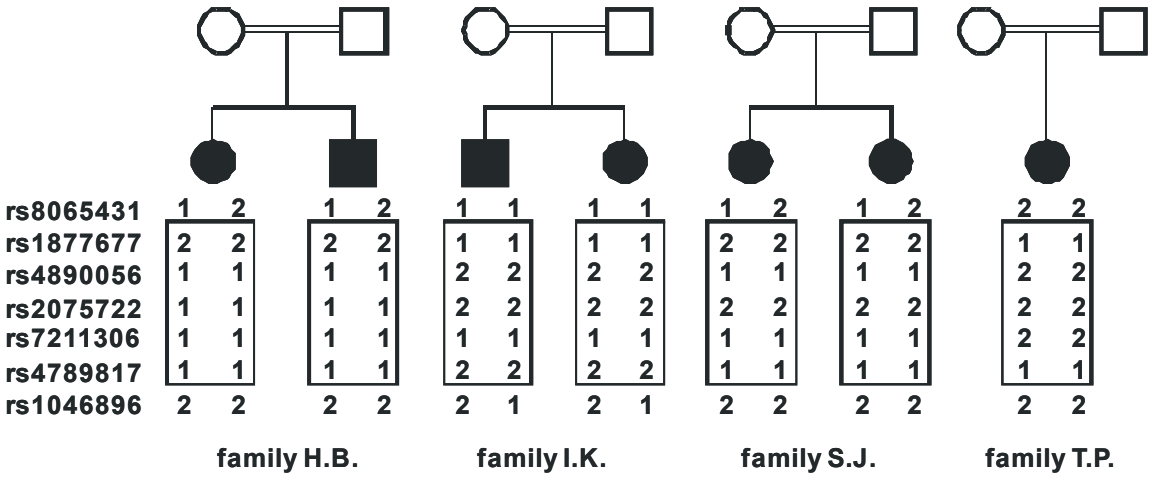

Fig 4.2 Fine mapping in 5 consanguineous families with cutis laxa defined the loci on chromosome 17 between the rs8065431 and rs1046896 markers.

Our newly identified homozygous region included 59 genes in total. Among these genes 8 were already known to be causative for different disorders or partially associated with a phenotype, 4 were pseudogenes and 4 were described as not being expressed in human skin fibroblasts (ncbi-Unigene-EST data).

Furthermore, we took into account the fact that two of the overlapping cutis laxa phenotypes, ARCLII and GO, were caused by mutations in genes involved in processes associated with the Golgi apparatus. Genes, encoding proteins involved in glycosylation would also be interesting candidates as the highly similar phenotype of ARCLII is combined with a clear glycosylation defect of type II (CDGII)(79). Thus, we ranked the remaining 43 genes according to their function, sub-cellular localisation and their expression levels in different tissues.

In order to identify the gene, mutations in which would be causative for the observed phenotype in our cohort, we performed sequence analysis (s.3.2.1.6) at first in the samples of our homozygous families according to this hierarchy. Sequencing analysis of 16 genes yielded mutations in the gene encoding the enzyme D1-pyrroline-5-carboxylate reductase 1 (*PYCR1*) (Location

Chromosome 17: 79,890,269-79,895,172) in the affected members of all five families. We sequenced the rest of the families in our cohort as well as the sporadic cases and we identified, in total, eight missense mutations, one frameshift mutation, five splice-site mutations and one 22-bp deletion encompassing the exon-intron boundary of exon 5 (Table 4.1and fig 4.3). No nonsense mutations were found in any of our patients.

Table 4.1. Results of sequencing analysis in 22 families.

Family	Origin	Number of affected	Status	Position in cDNA	Protein	Aff. Exon
J.I.	Iraq	1	Hom	138+1G>A	ND	2
T.P.	Palestine	1	Hom	616G>T	G206W	5
S.P.	Palestine	3	Hom	617_633+6del	ND	5
I.K.	Kuwait	2	Hom	797G>A	R266Q+ splicing	6
F.S.	Kuwait	1	Hom	797G>A	R266Q+ splicing	6
S.I.	Jordan	4	Hom	797+2_797+5del	K215_D319del	6
D.I.	Italy	1	Het Het	11delG 355C>G	G4fsX50 R119G	1 4
S.O.	Oman	1	Het Het	356G>A 566C>T	R119H A189V	4 5
G.O.	Oman	3	Hom	356G>A	R119H	4
H.B.	Bahrain	2	Hom	535G>A	A179T	4
M.A.	Austria	1	Hom	540+1G>A	ND	4
M.Q.	Qatar	1	Hom	616G>A	G206R	5
H.U.	U.S.A	1	Hom	633+1G>C	ND	5
N.A.	Australia	1	Het Het	633+1G>C 797+1G>T	ND ND	5 6
A.S.	Syria	1	Hom	797+2_797+5del	K215_D319del	6
D.T.	Turkey	1	Hom	355C>G	R119G	4
M.F.	Italy	1	Het Het	355C>G 356G>A	R119G R119H	4 4
S.T.	Turkey	2	Hom	540+1G>A	ND	4
E.U.	U.S.A.	1	Hom	752G>A	R251H	
J.A.	Australia	3	Hom	769G>A	A257T	6
K.T.	Turkey	1	Hom	797G>A	R266Q+ splicing	6
I.T.	Turkey	1	Hom	797+2_797+5del	K215_D319del	6

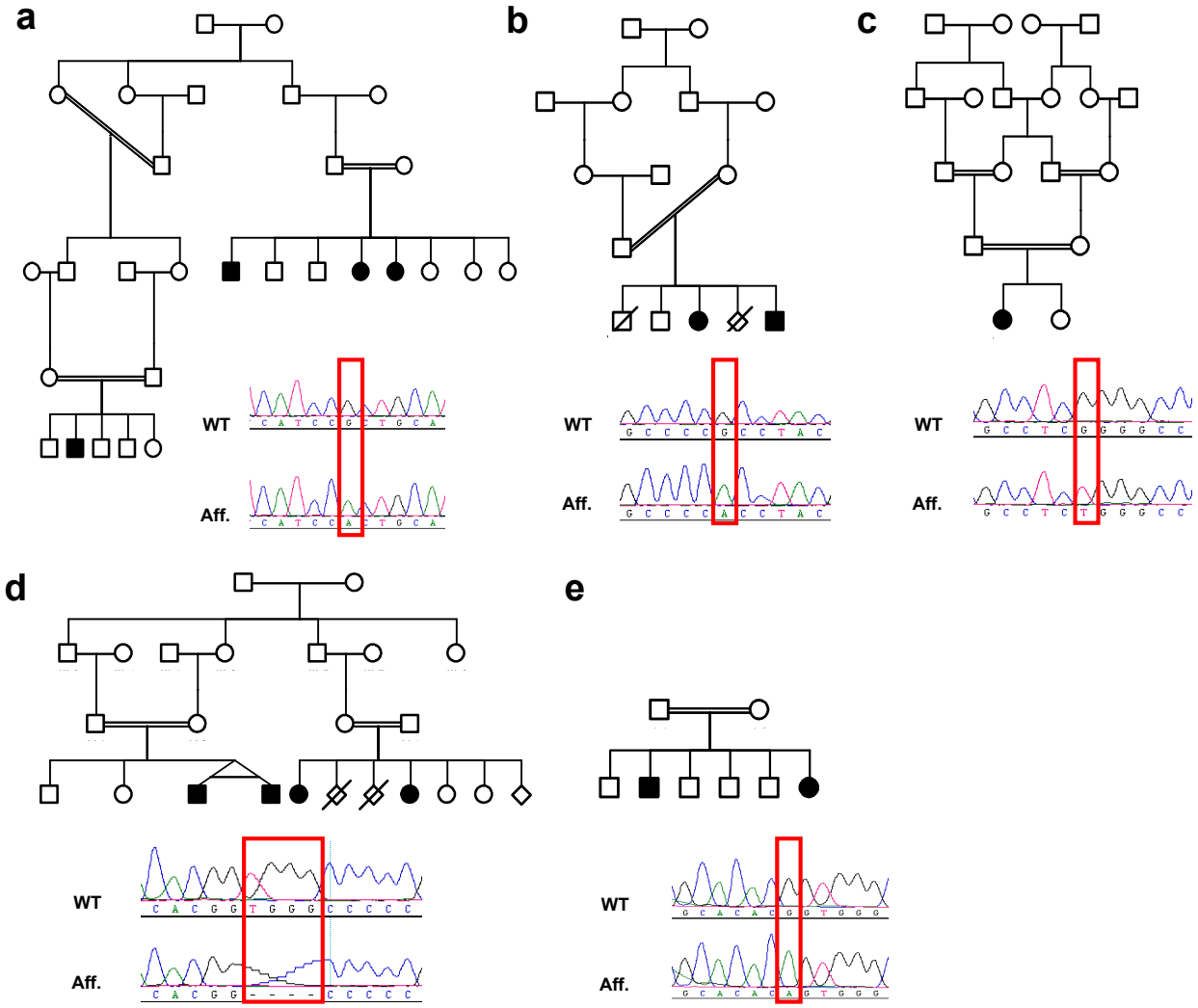

Fig. 4.3 Complete pedigrees and mutations identified in the affected members.(a)family G.O., g.2787G>A, (b) family H.B., g.2966G>A, (c)Family T.P., g.3227G>T, (d) family S.J., g.3573-3576del, (e) family I.K., g.3571G>A

As shown in table 4.1, six of these mutations were recurrent, although the affected individuals did not share a common ethnic background. Among the patients 4 were found to be compound heterozygotes for mutations in *PYCR1*gene. The mutations show a clustering pattern between exons 4 and 6 with only two exceptions in exons 1 and 2. No mutations were found in exons 3 and 7 of the *PYCR1* gene in the examined samples (fig 4.4).

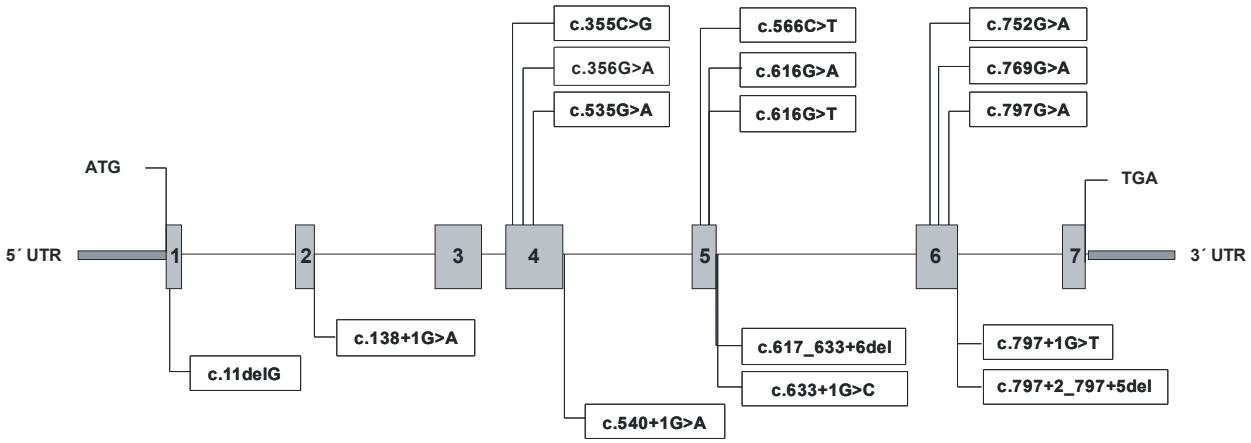

Fig. 4.4 Mutational distribution in *PYCR1* gene: The identified mutations are spread between exons 4-6 with only two exceptions.

We then investigated whether the mutations found could affect the structure and the function of the protein first by comparing the degree of conservation of each affected amino acid in the protein sequence through evolution, as highly conserved amino acids are usually essential for the maintenance of the physiological properties of proteins.

The PYCR1 protein is generally highly conserved through evolution, showing strong similarities from human down to E.coli. We aligned the protein sequences of PYCR1 of eight species and found that among the eight missense mutations identified so far, three are found to affect amino acids conserved in all eight species and five affect amino acids that are higher than 80% conserved (fig.4.4,4.5).

For the same reason we looked into the crystal structure of PYCR1 protein, which was described by Meng *et al.* (2006) (89). The sites consisting of amino acids affected by mutations appear to have an important predicted role. All missense mutations found in our patients affect residues which have been shown to take part in forming the binding site of the protein and more specifically the “charged pocket”, which stabilizes the binding of NADH with hydrogen bonds (89).

Pyrroline-5-carboxylate reductase (P5CR) is a universal housekeeping enzyme that catalyzes the reduction of Δ1-pyrroline-5-carboxylate (P5C) to proline using NAD(P)H as the cofactor. We conclude that the mutations identified in our patients are causative for the observed phenotype, if we take into account that NADH cannot bind as a cofactor and consequently the enzyme cannot perform its catalytic function.

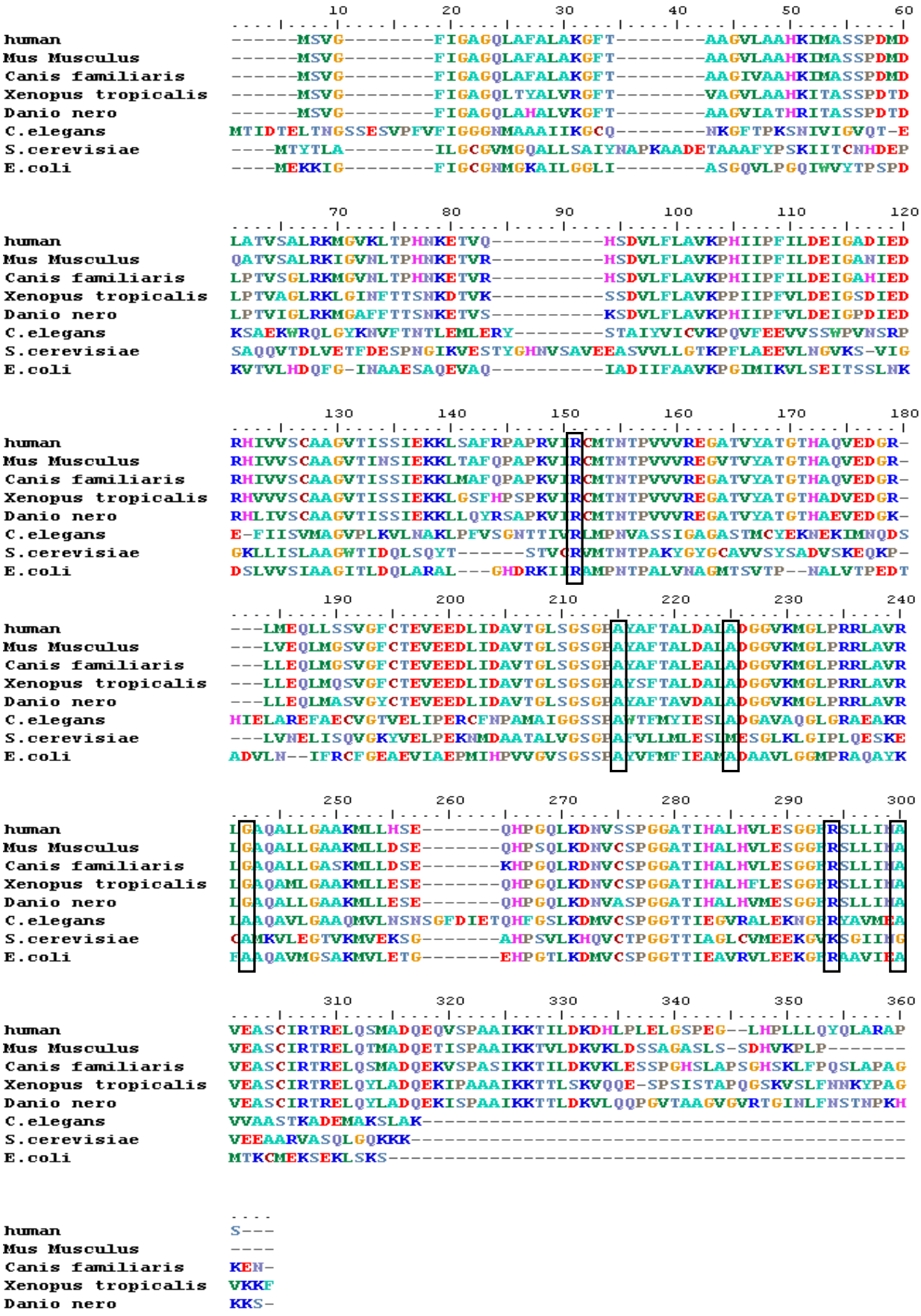

Fig 4.5 Alignment of the PYCR1 protein sequence from eight species. The identified mutations are indicated with the black margins (Bio Editor).

4.2 Phenotypic analysis

We showed that mutations in PYCR1 gene result in a phenotype reminiscent of those already known to belong in the ARCL-spectrum. The molecular elucidation of a great part of our complete cutis laxa cohort has enabled us to identify the features which characterise each genetic disorder. All ARCL patients show wrinkled inelastic skin most evident on the dorsum of the hands and feet, joint laxity and general connective tissue abnormalities. The patients bearing mutations in *PYCR1* gene, apart from exhibiting the common features of cutis laxa, appear to have a more distinct facial dysmorphism. This involves a triangular face with sagging cheeks and malar hypoplasia combined with big protruding ears and prognathism in most of the cases (fig 4.6), which give those affected a progeroid appearance.

Fig 4.6 Facial characteristics of the patients with PYCR1 mutations. (a-c) Affected girl from family T.P. (90), initially diagnosed with WSS, in the neonatal period, at the age of 2 and 6 years, (d) affected boy from family F.S. (91) (e) affected boy from family I.K., both were reported as GO/WSS cases (91), (f-g) two affected siblings from family G.O.(80), (h-j) two affected sisters and one of the affected twins from family S.J. (k) patient E.U. in the neonatal period, initially diagnosed as DBS, (l) patient H.U. at the age of 7 years (92), (m) affected 18-month-old girl from family D.I. clinically categorized as having GO, (n) affected sibling from family S.P., diagnosed as GO/WSS (93),(o) affected sibling from family J.A., reported as DBS (84).

The skeletal phenotype in these patients reveals osteopenia of varying degrees but not as severe as in GO. This effect could be secondary to the hypotonia also seen in almost all individuals. Contractures of the finger phalanges were described and dental anomalies were also present in some of the cases (fig 4.6, 4.7). Among the phenotypes of the cutis laxa spectrum with a known molecular defect, the patients with mutations in *PYCR1* show the highest rate of mental retardation. Among the 22 families and in total 34 affected members only one showed no signs of cognitive involvement. In four patients mental retardation was combined with neurological signs of athetosis. MRI (magnetic resonance imaging) scans were available for 13 of our patients. Abnormalities of corpus callosum were obvious in eight of the examined probands (fig 4.7). The affected girl of family T.P. was the only patient showing conductive hearing loss. Interestingly, eye abnormalities, in terms of early-onset cataract, was seen in three of our patients (Tables 4.2,4.3).

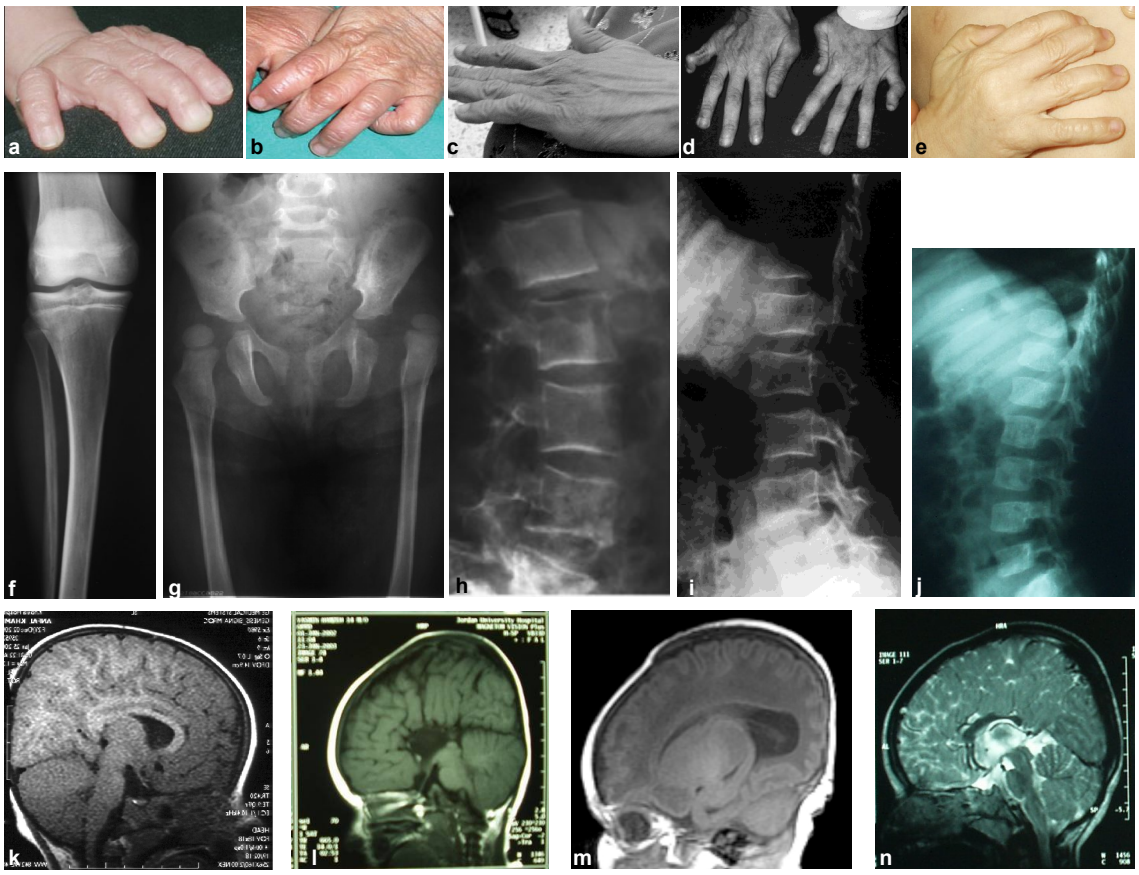

Fig.4.7. Clinical features. (a-e)Wrinkly skin of the dorsum of the hands, (a,) index family T.P, (b) index family I.K., (c) index family G.O. (80), (d) index family S.P. (93), (e) index family S.J. (f-j) X-Ray pictures, (f,h) family G.O.(80), pronounced osteopenia of the vertebrae and the long bones (80), (g) osteoporotic femoral necks in patient from family S.P. (93), (j) osteopenia of the vertebrae in index patient from family S.J., (k-n) brain-MRT, normal presentation of corpus callosum in patient S.O.(k), abnormal (agenesis) corpus callosum in patients T.P (l), E.U. (m) and S.J. (n).

Important feature of cutis laxa are the ultrastructural alterations found in the dermis of affected individuals. Skin biopsy was available for the patient from family D.I. (fig 4.8). Weigert staining revealed the recurrent finding, common in all ARCL forms, of reduced and fragmented elastic fibres whereas the collagen structure remains intact. Electron microscopy confirms the result, showing reduced number and size of the elastic fibres affecting both its fibrillar and amorphous components in the patient D.I., when compared with controls. The same alterations were seen in three more patients that were formerly diagnosed as GO and WSS or DBS in previous publications (93,94).

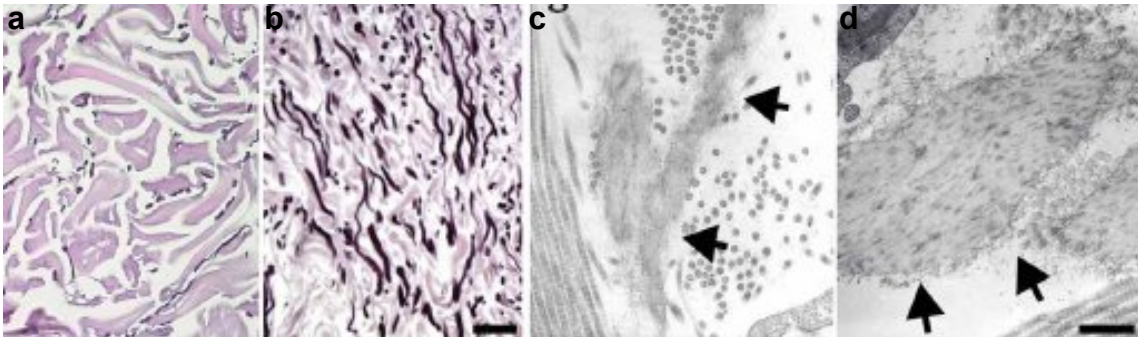

Fig 4.8 Skin biopsy from affected individual from family D.I..(a,b) Weigert staining reveals sparse, thinned and fragmented elastic fibres in the reticular dermis compared to control (b); scale bar, 100 mm. (c,d) Ultrastructural analyses corroborate the markedly reduced elastic fibre (arrows) size with a reduction in both the fibrillar and amorphous components in an affected individual from family D.I. compared to control (d); scale bar, 500 nm.

Table 4.2 Summary of the clinical features in our patients with PYCR1 mutations

Fam.	Initial Diagnosis	Origin	IUGR	Lax, wrinkly skin	Hip Dis-location	Hernias	Osteo-penia	Abnormal Corpus callosum	MR	Athe-tosis	Cata-ract
J.I.	WSS	Iraq	+	++	+	-	+	-	-	-	-
T.P.	WSS	Palestine	+	+	-	-	ND	+	+	+	-
S.P.	GO/WSS	Palestine	+	++	+	-	+	+/-	+/-	-	-
I.K.	GO/WSS	Kuwait	+	++	++	++	++	-	+	-	+
F.S.	GO/WSS	Kuwait	+	+	++	++	++	-	+	-	-
S.I.	WSS	Jordan	+	++	-	+	ND	+	+	-	-
D.I.	GO	Italy	+	++	-	++	++	ND	+	-	-
S.O.	GO	Oman	-	++	+	-	+	-	+	-	-
G.O.	GO	Oman	ND	++	-	-	+	ND	+	-	-
H.B.	GO	Bahrain	+	++	++	+	-	ND	+	-	-
M.A.	GO	Austria	+	+	++	+	++	ND	+	-	-
M.Q.	GO	Qatar	ND	++	++	+	++	ND	+	-	-

H.U.	GO	U.S.A	+	+	-	-	-	+	+	-	-
N.A.	GO	Australia	+	++	+	+	ND	ND	+	-	-
A.S.	GO	Syria	+	+	-	+	+	+	+	-	-
D.T.	DBS	Turkey	+	++	+	-	ND	ND	+/-	-	-
M.F.	DBS	Italy	+	++	ND	++	ND	ND	+	+	-
S.T.	DBS	Turkey	+	+	+	-	ND	+	+	+	-
E.U.	DBS	U.S.A.	+	++	+	++	ND	+	+	-	+
J.A.	DBS	Australia	+	++	-	-	ND	ND	++	+	+
K.T.	DBS	Turkey	-	+	+	-	ND	+	+	-	-
I.T.	DBS	Turkey	+	+	+	-	ND	-	+	-	-

Table 4.3 Recurrence rates of CL features in ARCL with progeroid features.

Feature	ARCL with progeroid features
Lax skin	34/34
Triangular facies with big Prodruding ears	34/34
Mental retardation	33/34
Osteopenia	15/18 (BMD not available for all patients)
IUGR	28/30
Hip dislocation	21/33
Hernias	17/34
Emphysema	1/34
CDG II	0/34
Abnormalities of CC	8/13 (MRI not available for all patients)
Athetosis	7/34
Cataract	3/34

4.3 Expression analysis

The most prominent and stable feature of our patients is the wrinkled, lax skin. Skin was therefore considered to be the mostly affected tissue. The investigation of the remaining protein levels in skin would be an important evidence of the effect the mutations found in *PYCR1* have on the protein. In order to examine the expression status of the PYCR1 protein, we isolated fibroblasts obtained from skin biopsies taken from patients and healthy controls.

4.3.1 Q-PCR analysis (quantitative-polymerase chain reaction)

We determined the gene expression levels means q-PCR in order to examine whether the transcription of the gene is also affected. The determination of the expression levels was the result of a relative quantification, relative to one endogenous control and one calibrator (s.3.2.1.3,3.2.1.8). The q-PCR analysis showed that the remaining mRNA levels were most strikingly reduced, 50% and 80% respectively, in subjects S.J. and D.I. most probably due to nonsense-mediated decay, whereas in the missense-bearing subject (T.P.) there was no difference compared to the controls (fig.4.9). There are two paralogues of PYCR1 in humans, the highly similar PYCR2 and the more distantly related PYCRL. In the pathway of proline synthesis, P5CS (Δ1-pyrroline-5-carboxylate synthase) catalyzes the reduction of glutamate to delta1-pyrroline-5-carboxylate, a critical step in the de novo biosynthesis of proline, ornithine and arginine (95). We conducted expression analysis of PYCR1, its paralogues and the upstream enzyme, P5CS in samples from control and affected fibroblasts in order to find out whether their expression is up- or down-regulated through the abnormalities of PYCR1 (fig.4.9). We showed that the expression does not show any variation between the tested probands, which indicated a normal expression of these genes in patients with the cutis laxa phenotype. The defect of PYCR1 is not being compensated through its homologues or through P5CS which is involved in the same pathway.

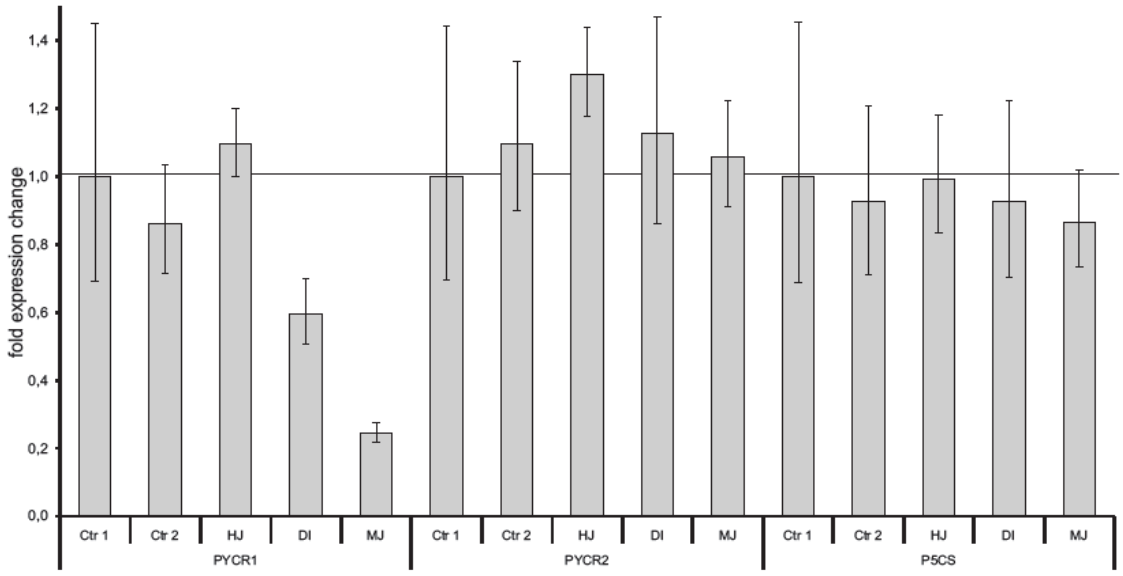

Fig 4.9 Gene expression changes in fibroblasts from individuals with PYCR1 mutations and controls. PYCR1 shows reduced expression levels in DI and MJ (= S.J.), but not in individual HJ (= T.P.). Expression of PYCR2 and P5CS is not affected.

4.3.2 Western blot analysis

For the analysis we used the protein-lysate from a control cell line and from four index patients bearing different mutations. The gel was transferred onto a nitrocellulose membrane and incubated with antibodies against PYCR1. Actin was used as loading control (s. 3.2.2.1 and 3.2.3).
The signal obtained through the development of the respective films was different in each sample, being almost absent or weaker in the patient samples compared with the control. The actin expression was consistent in all examined samples indicating that the analysis was successfully performed. The western blot showed a strong reduction of the protein levels in subject S.J., bearing a homozygous splice site mutation, and in a compound heterozygous subject (D.I.) with a missense and a frameshift mutation. The protein levels were mildly reduced in the patients bearing the missense mutations G206W (T.P.) and R251H (E.U.) (fig.4.10a).

4.3.3 Immunofluorescence

The changes observed in western blot analysis between control and affected fibroblasts were the first evidence indicating differences in the expression of PYCR1 protein. We then sought to test whether these findings are reproducible through alternative methods. We performed immunofluorescence studies in fibroblasts from our patients and controls. The cells were prepared as described (s.3.2.4.1), specific primary antibody against PYCR1 was incubated overnight and the protein was visualized using secondary antibodies. We used the same exposure times for collecting the images to render them comparable. We were again able to identify differences between controls and affected fibroblasts. The level of PYCR1 protein is slightly reduced in subjects T.P. and E.U., whereas in S.J. and D.I. it is almost undetectable (fig.4.9b). The immunostaining experiments performed in control and patient fibroblasts confirmed the western blot results.

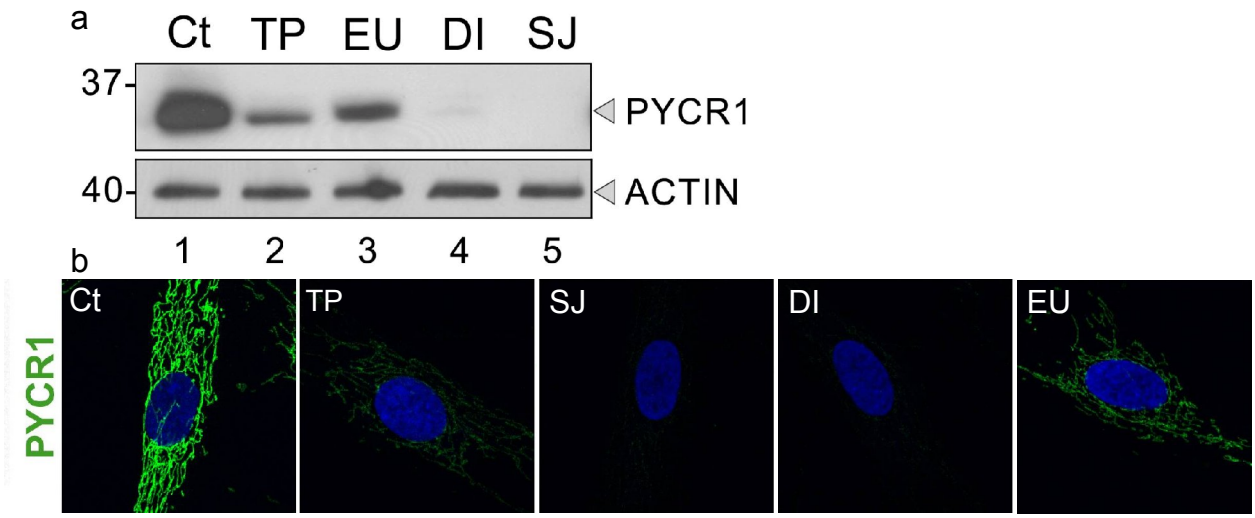

Fig. 4.10 Expression levels of PYCR1 protein in patients and healthy controls. a) Western blot, showing reduced expression in mutated fibroblasts, b) immunostainings of skin fibroblasts from the same individuals and controls confirm the results of the immunoblotting, showing reduced remaining protein in fibroblasts bearing mutations in *PYCR1*. PYCR1 is indicated by the green signal.

4.3.4 Expression analysis in mouse tissues

According to the EST data, human PYCR1 protein is described to show high expression levels in different tissues such as muscle, cervix bone, skin and eye (UniGene: www.ncbi.nlm.nih.gov). An interesting point was to examine whether this expression pattern would be reproducible in tissues from other species and we decided to test the expression of PYCR1 in mouse tissues. For that we used 4-day-old control mice, from which we prepared eight tissues along with osteoblasts and osteoclasts. RNA and whole protein lysates were extracted as described before (s.3.2.1.8).

Furthermore, as mentioned, two paralogs of PYCR1 exist in humans, PYCR2 and PYCRL. We conducted expression analysis of PYCR1, its paralogues and the upstream enzyme, P5CS, in different tissues from 4-day-old mice normalized to expression levels in the heart determined by quantitative PCR. We observed extremely high Pycr1 expression levels in osteoblasts and in skin. Pycr2 and Pycrl also show the highest expression levels in osteoblasts, but otherwise show uniform expression, as does P5cs (fig. 4.11a). The high expression levels of Pycr1 protein were confirmed by Western blot analysis, performed on the same tissues, with exception of osteoblasts and osteoclasts (fig. 4.11b). Interestingly, in the western blot, high expression is also apparent in the eye. Our experiments have shown that Pycr1 is expressed in tissues that are mostly affected in our phenotype.

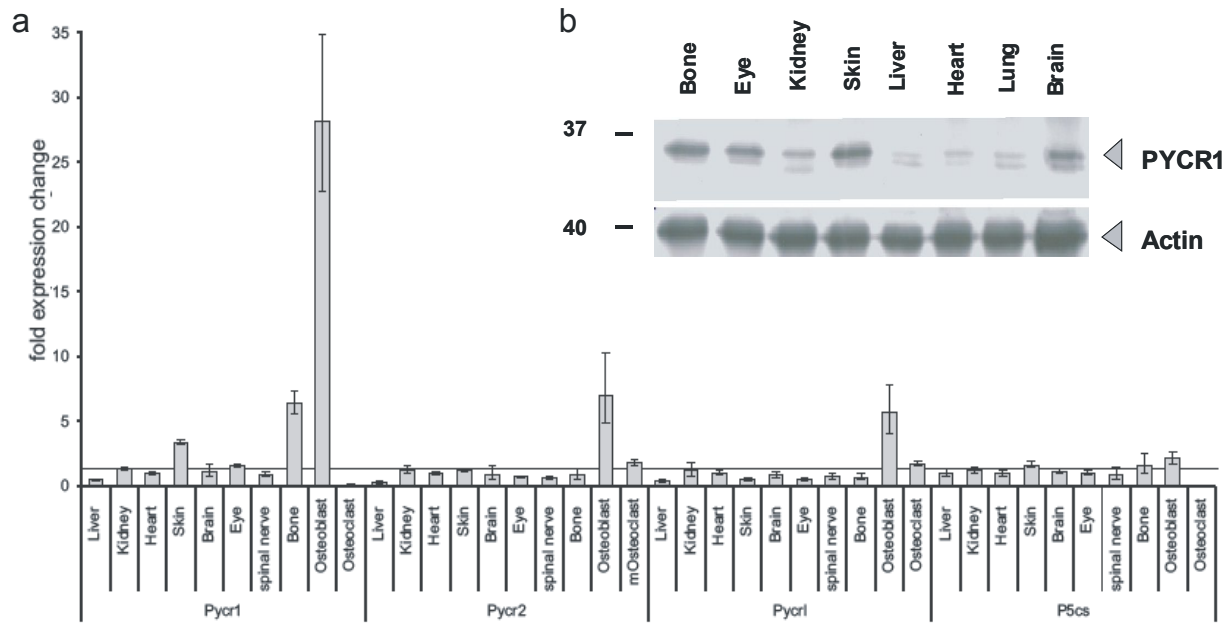

Fig 4.11 Expression analysis in mouse tissues. (a) Expression of PYCR1 homolog genes and P5cs, which is involved in the proline metabolic pathway determined by quantitative PCR. Note the high expression in osteoblasts in all four genes. Pycr1 is also highly expressed in skin and bone (b) expression of Pycr1 protein by immunoblotting reveals the same pattern, confirming the results of Q-PCR. Actin was used as loading control.

4.4 Biochemical analysis - proline metabolism

L-proline concentration is primarily related to the balance of enzymatic activities of proline dehydrogenase [proline oxidase (POX)] and D-1-pyrroline-5-carboxylate (P5C) reductase (96). Pyrroline-5-carboxylate reductase (P5CR) is a universal housekeeping enzyme that catalyzes the reduction of Δ1-pyrroline-5-carboxylate (P5C) to proline using NAD(P)H. As a result, P5C plays a pivotal role in maintaining the concentration of proline in body fluids. The enzymatic cycle between P5C and proline is very important for the regulation of amino acid metabolism (89). Inborn errors of P5C metabolism lead to disturbance of proline metabolism (96).

4.4.1 Proline level measurements

Since the underlying genetic defect in our patients was affecting a main enzyme of the proline synthesis pathway, we assumed that the production of proline could also be affected. In order to confirm this assumption we examined whether our patients showed hypoprolinemia, which in that case could serve as a useful diagnostic marker. We measured the proline levels in the serum of 13 patients in comparison with healthy controls and also compared them with the levels of an-

other amino acid, ornithine. The measurements showed no significant differences between controls and patients in proline and ornithine levels (fig. 4.12a). We then performed the measurements in fibroblast lysates from 4 patients and 4 control cell lines in order to exclude an intracellular reduction of proline. We were not able to detect any significant differences in the proline levels of our subjects compared to the healthy controls (fig. 4.12b). This finding suggests that the intracellular production of proline is not affected, although one of the main pathway enzymes, the one catalyzing the final step in proline metabolism, is mutated. That could lead to the hypothesis that this enzyme has further alternative functions, which are affected when the responsible gene is mutated.

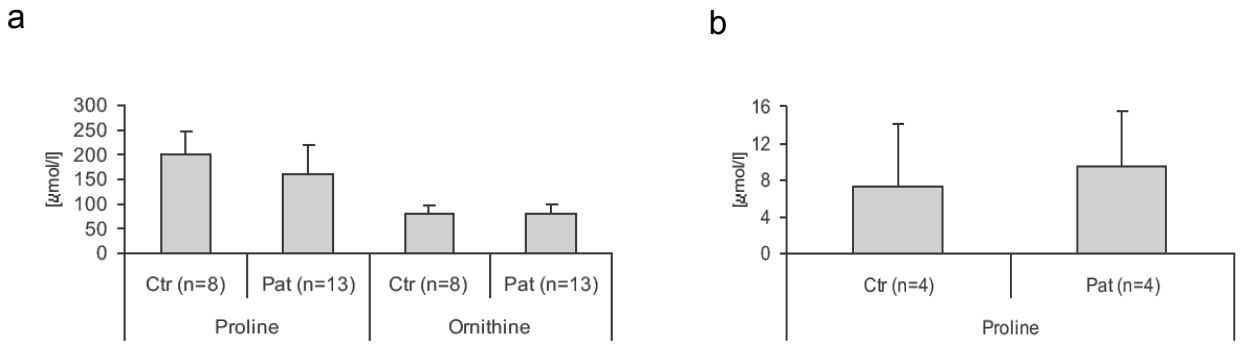

Fig 4.12 Proline levels in serum and in skin fibroblast from affected individuals and controls:(a)Proline and ornithine levels in individuals with PYCR1 mutations (Pat) compared to controls (Ctr). Note non-significant (p=0,051) reduction of proline concentrations in affected individuals. (b) Proline levels in fibroblast lysates from controls and from individuals with PYCR1 mutation. No significant differences were detectable.

4.4.2 Proline and cell metabolism

Proline can be derived from dietary proteins and from the degradation of endogenous proteins (97). Proline can be biosynthesized from glutamate and ornithine (95), making it nutritionally nonessential. We showed that its levels in serum and in fibroblasts are not influenced by the fact that the enzyme PYCR1, which catalyzes the final step of its *de novo* production, is affected. Proline is implicated in different cellular processes, but it is mainly important as an essential structural component of proteins.

We wanted to examine whether the complete absence of exogenous proline would have any affect on the cell metabolism. In that way we wanted to verify that no proline auxotrophy occurs. A simple marker for the cell autonomy is its ability to proliferate. Control and affected fibroblasts were cultured in medium with different concentrations of proline in order to investigate the proliferation rates of affected fibroblasts in comparison to controls. We extracted proline from the normal medium using fetal chicken serum which was first dialysed overnight. The cells

were cultured in medium with 0 mM, 0,2 mM (normally included in the serum) and in medium supplemented with 5 mM proline. The cells were incubated for 8 hours in medium containing 10µM Bromdesoxyuridin (BrdU). They were then fixed after 24, 48 and 72 hours and then incubated in HCL. They were then permeabilized and specific antibody against BrdU was incubated for 1 hour in RT. For visualization an anti-mouse conjugate was applied. DNA was stained with DAPI (s.3.2.4.4). In total we examined on average 200 cells from each cell line, three control and three affected, at each time point. The experiment was performed twice in order to achieve statistical significance. We were not able to identify significant differences, whereas mutant cells showed slightly higher proliferation (fig. 4.13). Furthermore, there were no differences in the proliferative behaviour among the patient fibroblasts with different types of mutations (Pat = 3, S.J., D.I. and E.U). This observation suggests that the absence of exogenous proline in fibroblasts from patients with mutations in PYCR1 is not capable of affecting the cell metabolism. It could then be assumed that the catalytic function of our protein is compensated through alternative mechanisms or enzymes, which take over when the levels of PYCR1 protein drop below a critical point.

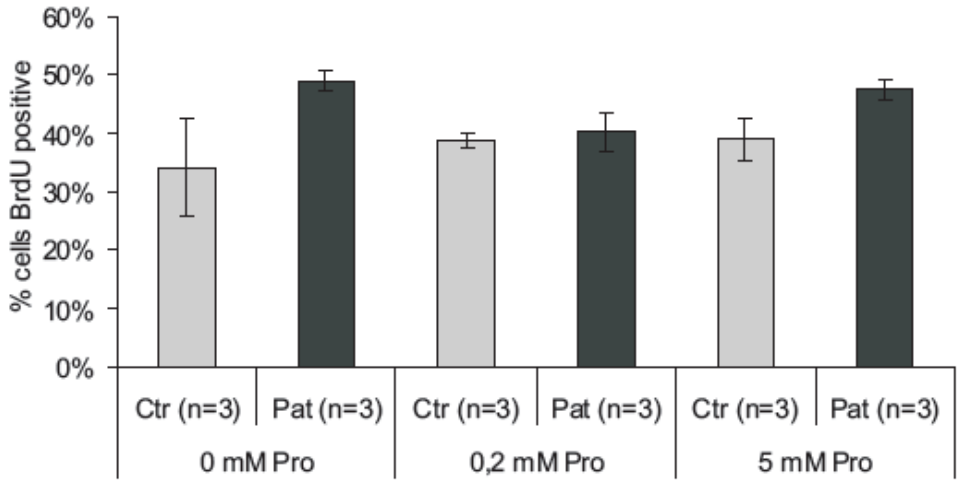

Fig. 4.13 Proliferation rates of fibroblasts from individuals with PYCR1 mutations (Pat) and controls (Ctr) grown in medium with different proline concentrations. No significant differences in the proliferation rates are observed. Errors are given as s.d..

4.5 Localization and morphological studies

After identifying the underlying genetic defect in our cutis laxa patients, we also wanted to define some of the properties of the encoded protein. At first we wanted to investigate its sub cellu-

lar localization because the existing descriptions demand further analysis as they are unclear and incomplete. The precise characterisation of this feature could eventually give us the first hint about its functional role, as each compartment is associated with specific cellular procedures.

4.5.1 Cellular localization of PYCR1 protein

4.5.1.1 PYCR1 and cellular marker proteins

PYCR1 was, until now, believed to be a cytosolic protein (96,97). On the other hand almost all other enzymes taking part in proline metabolism are known to reside in the mitochondrial inner membrane or matrix except for prolidase, which is also found in the cytoplasm (96). As there were no clear data indicating a specific localization of the protein, we looked into the cellular localization of the protein in order to verify or refute the existing knowledge. For that reason we examined proteins known to reside in certain cellular compartments and compared the results with PYCR1 stainings. Again, control cells were seeded on glass coverslips and cultivated until 50% of confluence. Specific primary antibody against the PYCR1 protein was co-incubated with antibodies against cellular-marker proteins overnight and the result was visualized using secondary antibodies. For this study we used antibodies against α-Adaptin, which is known to reside at the cytosolic side of the cell membrane, against a marker protein for Endoplasmatic-Reticulum-Golgi-intermediated compartment, ERGIC-53, and against TGN46, which is a representative protein for the trans-golgi network. DNA was stained with DAPI diluted in PBS. Images were collected as described before (s.3.2.4.1). The fine structures of the cell membrane, the ER and the trans-golgi were clearly visualized, while PYCR1 protein was forming structures evenly spread through the cell, without showing any co-localization with the examined compartments. Moreover, a cytosolic residence of the PYCR1 protein was excluded, as its cellular distribution showed a distinct network (fig. 4.14).

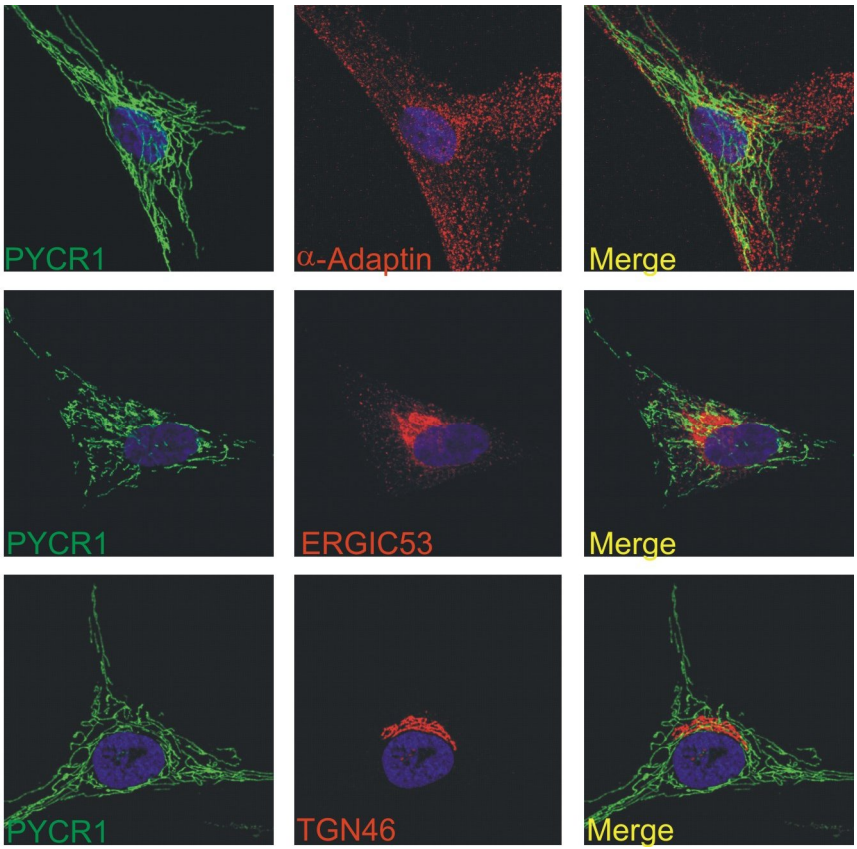

Fig 4.14 PYCR1 protein does not co-localize in control skin fibroblasts with cellular markers localizing in cell membrane (α-Adaptin), in the ER-Golgi intermediate compartment, ERGIC (ERGIC-53) or the trans-Golgi network (TGN46). PYCR1 is indicated by the green signal, whereas the different markers by the red signal.

4.5.1.2 PYCR1 and mitochondria

PYCR1 formed a very specific linear network structure distributed throughout the cell. The only cellular organelle known to form similar structures are the mitochondria. Mitochondria are usually depicted as stiff, elongated cylinders with a diameter of 0.5–1 μm, resembling bacteria (98). Each mitochondrion is bounded by two highly specialized membranes, the inner and the outer membrane. Together they create two separate mitochondrial compartments: the internal matrix and a much narrower intermembrane space. The inner membrane is usually highly convoluted, forming a series of infoldings, known as cristae, that project into the matrix. As mentioned before, most of the other enzymes involved in the proline metabolism reside in mitochondria. In order to test whether the protein was actually localized to the mitochondria, we repeated the same experiments. Instead of other cellular markers, we used proteins that are known to be associated with mitochondria. For that reason we used antibodies against cytochrome C, found in the inner membrane of the mitochondrion as an essential component of the electron transport chain,

against mitofilin, which is a transmembrane protein of the inner mitochondrial membrane (99) and against D1-pyrroline- 5-carboxylate synthase (P5CS), which has also been described as a mitochondrial protein (94). The stainings were performed on healthy control fibroblasts, that were seeded on glass coverslips and cultivated until they reached 50% of confluence. The fixation and permeabilization took place as described before (s.3.2.4.1) and the cells were co-incubated with antibodies against PYCR1 and cytochrome C, mitofilin and P5CS respectively. The result was visualized using secondary antibodies and DNA was stained using DAPI. The mitochondrial stainings showed a clear network structure which co-localized with that of PYCR1 through merging the fluorescence-channels, indicating a mitochondrial residence of the PYCR1 protein (fig. 4.15a-c). In order to further confirm the result, we treated the control cells with a highly mitochondria-specific substrate, the MitoTracker Red CM-H2XRos (Invitrogen), which is a reduced, nonfluorescent substrate that fluoresces upon oxidation and whose signal is dependent upon membrane potential. After fixation and permeabilization these cells were incubated with the PYCR1 specific primary antibody. Once more, the two stainings appeared to overlap completely (fig. 4.15d), verifying the former observation that PYCR1 is localized on the mitochondrion.

After co-stainings in control fibroblast using specific antibodies against different cellular markers and against the studied protein, we were able to show that PYCR1 does not reside in the respective compartments, as it could not co-localize with any of the examined proteins. By contrast, we were able to show that PYCR1 protein co-localizes with different mitochondrial markers, among them D1-pyrroline- 5-carboxylate synthase (P5CS), which also belongs to the proline metabolic pathway (100) and mitotracker, which is highly specific for mitochondria. We therefore conclude that PYCR1 is a mitochondrial protein.

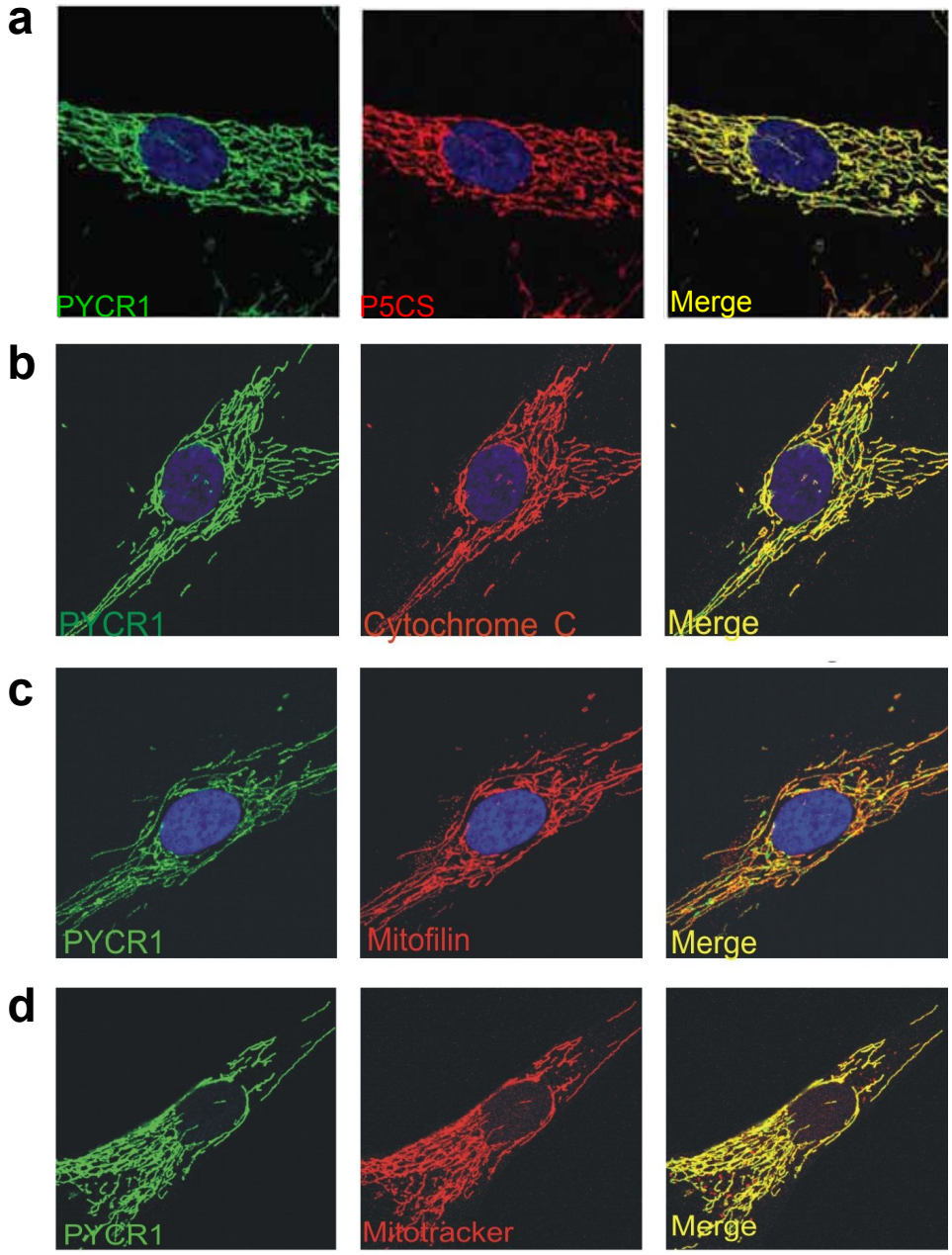

Fig 4.15 Immunofluorescence detection of PYCR1 in mitochondria from control skin fibroblasts (a)PYCR1 and P5CS, (b) PYCR1 and Cytochrome C, (c) PYCR1 and mitofilin co-localize (d) PYCR1 and mitotracker signal overlap, indicating a mitochondrial residence of PYCR1.PYCR1 is indicated by the green signal and the mitochondria specific marker proteins by the red.

4.5.2 Mitochondria structure in *PYCR1*-mutated fibroblasts

The designation of PYCR1 as a mitochondrial protein gave rise to the question whether the mitochondrial structure and subsequently their function is affected by the mutations found in the responsible gene. The mitochondrial cristae and the matrix play distinct functional roles, with the

matrix and inner membrane representing the major working compartments of mitochondria (101). The mitochondria in living cells are seen to be very dynamic—frequently dividing, fusing, and changing shape (101). Division (fission) and fusion of these organelles are topologically complex processes, because the organelles are enclosed by the double membrane and the integrity of the separate mitochondrial compartments must be maintained (98). In order to examine the maintenance of the mitochondrial structure, we performed immunofluorescence and electron microscopy studies.

4.5.2.1 Immunofluorescence study

After concluding that PYCR1 is a mitochondrial protein, we examined the mitochondrial network in our patient fibroblasts using immunofluorescence by repeating the stainings of the mitochondrial protein mitofillin and with mitotracker (s.3.2.4.2). The stainings were performed on healthy control fibroblasts and on affected ones as described before and the cells were incubated with primary antibody against PYCR1 and the inner mitochondrial membrane protein mitofilin. Fifty-percent-confluent fibroblasts were loaded with 100 nM Mito Tracker Red CM-H2XRos (Invitrogen). Control fibroblasts showed a normal tubular appearance. Both stainings appear altered in affected fibroblasts (fig.4.16a,b). The mitochondrial morphology is clearly disrupted and its typical network structure is only partially maintained.

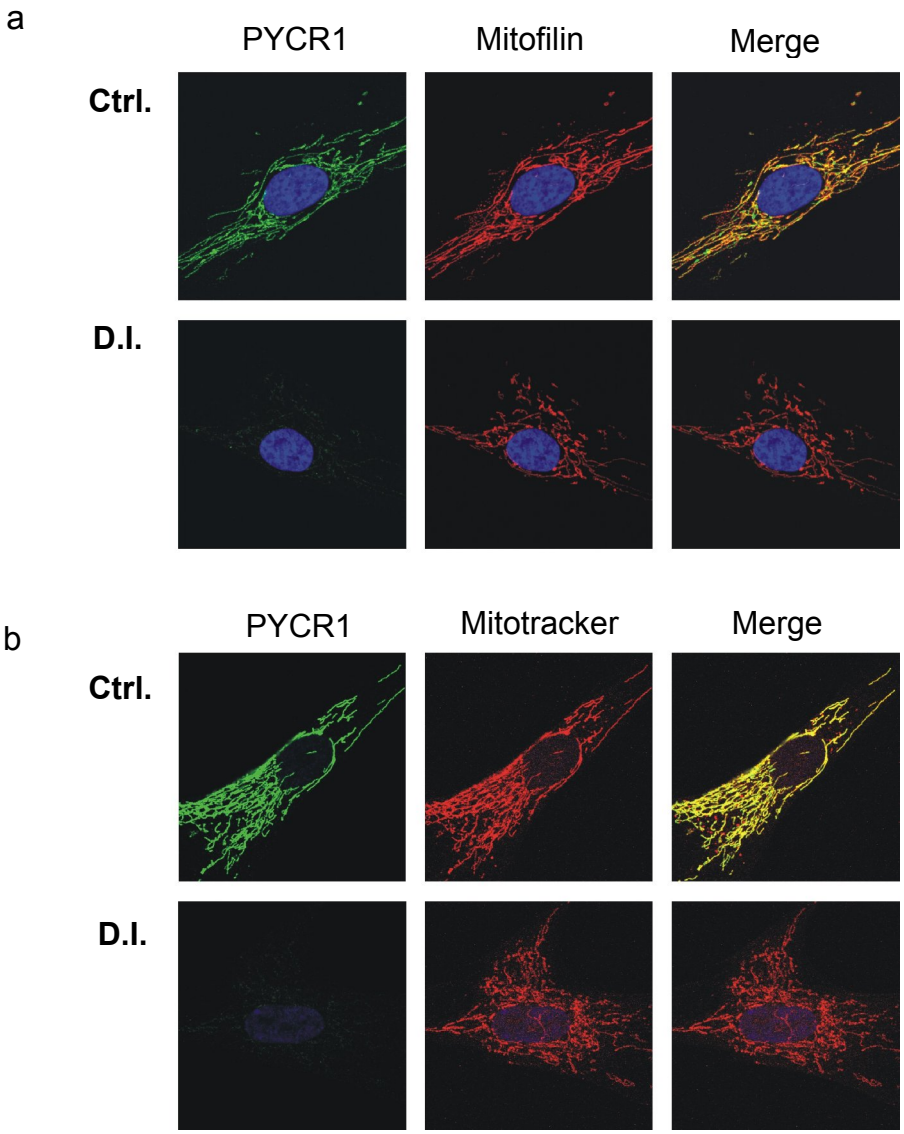

Fig 4.16 Alteration of mitochondrial morphology in immunofluorescence. Mitochondria from affected individual D.I. show an altered mitochondrial morphology (sparse, disrupted mitochondria) in comparison with control fibroblasts in a) mitofilin staining, and b) after incubation with mitotracker. PYCR1 is indicated by green signal and the mitochondrial markers by the red signal.

4.5.2.2 Electron microscopy studies

Mitochondria are among the largest organelles in the cell, each one being about the size of an E. coli bacterium. Most eukaryotic cells contain many mitochondria, which collectively can occupy as much as 25 % of the volume of the cytoplasm. They are large enough to be seen under a light microscope, but the details of their structure can be viewed only with the electron microscope (101). After observing alterations in the immunofluorescence we wanted to confirm that the fine

structure of the mitochondria is disrupted in fibroblasts bearing mutations in the *PYCR1* gene by performing an ultrastructural analysis means electron microscopy (s.3.2.4.3). We were able to show clear differences in the mitochondrial structure between the cell lines. In control fibroblasts, the mitochondrial cristae are regularly arranged, showing as expected, a homogenous structure of the inner membrane (fig 4.17a). By contrast, in patient fibroblasts the cristae appear to be altered lacking the lineal structure that was seen in control mitochondria. The inner mitochondrial membrane appears to form non canonical, disorientated and interrupted folds in the mitochondria. Furthermore, the mitochondria of the patient fibroblasts showed a smaller diameter in comparison with the normal control mitochondria (fig. 4.17b). This finding can indicate a role of PYCR1 protein in the maintenance of the mitochondrial fine structure, as this structure appears to be affected in the absence of the protein.

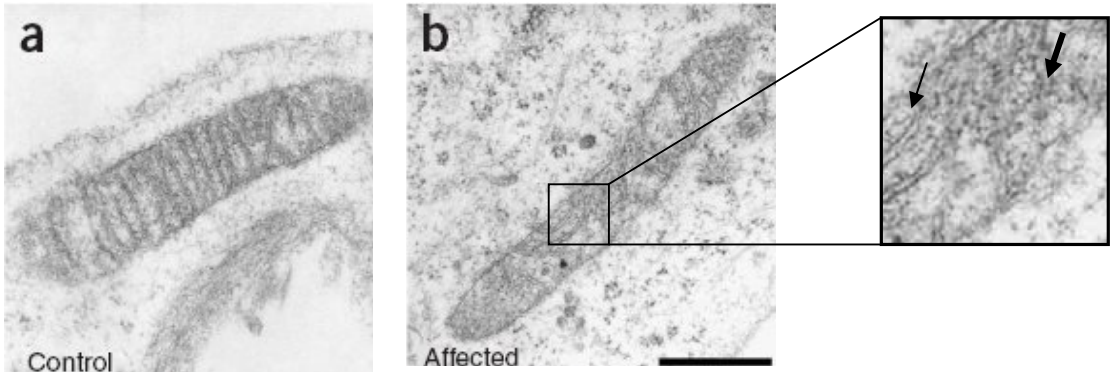

Fig. 4.17 Ultrastructural alterations of mitochondrial morphology. a) control fibroblasts show normal mitochondrial morphology, whereas b) mitochondria from affected individual D.I. show altered cristae and a smaller diameter. Scale bar, 1 mm.

4.5.2.3 Oxidative stress in *PYCR1*-mutated fibroblasts

Proline is considered a nonenzymatic antioxidant (102). As mitochondria are the main source of reactive oxygen species (ROS) and the organelles responsible for the maintenance of oxidative balance, we investigated the reaction of healthy and affected fibroblasts to oxidative stress. Control and affected fibroblasts were again seeded on glass coverslips and the cell culture medium was supplemented with 500mM hydrogen peroxide (H_2O_2) in which the cells were incubated for 10 min. The mitochondrial network was visualised using mitotracker (s.3.2.4.2). Upon H_2O_2 stress, we observed a breakdown of the mitochondrial network in affected fibroblasts. The mitochondria appeared fragmented, lacking their typical tubular appearance. In control fibroblasts we

were able to see only a slight fragmentation of the mitochondrial network (fig. 4.18a,b). In order to obtain a quantification of this effect we defined the percentage of tubular, intermediate and fragmented mitochondria in the control and in the affected cells. On average, 200 cells were estimated from each cell line, three control and four affected. The experiment was performed three times in order to achieve statistical significance. An increase of the fragmented mitochondria was obvious in both cell types, but significantly more intense in the affected fibroblasts (fig. 4.18c).

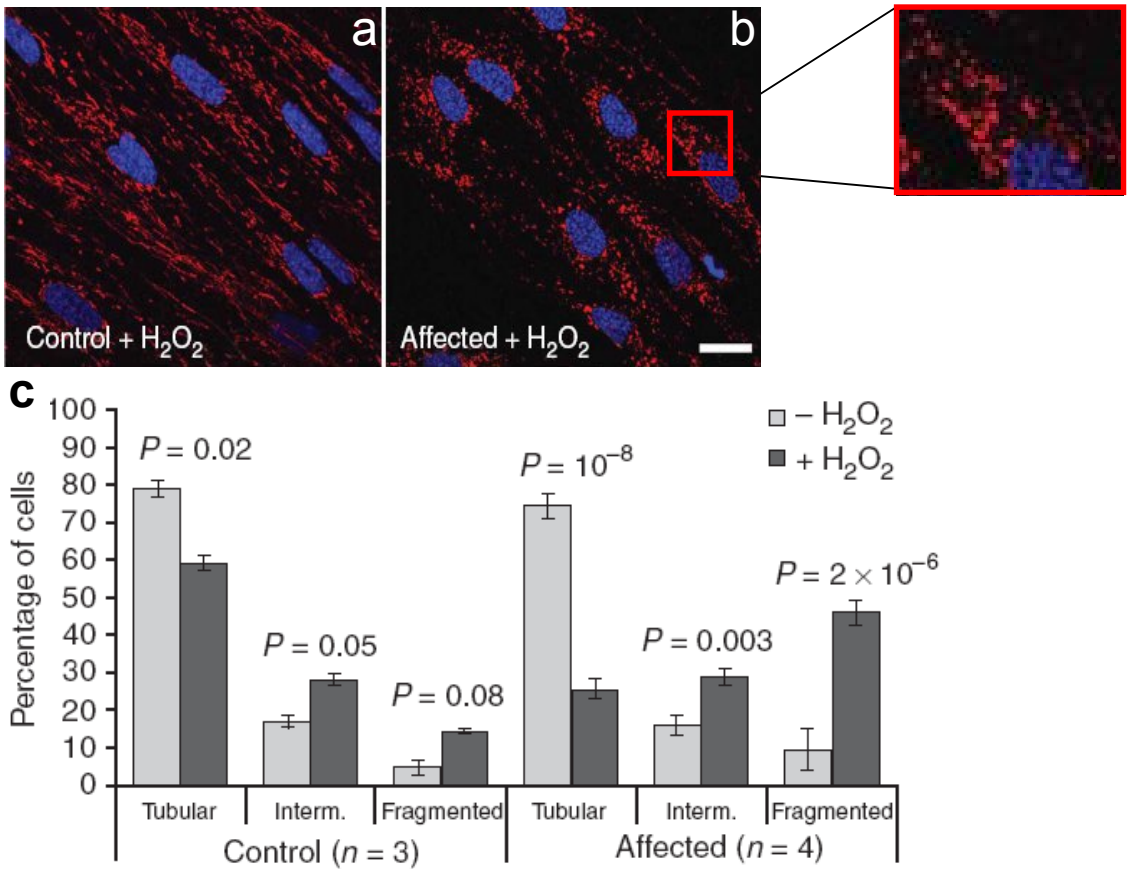

Fig. 4.18 Changes in mitochondrial morphology upon oxidative stress. After addition of 500 mM H2O2 to cell culture medium for 10 min, a) tubular mitochondrial network remains largely intact in control cells, whereas b) mitochondrial network collapses in fibroblasts from affected individual from family S.J. Scale bar, 20 µm c) quantification of the effect on mitochondrial morphology. Note the increase of the rate of fragmented mitochondria of affected fibroblasts after treatment with H_2O_2.

The differences in mitochondrial morphology seen through immunofluorescence were exacerbated upon oxidative stress. Addition of 500 mM H_2O_2 to cell culture medium for 10 min induced the collapse of the filamentous mitochondrial network in cells from affected individuals, whereas almost no changes were observed in mitochondria of control cells.

4.6 Apoptosis rates after oxidative stress in *PYCR1*-mutated fibroblasts

Pyrroline-5-carboxylate reductase has been implicated to be an important control point to regulate apoptosis (89). It has been shown that in Colletotrichum trifolii, a fungal pathogen of alfalfa (Medicago sativa), the mutationally activated oncogenic fungal Ras (DARas) elevates levels of ROS, causing abnormal fungal growth and development and eventual apoptotic-like cell death when grown under nutrient-limiting conditions. Remarkably, restoration to the wild-type phenotype requires only proline. Thus, it was suggested that proline has the ability to scavenge intracellular ROS and inhibit ROS-mediated apoptosis and that this may be an important and broad-based function of this amino acid in responding to cellular stress (102). In order to examine whether our protein does play a role in apoptosis, because of the fact that it catalyzes the final step of proline production, we conducted the TUNEL assay in healthy and affected cell lines. This assay detects the DNA fragmentation, which is commonly used as an apoptosis marker (s.3.2.4.5).

Fibroblasts from healthy controls and affected individuals were seeded on glass coverslips. For apoptosis determination, the TUNEL assay was performed for both normal and H_2O_2 stress conditions according to manufacturer specifications. Each experiment was performed three times and more than 2,000 cells were analyzed per assay. The quantification of these assays was not able to point out any differences in the apoptotic rates between control and affected fibroblasts under normal conditions. The treatment with hydrogen peroxide revealed a massive, fivefold increase of the number of cells in which apoptosis is induced in the affected fibroblasts. After the same treatment control cells do not show any elevated apoptotic rates (fig 4.19).

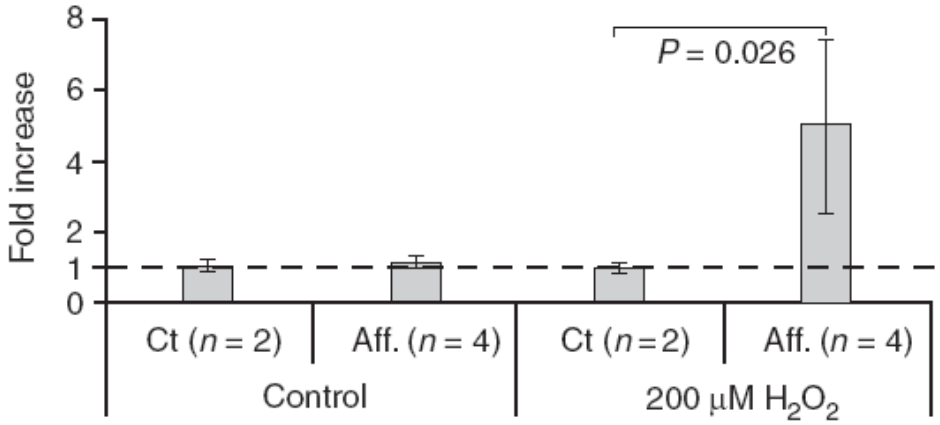

Fig. 4.19 Quantification of apoptotic cell death by TUNEL. Fibroblasts from control (Ct; n = 2) and affected individuals (Aff; n =4) under normal culture conditions (control) and 24 h after a 10 min incubation with 200 mM H2O2. Normalized to Ct cells in control experiment. Note the 5-fold increase of the apoptotic rate in affected fibroblasts (error bars, s.d.).

This result suggests that the PYCR1 protein plays a role in the cells' ability to react against oxidative stress.

5 Discussion

5.1 Autosomal recessive cutis laxa phenotypes.

We were able to identify mutations in the *PYCR1* gene as a new cause of autosomal recessive cutis laxa. The phenotype caused by *PYCR1* mutations shares many features with the other ARCL forms. Nevertheless, some typical traits also allow to differentiate the phenotype.

5.1.1 Comparison of the subtypes-differential diagnosis

The term cutis laxa implies a skin anomaly with loose, redundant skin folds and abnormal elasticity of the skin. Among the different forms of inborn cutis laxa, the autosomal recessive cutis laxa (ARCL) appears to be the most heterogeneous in terms of phenotypic features and underlying molecular defect. The identification of mutations in the *PYCR1* gene as an additional cause for autosomal recessive cutis laxa has further contributed to the genetic heterogeneity of this group of disorders.

The fact that the cutis laxa phenotypes show significant overlap gives rise to the question whether these phenotypes can be clinically distinguished. The elucidation of the molecular basis of the majority of these disorders helps to group the existing cases and delineate characteristic features of each subform.

Common features of all ARCL-phenotypes are inelastic and wrinkly skin, joint laxity, delayed motor development and abnormal skin biopsy revealing fragmentation of the elastic fibres. This last feature is considered to be one of the major diagnostic criteria for ARCL (66). Involvement of inner organs can differentiate the main types of ARCL (I, II and III). At the most severe end of the spectrum, the ARCL type I manifests itself through lung disease and anomalies of the vascular, gastrointestinal and genitourinary systems. Patients diagnosed with the milder phenotypes of ARCL type II (Debré Type) and Wrinkly Skin Syndrome (WSS) show more constantly a delayed closure of the frontal fontanel, a generalised skin wrinkling and a congenital hip dislocation, while MRI scans have revealed pachymicrogyria in some of the individuals. The patients show a unique biochemical feature of a combined N- and O-linked glycosylation defect (Congenital Disorders of Glycosylation, CDG type II). This defect can be used as a key differential feature from the highly similar phenotype of ARCL with progeroid appearance, also referred to as ARCL Type IIb. These patients show the most prominent mental retardation among the cutis

laxa phenotypes and bear an exclusive facial dysmorphism, not observed in any of the other overlapping phenotypes. Patients with gerodermia osteodysplastica do not show cognitive impairment but a more severe bone phenotype, with osteoporosis and increased fracture risk. ARCL type III, mostly known as De Barsy syndrome, overlaps significantly with ARCLII, but shows no signs of CDG.

Interestingly, the patients finally found to bear mutations in *PYCR1* were at first diagnosed mostly as GO (table 4.2). In both subtypes the skin wrinkling is milder in comparison with ARCLII and is restricted to certain loci rather than generalised. In ARCLII the skin phenotype tends to improve with time, whereas in GO and ARCLIIb the patients sustain the progeroid appearance to a grater degree. Furthermore, dental abnormalities and contractures leading to camptodactyly have been reported for GO patients and were also observed in the present cohort. The facial appearance in GO as described first by Bamatter *et al.* (1950) with droopy face, maxillary hypoplasia and mandibular prognathism (88) is common in both disorders but ARCLIIb patients also show triangular facies accompanied by large protruding ears, which can differentiate the two forms.

A number of families presented in this study have been previously reported or diagnosed as De Barsy syndrome cases (table 4.1, 4.2.). Mental and growth retardation and eye anomalies such as corneal clouding or cataract were considered to be the typical features of this phenotype (86). ARCLIIb significantly recapitulates the De Barsy phenotype and it could therefore be suggested that mutations in *PYCR1* is the underlying genetic defect. Despite that, a number of cases diagnosed as De Barsy were found negative for mutations in *PYCR1*, indicating a heterogenous genetic background of this phenotype.

As ARCL comprises a heterogeneous group of phenotypes, we suggest that the differential approach based on these clinical and biochemical features should be performed before the molecular diagnostic procedure of the underlying genetic defect (fig 5.1).

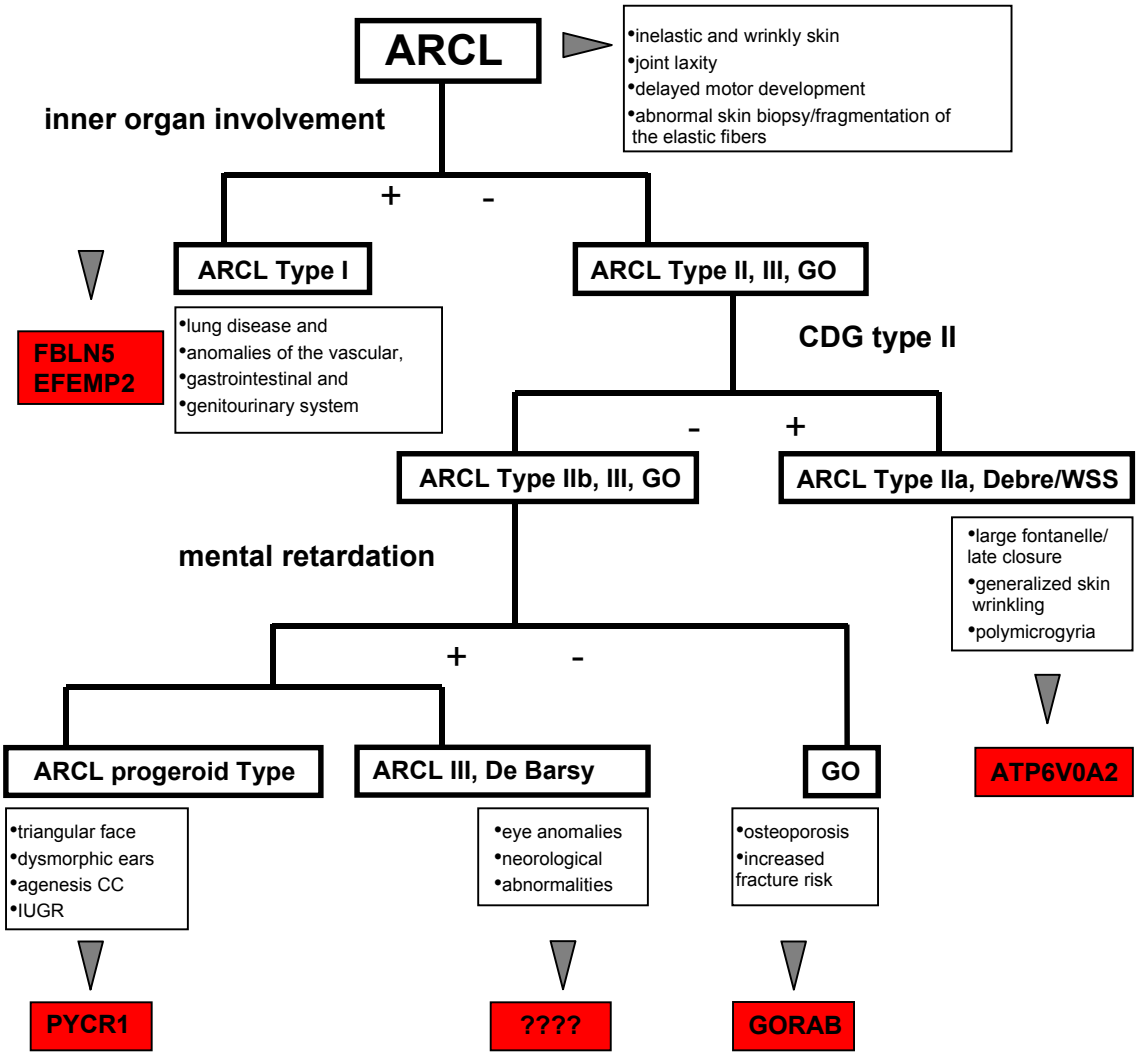

Fig. 5.1 Differential diagnosis schema in autosomal recessive cutis laxa.

5.1.2 Is ARCL with progeroid features a new segmental progeroid syndrome (PS) ?

The progeroid syndromes are a group of disorders characterized by premature or accelerated ageing. These syndromes recapitulate the features of chronological ageing in a partial way and for that reason they have been given the name of "segmental progeroid syndromes" (39). Common feature of these syndromes is the progressive character, which ultimately leads to shortened lifespan. Alterations in skin, fat distribution and skeleton, neurological degeneration, inner organ failure and early onset of age-related diseases such as cardiovascular abnormalities, diabetes and cancer are some of the typical observations in progeroid syndromes (39,104).

Autosomal recessive cutis laxa with progeroid appearance shares some characteristics with the PSs, which could partially justify its classification into this group of disorders. The wrinkled, inelastic skin, the droopy-sagging facial appearance, the growth retardation, the osteopenia and the contractures as well as the early-onset cataract observed in some cases could argue in favour of a premature ageing phenotype. Nevertheless, this cutis laxa form is not progressive (fig.5.2), a feature which significantly differentiates it from the known progeroid syndromes. On the contrary, the skin phenotype becomes milder with time. It is rather difficult to say whether the life-expectancy is affected, because most of the patients are relatively young and also because of the lack of follow-up data, as our collective consists of patients seen by clinicians at the place of origin. To date, no high susceptibility for cancer or cardiovascular diseases has been noted.

Fig. 5.2 Patient bearing mutations in PYCR1 gene at different ages. Note the progeroid appearance, which do not deteriorates with time (89).

All the characterized PSs belong to a group of rare monogenic disorders and several causative genes have been identified. These can be separated into subcategories corresponding to (i) genes encoding DNA repair factors, in particular, DNA helicases, and (ii) genes affecting the structure or post-translational maturation of lamin A, a major nuclear component (49). In addition, several animal models featuring premature aging have abnormal mitochondrial function or signal transduction between membrane receptors, nuclear regulatory proteins and mitochondria: no human pathological counterpart of these alterations has been found to date (49). It could be claimed that the ARCL with progeroid features fits in the wider spectrum of the last category and thus can be characterised as a progeroid syndrome.

5.1.3 Mutation frequencies

Up to the present time, we were able to confirm the diagnosis at the molecular level in almost 65% of the patients in our cohort. It appears that mutations in *ATP6V0A2* are responsible for the majority of the affected individuals, while mutations in *PYCR1* are presented as the second most frequent genetic defect among the cutis laxa patients (fig5.3). Despite these data, it is difficult to evaluate the prevalence of each disorder, as the overall occurrence of cutis laxa is itself very limited.

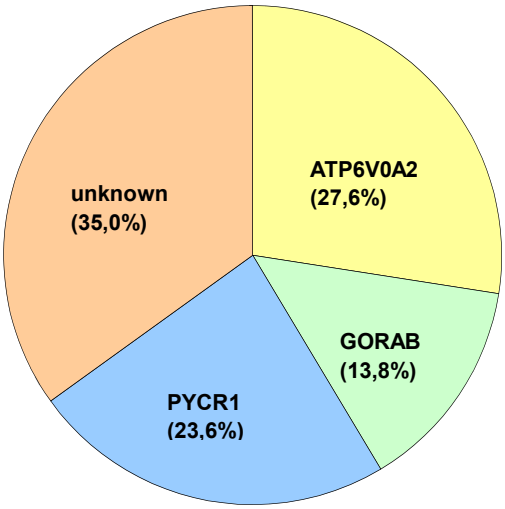

Fig. 5.3 Percentage of each ARCL phenotype in our cohort.

5.2 Molecular genetic studies

5.2.1 Mutation analysis and genotype-phenotype correlations

We defined, through homozygocity mapping, a minimal homozygous interval on chromosome 17q25 in five out of the 10 families examined in our cohort. The sequence analysis of the genes included in this region resulted in the identification of mutations in *PYCR1* gene. We were able to recognise 16 different mutations in our cohort of 22 families and sporadic cases. Among these mutations six were recurrent in patients with no common ethnic background. Interestingly, the majority of the mutations resides between exons 4 and 6, with only two exceptions, resulting in a

C-terminal clustering pattern. Furthermore, some codons appear to be more often affected than others, while no nonsense mutations were detected in our study.

The severity of the phenotype or the presence of special features could not be associated with a specific genotype or a certain mutation type. Individuals that bear frame shift mutations that lead to a premature stop codon, such as the Gly4fsX50, or splice site mutations most probably resulting in exon skipping, in other words affecting the protein to a higher degree than missense mutations, do not show a more pronounced phenotype. The same conclusion was drawn by clinically comparing patients with different missense mutations, e.g. mutations affecting highly or moderately conserved residues.

5.2.2 Mutations and probable effect on the protein

According to the crystal structure of PYCR1 protein, presented by Meng *et al.* (2006), the refined structures of the human pyrroline-5-carboxylate reductase demonstrate a decameric architecture with five homodimer subunits and ten catalytic sites arranged around a peripheral circular groove (89).

The N-terminal domain (domain A, residues 1-176) is formed by seven α-helices and eight β-strands, and has a modified NAD(P)-binding Rossmann-fold. The C-terminal domain (domain B, residues 177-275), where most of the mutations are located, is formed by six relatively longer α-helices. The basic biological unit is formed when one molecule binds to the equivalent part of another molecule via hydrophobic interactions. Domain B is important for dimerization, and in dimer–dimer interactions for decamer formation (89).

There are two main parts that constitute the NADH-binding site: the hydrophobic wall and the charged centre (89). Two different missense mutations G206W and G206R in the same codon affect an amino acid which is located between R204, a residue described to participate in forming the hydrophobic wall of the binding site and Q208, described to form one of the side walls of the charged pocket. Neighbouring two critical residues, G206 is very likely to also have a significant function in the binding site.

Apart from G206, another codon seems to be highly susceptible to mutagenesis: R119, a 100% conserved residue, which is mutated into R119G and R119H. Arginine at this position is located on the β6-strand of the A domain, the residues of which are implicated in the formation of the charged pocket of the binding site, which stabilizes NADH (89) (fig5.4). Its substitution by a

much smaller amino acid, such as glycine, or by an aromatic such as histidine could potentially change the molecular structure of this site, affecting eventually its properties.

In the study of Meng et al. (2006), in order to characterize the functional roles of the key residues in the active site, which is responsible for the recognition of the NADH moiety in the structure, the point mutants E221A, E221G were constructed. Glu221 and the C-terminal residues are specific to human P5CR. The affinity of wild-type P5CR for NAD+ is 20-fold higher than for NADP. However, the affinity of the E221A mutant for NAD+ was only twofold higher than for NADP+ (89), implying a significant alteration of the functional abilities of the protein caused by a missense mutation, which can also be the case for the missense mutations found in our cohort.

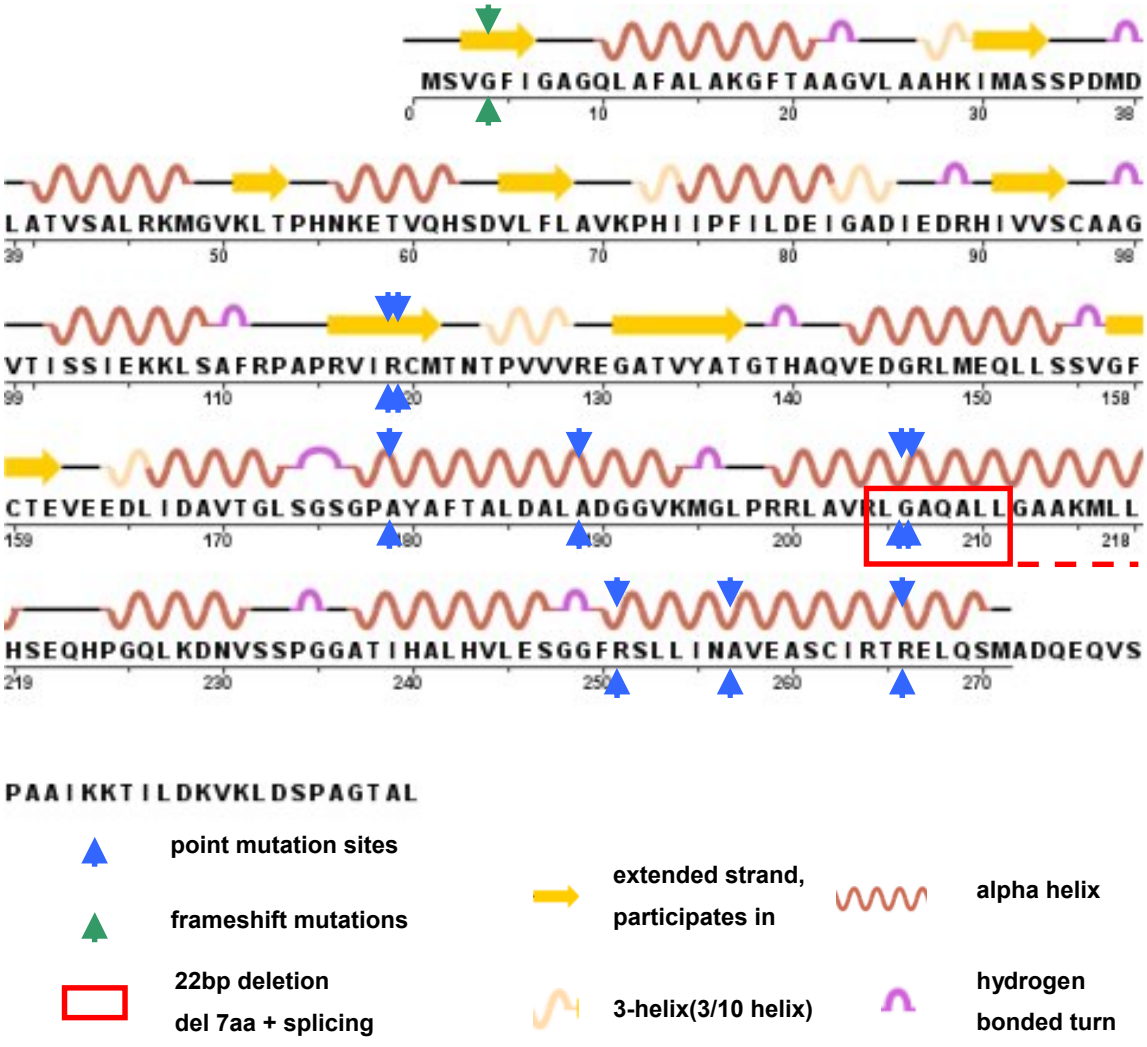

Fig.5.4 Schematic representation of the structure of the human pyrroline-5-carboxylate reductase (http://www.rcsb.org). The mutated residues are indicated with arrows.

5.3 Expression of the PYCR1 protein

5.3.1 Expression of the PYCR1 protein in fibroblasts from affected individuals

The determination of PYCR1 protein levels in fibroblasts from patients bearing mutations in the respective gene revealed an expression pattern consistent with the mutation type. It was shown by quantitative PCR that missense mutations do not affect the mRNA levels, while the combination of a missense and a frameshift mutation leads to a 40% reduction of the expression and finally a homozygous splice site mutation results in 80% reduction, most probably through nonsense-mediated decay (NMD). On the other hand, the expression of the protein in immunofluorescence and Western blot studies reveal a slightly different pattern. The signal obtained is very weak, but still existent in fibroblasts bearing the homozygous splice site mutation and in the compound heterozygotes, while the protein expression is mildly reduced in cells with homozygous missense mutations.

The fact that the cellular phenotype of the cells bearing missense mutations is milder is not correlated to the human phenotype (fig 4.6 and 4.9 results), which is also severe in these individuals. This implies that the mutations in the respective residues do not lead to a strong degradation of the protein but probably to a significant inability to function properly. A residual protein level suggests that in all cases a small amount of protein is not subject to degradation. This is also consistent with the fact that no nonsense mutations were identified, implying that the complete loss of the protein is probably lethal for the cell.

The expression analysis of PYCR1-paralogs and of the upstream enzyme P5CS in samples from control and affected fibroblasts showed that their expression does not show any variation between the tested probands. This finding indicated a normal expression of these genes in patients with the cutis laxa phenotype, arguing against a functional compensation of the PYCR1 defect through its homologs or through P5CS, which is involved in the same pathway.

5.3.2 Expression of PYCR1 protein in mouse tissues

We defined the expression levels of *Pycr1*, the murine ortholog of *PYCR1*, in different mouse tissues from P4 mice. The analysis showed high expression of the protein in skin, bone, eye and osteoblasts. The latter tissues also showed increased expression of Pycr2, Pycrl and P5cs.

This expression pattern allows some interesting speculations. The main tissues, skin and bone, affected in our phenotype do show a high expression of the protein, whereas the very interesting finding of the selective increased levels in osteoblasts is also consistent with the bone phenotype observed in these patients. Furthermore, the eyes are also significantly represented in this pattern, which is in line with early onset cataracts described in our patients. It is obvious that only speculations about potential correlations can be made on that ground, as the human and murine expression patterns are not necessarily identical.

These results, when compared to the existing data for the expression profile of the human Pyrroline-5-carboxylate reductase 1 (NCBI, Unigene, EST-profile), do not appear to overlap significantly (fig5.5 representative data shown). Again, compared to the heart, the expression is higher in eye, skin and bone, but in other tissues as well. Unfortunately, no expression analysis in human tissues was possible except for human skin fibroblasts obtained from patients with mutations in PYCR1, where the levels of the mRNA and protein were described above.

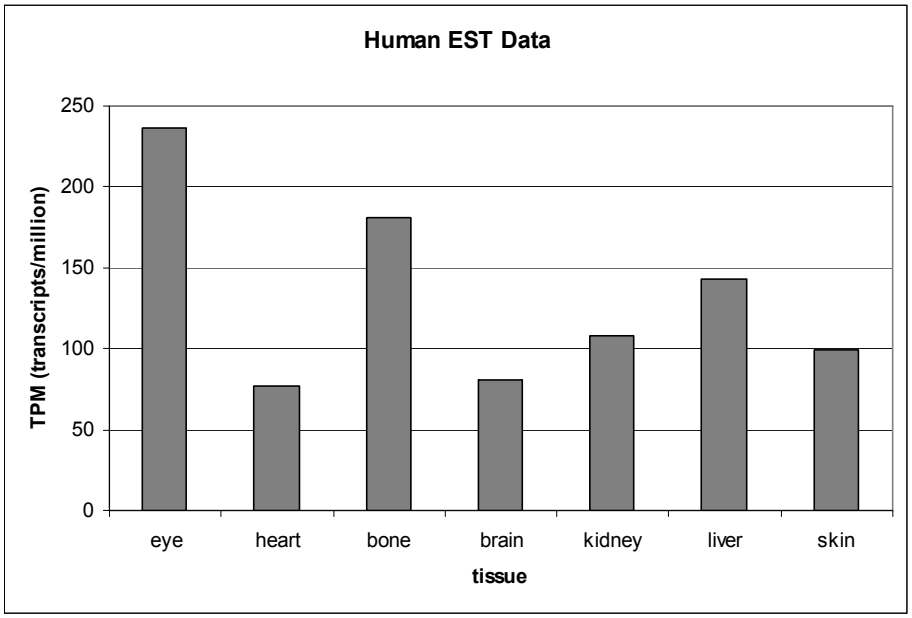

Fig. 5.5 Expression of PYCR1 -selected EST data of human PYCR1, as reported in www.ncbi.nlm.nih.gov/.

5.4 Proline metabolism

Among the 20 amino acids known to constitute proteins, proline is the most interesting, having its side chain cycling back to the backbone amino group and generating a pyrrolidine ring not susceptible to generic peptidase cleavage. Due to this structure, its presence effects the conformation, properties and biological functions of various molecules such as structural proteins like

collagen, peptides involved in immunomodulation and coagulation, cytokines, growth factors, and neuro- and vasoactive peptides (105). Proline can be obtained from dietary proteins and from the degradation of endogenous proteins (97) and it can be biosynthesized from glutamate and ornithine (95), making it nutritionally nonessential.

5.4.1 Proline synthesis cycle

Proline synthesis cycle has been hypothesised based upon purely enzymatic data almost 30 years ago after the primer identification of the participating enzymes. In mammals proline metabolism involves two further amino acids, glutamate and ornithine, and five enzymatic activities, D1-pyrroline-5-carboxylate (P5C) reductase (P5CR), proline oxidase, P5C dehydrogenase, P5C synthase (fig5.6) with D1- pyrroline-5-carboxylate (P5C) as the obligatory intermediate (106). P5C is the obligatore substrate for proline biosynthesis, and is reduced to proline by the cytosolic NAD(P)H-dependent enzyme P5C reductase (P5CR).

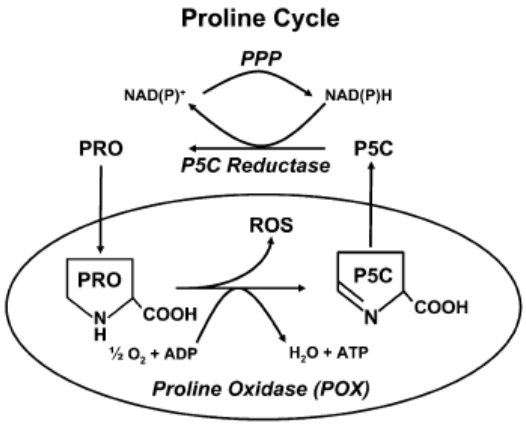

The central enzyme in the proline cycle is proline dehydrogenase (PRODH), which is tightly bound to mitochondrial inner membranes and which catalyzes the degradation of proline back to P5C. The oxidation of proline by POX to yield P5C and the conversion of P5C into proline by P5CR constitutes a proline-P5C cycle that involves two subcellular compartments, mitochondrion and cytosol. In order for this conversion to take place, P5C must leave the mitochondria, because P5CR isozymes are localized to the cytoplasm and/or loosely associated with the cytosolic side of the outer mitochondrial membrane, indicating the presence of unidentified transport systems across the mitochondrial and plasma membranes (106). These mostly mitochondria-based pathways involved in the biosynthesis and degradation of proline interact with the urea cycle, pentose phosphate pathway, and TCA cycle (tricarboxylic acid cycle) (106). Proline biosynthesis coupled to the pentose phosphate pathway stimulates the synthesis of $NADPH_2$ and sugar phosphates for anabolic pathways, including phenolic and antioxidant response pathways. The reducing equivalents for mitochondrial oxidative

phosphorylation are provided by proline-replacing NADH, with oxygen being the terminal electron acceptor (107). The proline-P5C cycle plays an important role in the regulation of gene expression, purine biosynthesis, cellular redox state, apoptosis and cell proliferation (89,97,106).
Up to now, apart from taking part in the proline biosynthesis, little is known about a potential alternative function of the PYCR1 protein. Studies on the properties of human erythrocyte P5CR concluded that besides the traditional role, isozymes of P5CR (*PYCR1* and *PYCR2*) may play a physiologic role in the generation of NADP+ in some types of cell including erythrocytes (108). Further studies have revealed an increased activity of PYCR1 in pulmonary and colorectal tumors (89).

5.4.2 Loss of PYCR1 does not affect proline levels

The human P5C reductase, as already mentioned, catalyzes the NAD(P)H-dependent reduction-conversion of Δ1-pyrroline-5-carboxylate (P5C) to proline, the first committed step in de novo biosynthesis of proline (106). Since the mutations found in our families affect the gene encoding this enzyme, we expected reduced production of proline. However, the measurement of proline in both serum and cell lysates (fibroblasts) from affected individuals appeared to be in the normal range, suggesting that the pathogenesis is not based on lower proline levels. This was also confirmed by the fact that addition or depletion of proline from the culture medium was not able to cause any significant effect to the results obtained from experiments performed on affected fibroblasts, or rescue their cellular phenotype. Alterations of the proline levels in the microenvironment of mitochondria for instance cannot be ruled out.
This might be explained by the fact that proline synthesis in the absence of PYCR1 is taken over by other enzymes, which in that case would be up-regulated, or that alternative pathways of proline synthesis are being activated. Expression studies of all genes involved could maybe indicate a compensating mechanism upon loss of PYCR1.
Mutations in genes encoding for enzymes of the same pathway do show an altered pattern of proline levels (fig 5.5). Hyperprolinemia type I (HPI; MIM 239500) is caused by a deficiency in proline oxidase (POX), the mitochondrial inner-membrane enzyme that converts proline to P5C, the first step in the conversion of proline to glutamate. HPI is biochemically diagnosed by high plasma proline levels and is characterised by renal abnormalities (109), neurologic involvement and increased susceptibility to schizophrenia (110).

Hyperprolinemia type II (HPII; MIM 239510) is due to absence of D-1-pyrroline-5-carboxylic acid dehydrogenase (P5CDh) activity. P5CDh is a mitochondrial matrix NAD(1)-dependent dehydrogenase which catalyzes the second step of the proline degradation pathway. Deficiency of this enzyme causes accumulation of P5C and proline (96), leading to recurrent seizures and mild mental retardation (111).

A phenotype similar to ARCL2b is caused by deficiency of P5C synthetase (MIM 138250) showing progressive neurodegeneration, joint laxity, skin hyperelasticity, and bilateral cataracts. The metabolic phenotype includes hypoprolinemia, hyperammonemia, and reduced serum levels of other amino acids, findings that, interestingly, are not observed in all patients (112,113).

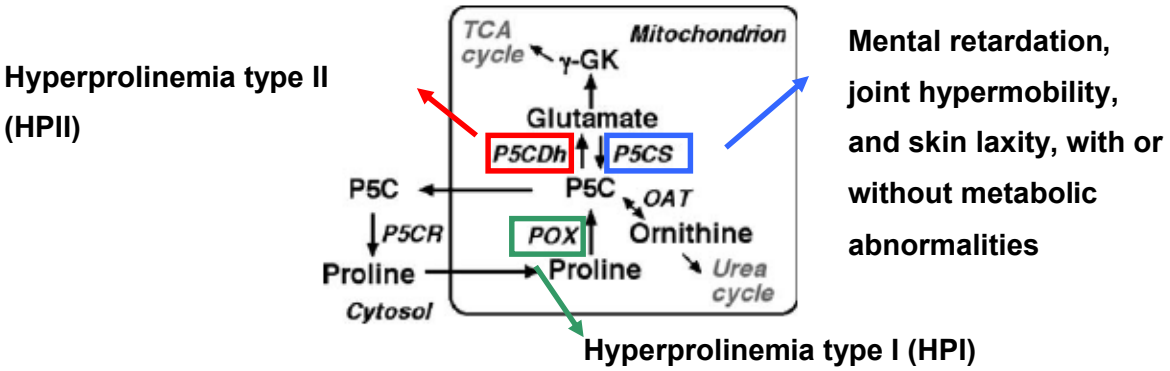

Fig. 5.6 Proline metabolic pathway and related disorders (modified, 106).

In both disorders characterised by hyperprolinemia, a neurological phenotype is the most prominent sign, although the mechanism through which this occurs is only poorly understood. Investigation of the effects of proline on cerebral cortex and hippocampus slices of rats identified a reduction of glutamate uptake and Na^+,K^+-ATPase activity associated with generation of free radicals (114,115), suggesting that physiological levels of proline are important for the maintenance of the oxidative balance in these cells. Na^+,K^+-ATPase is a crucial enzyme responsible for the generation of the membrane potential in the central nervous system (CNS) necessary to maintain neuronal excitability and cellular volume control. Thus, a reduction of glutamate uptake, Na^+,K^+-ATPase activity and oxidative stress may be involved in the brain dysfunction observed in hyperprolinemic patients (114,115).

On the other hand, hypoprolinemia seen upon mutations in P5CS is associated with a more complicated phenotype, including neurological signs but connective tissue abnormalities as well.

P5CS catalyzes an essential step in the pathways of proline, ornithine and arginine synthesis (112). Lack of these amino acids in the different tissues was proposed to be responsible for the observed phenotype. Proline serves as an antioxidant, lowering ROS levels and preserving the

intracellular glutathione pool, which is the major redox buffer of the cell (116). Additionally, proline is essential for the synthesis of brain polypeptides with neuroprotective and neuromodulatory effects (117) which could account for the neurological disorders observed in humans with P5CS deficiency. Low levels of proline also impair collagen synthesis, causing hyperelasticity. Additionally, proline deficiency could affect the levels of P5C and the redox state of the lens, leading to cataracts (118).

5.5 PYCR1 and mitochondria

5.5.1 Mitochondrial localization of PYCR1 protein

We investigated the cellular localization of PYCR1 protein and concluded that it resides on the mitochondrion as the immunofluorescence studies revealed a clear co-localization with known mitochondrial proteins. This finding provides new insights into the proline synthesis cycle, as a transport of P5C from mitochondria to cytosol does not appear any more to be necessary for its final conversion to proline. A mitochondrial residence of PYCR1 seems logical, considering the mitochondrial localization of the other enzymes participating in the same pathway, indicating that the whole biosynthetic pathway takes place in mitochondria.

Thus, this result contradicts the cytosolic localization of the enzyme described so far but not a potential association with the cytosolic side of the outer mitochondrial membrane, as further studies have to be performed in order to define the precise localization of the protein.

P5CR catalyzes the synthesis of proline from P5C, which is thought to be linked with pentose-phosphate pathway, driving the synthesis of NADPH(2) and sugar phosphates for anabolic pathways. The proven mitochondrial localization of PYCR1 should establish new perspectives on the way that these pathways may relate to each other.

5.5.2 PYCR1 and maintenance of the mitochondrial structure

Comparing the mitochondrial morphology of control and mutant fibroblasts, we were able to identify, by electron microscopy and immunofluorescence, a disruption of the mitochondrial

cristae and its network structure in fibroblasts bearing mutations in *PYCR1*. Therefore it could be concluded that the encoded protein plays a critical role in the maintenance of the normal mitochondrial morphology.

Mitochondrial fragmentation is very tightly correlated with their function. It has been described to impair cellular function in different neurodegenerative disorders. Compared with other cell types, neurons seem to be particularly vulnerable to changes in mitochondrial morphology and connectivity, probably due to their great energy requirements and unique energy transmission demands (119).

Furthermore, the impact of mitochondrial morphological changes on bioenergetics is strongly established, as it appears to be a key player regulating fusion and fission of mitochondria (120). Several observations indicate that mitochondrial energy production may be controlled by structural rearrangements of the organelle, including the remodelling of cristaes' morphology and elongation or fragmentation of the tubular network organization, respectively (121). Human phenotypes resulting from mutations in genes encoding for proteins involved in the mitochondrial procedures of fusion and fission are already known.

A neurodegenerative process is not observed in our patients, although a neurological phenotype is present in terms of mental retardation, brain malformations and athetosis. Neuropathy is not noted either, although no nerve biopsies or electrophysiological studies have ever been performed on the affected individuals.

5.5.3 Loss of PYCR1 induces the collapse of the mitochondrial network upon oxidative stress

The changes observed in the morphology and structure of the mitochondria in fibroblasts from patients bearing mutations in *PYCR1* were aggravated upon oxidative stress. PYCR1 apparently participates in maintaining the normal mitochondrial function and integrity, although its exact role is yet to be identified. The orthologs of PYCR1 in other species, such as *Saccharomyces*, *Arabidopsis* and *Drosophila*, have been associated with stress resistance, which suggests that human PYCR1 as well may provide adaptive protection against stress by reducing equivalents in mitochondria and maintaining a reservoir of rapidly mobilizable proline, which as substrate is stored as collagen in extracellular matrix, connective tissue, and bone and it is rapidly released from these sources by the eventual action of matrix metalloproteinases, peptidases, and prolidase (89,97).

Proline was observed to protect cells against H_2O_2, tert-butyl hydroperoxide, and carcinogenic oxidative stress inducers (97, 116). In different mammalian cell lines exposed to physiological H_2O_2 levels, increased endogenous P5CS and P5CR expression was observed, indicating that upregulation of proline biosynthesis is an oxidative stress response, while overexpression of the proline biosynthetic enzymes Δ1-pyrroline-5-carboxylate (P5C) synthetase (P5CS) and P5C reductase (P5CR) resulted in 2-fold higher proline content, significantly lower ROS levels, and increased cell survival relative to control cells (116). In our study, increased expression of P5CS was not observed in affected cells in the absence of P5CR and at the same time extraction or addition of proline did not show any measurable effect on the cellular behaviour.

5.5.4 Loss of PYCR1 induces increased apoptosis in mutated fibroblasts

Δ1-pyrroline-5-carboxylate (P5C) was found to be able to generate oxygen species that induce apoptosis (122,123), while proline is considered to be a non enzymatic antioxidant that suppresses apoptosis (102). PYCR1 catalyzes the reduction of P5C to proline, suggesting that this protein should be an important control point to regulate apoptosis (89). Affected and control fibroblasts showed no differences in their apoptosis rate when cultured under normal conditions. However, short treatment with H_2O_2 leads to a fivefold increase in cell death in affected fibroblasts compared to controls. This result implies that the PYCR1 protein plays a role in the cell reaction to oxidative stress, probably by inhibiting apoptosis.

Apoptosis is initiated by extracellular or intracellular signals in which a complex machinery is activated to start a cascade of events ultimately leading to the degradation of nuclear DNA and dismantling of the cell. Dysregulation of apoptosis is associated with many pathologic conditions and may even be central in the pathogenesis of many diseases. While too little apoptosis may result in cancer, autoimmune or other chronic inflammatory diseases, too much apoptosis is involved in neuronal damage and neurodegenerative disorders (124).

According to our findings, PYCR1 protects against stress. Inability to react properly under stress conditions could trigger apoptosis in cells lacking PYCR1. As mentioned before, oxidative stress can lead to irreversible damage of proteins, nucleic acids and lipids (125), which can activate apoptosis check-points and ultimately drive a dysfunctional cell to death and apoptosis. Increased apoptosis rates are associated with disorders such as Hutchinson-Gilford Progeria syndrome (HGPS), where p53 pathway is upregulated in response to increased rates of DNA damage due to defects of the nuclear envelope (*LMNA*) (89).

Disorganisation of the mitochondria structure could be an additional disturbing factor as mitochondria are implicated in the regulation of apoptosis. During apoptosis, the integrity of the mitochondria is altered, the mitochondrial transmembrane potential drops, the electron transport chain is disrupted, and proteins from the mitochondrial intermembrane space (MIS) are released into the cytosol (126). Mitochondrial membrane permeability transition (PT) was reported to be a critical event of apoptosis as the point-of-no-return (127), and the mitochondrial control of apoptosis is well established (128,129).

5.5.5 Is ARCL with progeroid features a mitochondrial disorder?

Mitochondrial diseases are a heterogeneous group of clinical disorders that arise as a result of dysfunction of the mitochondrial respiratory chain. The mitochondrial respiratory chain is the essential final common pathway for aerobic metabolism, and tissues and organs that are highly dependent upon aerobic metabolism are preferentially involved in mitochondrial disorders (130). They can be caused by mutations of nuclear or mitochondrial DNA (mtDNA). Some mitochondrial disorders only affect a single organ, but many involve multiple organ systems in a syndromatic manner and often present with prominent neurological and myopathic features. Mitochondrial disorders may manifest at any age. In general terms, nuclear DNA mutations present in childhood and mtDNA mutations present in late childhood or adult life (131,132).

Common clinical features of mitochondrial disease include ptosis, external ophthalmoplegia, proximal myopathy and exercise intolerance, cardiomyopathy, sensorineural deafness, optic atrophy, pigmentary retinopathy, and diabetes mellitus (133). The central nervous system findings are often fluctuating encephalopathy, seizures, dementia, migraine, stroke-like episodes, ataxia, and spasticity. Chorea and dementia may also be prominent features (134).

It could be suggested that ARCL with progeroid features is a mitochondriopathy, caused by mutations in a nuclear gene, which encodes a protein localized in mitochondria and contributing to their normal function. Nevertheless, the clinical features of our patients do not recapitulate the typical signs of those disorders. Myopathic and neuropathic changes are absent, whereas the neurological phenotype is restricted to mental retardation and athetosis in very few cases. Furthermore it does not show any progression, arguing against an accumulative character of the underlying pathomechanism. Endocrine alterations have not been described in any of our patients, while sensorineural deafness was observed in one out of the 34 affected individuals. Moreover, up to

now, no dysfunction of the respiratory chain - oxidative phosphorylation - is proven, a finding which actually defines a mitochondriopathy.
Mitochondrial dysfunction is also seen in a number of different genetic disorders, including dominant optic atrophy (mutations in OPA1)(135), Friedreich ataxia (FRDA) (136), hereditary spastic paraplegia (SPG7) (137), and Wilson disease (ATP7B) (138) and also as part of the aging process. These are not strictly mitochondrial disorders and under this condition it could be postulated that this phenotype does not represent a mitochondriopathy, albeit its pathology probably results from mitochondrial dysfunction.

5.6 Common features in ARCL subtypes- common pathomechanism?

It could be claimed that the different genetic defects in a way lead to the same ultimate result, the alteration of the elastic fibre unit. This is most probably achieved through alternate triggering events, which eventually disturb similar pathways or cellular procedures, suggesting a common pathomechanism shared by all of these separate entities.

5.6.1 Elastic fibres and disease

The autosomal recessive cutis laxa phenotypes show great similarities, while some features are constant in all four genetically clarified forms so far. The indisputably recurrent finding is the wrinkled inelastic skin of different degree and its typical ultrastructural alterations, which indicate the main diagnostic criterion of ARCL (66). Skin biopsies reveal variable degrees of fragmentation and disorientation of the elastic fibres, whereas the collagen fibres are unaffected.
Elastic fibre abnormalities represent a non specific feature and are encountered in many different disorders. In healthy individuals, the mature elastin molecule is a stable, insoluble protein. Degradation of elastin is extremely slow due to the extensive crosslinking of tropoelastin within the elastic fibre. However, with aging, injury, or the onset of a variety of acquired diseases, the excessive or aberrant remodeling and degradation of elastic fibres becomes prominent in arteries, lung, skin, and ligaments (139). The correct assembly of the elastin polymer is critical for the proper elastic function, and therefore the physiological properties of these tissues become compromised. Examples of common disorders that involve abnormal elastic fibre assembly and/or degradation include aortic aneurysms, atherosclerosis, chronic obstructive pulmonary disease,

emphysema, and hypertension (140). Milewitz and colleagues (2000) reviewed the genetic disorders resulting from mutations in genes encoding for proteins which are involved in the genesis of the elastic fibres (141). One group of genetic disorders is due to mutations in the elastin gene (ELN), known as elastinopathies. The most important phenotypes resulting from mutations in this gene are supravalvular aortic stenosis SVAS, isolated or as part of Williams-Beuren Syndrome and autosomal dominant cutis laxa (ADCL). Attempts to correlate the severity of SVAS with the specific underlying genotype have so far been unsuccessful. The identification of three different ELN mutations in unrelated ADCL patients indicated a novel molecular cause for ADCL. These mutations were all single nucleotide deletions (60,142). Skin biopsies from ADCL patients reveal fragmentation and rarefaction of the elastic fibres (65). The second group includes disorders caused by mutations in *FBN1* and *FBN2*. Different *FBN1* mutations have been associated with several similar phenotypes such as typical Marfan syndrome, isolated ectopia lensis, marfanoid skeletal syndrome, atypical Marfan syndrome, autosomal dominant Weill-Marchesani syndrome, Shprintzen-Goldberg syndrome, isolated thoracic aortic aneurysms and associated aortic dissection, stiff-skin syndrome and others. Congenital contractural arachnodactyly is a rare, autosomal dominant connective tissue disorder, resembling Marfan syndrome caused by mutations in FBN2. The same group of disorders includes the former marfanoid phenotypes of isolated familial aortic aneurysms (Loeys-Dietz Syndrome 2B; MIM: 610380) caused by mutations in *TGFBR2* gene (143, 144), whereas mutations in *TGFBR1* gene were shown to cause Loeys-Dietz Syndrome 1A (MIM: 619192) which also includes neurologic and skeletal manifestations (145).

Autosomal recessive cutis laxa caused by mutations in *PYCR1* also represents a disorder of the elastic fibres, as skin biopsies of patients reveal abnormalities on this level. Despite that, the ARCL mainly differs because it does not manifest through alterations of the blood vessels with the tragic consequences seen in the mentioned syndromes. Biopsies of other tissues were not available in our study but the clinical evaluation did not provide any signs of a possible involvement. The underlying pathomechanism appears to selectively affect the connective tissue at specific loci such as skin, joints and bones, leaving inner organs, big and small arteries or lungs, intact. This can be due to the different expression pattern of the mutated gene but also due to the fact that the putative alternative role of the protein may be tissue specific.

5.6.2 Cellular pathomechanism

Up to now, structural defects (*FBLN5/FBLN4*), Golgi apparatus and mitochondrial involvement (*ATP6V0A2, GORAB* and *PYCR1)* are implicated in the pathogenesis of ARCL. No known common pathway directly connects these proteins and their functions, which at first seem to be very different. Moreover, the precise functional role of these proteins is in some cases unclear, multiple or even unknown, making it difficult to construct a general hypothesis concerning the major functional event that gives rise to the respective phenotypes.

In general, V-ATPases appear to play a role in the formation of endosomal carrier vesicles from sorting endosomes that transport the uncoupled ligands to later endosomal compartments (146). A direct association between V-ATPases and glycosylation has not been described, but loss of ATP6V0A2 is clearly accompanied by a combined N- and O- glycosylation defect, suggesting a defect at the Golgi apparatus level. Loss of function mutations in *ATP6V0A2* were also found to lead to tropoelastin (TE) aggregation in the Golgi, impaired clearance of TE aggregates and increased apoptosis of elastogenic cells (147). Studies on *ATP6V0A2* mutated cells suggest that the intracellular trafficking of TE-containing vesicles may be defective. This is underlined by the swelling and fragmentation of the Golgi apparatus and the accumulation of abnormal, TE-positive Golgi vesicles in affected fibroblasts (147).

GORAB is defined as the first golgin, whose defect lead to a hereditary human phenotype (87). The protein was found to specifically interact with Rab6 (87), whose main function is the recruitment of motor proteins that support vesicle movement. Rab6 is known to be involved in the retrograde transport from endosomes to the Golgi apparatus and to have a crucial role in the secretory pathway from the Golgi to the plasma membrane (148,149).

A disruption of the Golgi microenvironment either through its structural disorganization or through the aberrations of the intraluminal pH could lead to general abnormalities of the protein posttranslational modifications, to a large degree taking place during their passage through the Golgi compartment. A fundamental dysfunction of the Golgi apparatus is not yet thoroughly established in the ARCL phenotypes. A hint in this direction is given by the proven and constant finding of the glycosylation defect at the Golgi level, suggesting that maybe only certain modifications are obscured, in this case for instance when the luminal pH becomes more acidic and others when it becomes more alkaline .

These modifications may also form a signal sequence which determines their final destination (150), suggesting that a misplacement or degradation of the modified proteins due to wrong or missing signal is likely upon Golgi dysfunction.

Apart from such modifications, Golgi is responsible for sorting and packaging of macromolecules destined to be secreted and thus participating in exocytosis (150). The vesicles that leave the rough endoplasmic reticulum (ER) are transported to the *cis* face of the Golgi apparatus, where they fuse with the Golgi membrane and empty their contents into the lumen (150). A delayed fusion of Golgi membranes with the ER upon Brefeldin A (BFA) treatment was highly reproducible in skin fibroblasts bearing *ATP6V0A2* mutations (79), suggesting a trafficking defect.
Mitochondria are also implicated in participating in signalling events, as mitochondrially generated H_2O_2 can also act as a signalling molecule in the cytosol, affecting multiple networks that control cell cycle, stress response, energy metabolism, and redox balance (151,152). Within mitochondria, many new signalling effects of H_2O_2 have been uncovered over the past few years, including an important role in the activation of mitochondrial pathways, which are themselves key regulators of mitochondrial ROS generation (153). Whether the production of ROS is altered in mitochondria from *PYCR1*-mutated fibroblasts is yet to be determined, because in that case direct or secondary signalling effects can be hypothesised.
Thus, secretion of extracellular matrix proteins and signalling between the cellular compartments could be the basic mechanisms affected in these disorders, although such an association could only be partially proven. In order to be able to define more precisely the similarities of the pathogenesis of the autosomal recessive cutis laxa, the future studies have to be performed in parallel for all three phenotypes.

6 References

1) Callaghan TM, Wilhelm KP. A review of ageing and an examination of clinical methods in the assessment of ageing skin. Part I: Cellular and molecular perspectives of skin ageing. Int J Cosmet Sci. 2008 Oct;30(5):313-22. Review.
2) http://dermatology.about.com/
3) Kielty CM, Sherratt MJ, Shuttleworth CA. Elastic fibres J Cell Sci. 2002 Jul 15;115(Pt 14):2817-28. Review.
4) Sandberg LB, Weissman N, Gray WR. Structural features of tropoelastin related to the sites of cross-links in aortic elastin. Biochemistry. 1971 Jan 5;10(1):52-6.
5) Sakai LY, Keene DR, Engvall E. Fibrillin, a new 350-kD glycoprotein, is a component of extracellular microfibrils. J Cell Biol. 1986 Dec;103(6 Pt 1):2499-509.
6) Kagan HM, Sullivan KA. Lysyl oxidase: preparation and role in elastin biosynthesis. Methods Enzymol. 1982;82 Pt A:637-50
7) Wagenseil JE, Mecham RP. New insights into elastic fiber assembly. Birth Defects Res C Embryo Today. 2007 Dec;81(4):229-40. Review.
8) Uitto J, Christiano AM, Kähäri VM, Bashir MM, Rosenbloom J. Molecular biology and pathology of human elastin. Biochem Soc Trans. 1991 Nov;19(4):824-9. Review.
9) Swee MH, Parks WC, Pierce RA.Developmental regulation of elastin production. Expression of tropoelastin pre-mRNA persists after down-regulation of steady-state mRNA levels. J Biol Chem. 1995 Jun 23;270(25):14899-906.
10) http://ageing-research.blogspot.com/
11) Makrantonaki E, Zouboulis CC.. Molecular mechanisms of skin aging: state of the art. Ann N Y Acad Sci. 2007 Nov;1119:40-50
12) Makrantonaki E, Zouboulis CC, 2007 William J. Cunliffe Scientific Awards. Characteristics and pathomechanisms of endogenously aged skin. Dermatology, 214: 352–360.
13) Watson RE, Craven NM, Kang S, Jones CJ, Kielty CM, Griffiths CE. A short-term screening protocol, using fibrillin-1 as a reporter molecule, for photoaging repair agents.J Invest Dermatol. 2001 May;116(5):672-8.
14) Contet-Audonneau JL, Jeanmaire C, Pauly G. A histological study of human wrinkle structures: comparison between sun-exposed areas of the face, with or without wrinkles, and sun-protected areas. Br J Dermatol. 1999 Jun;140(6):1038-47.
15) Braverman IM, Fonferko E. Studies in cutaneous aging: II. The microvasculature. J Invest Dermatol. 1982 May;78(5):444-8.
16) D. Harman, Aging: a theory based on free radical and radiation chemistry, J. Gerontol. 11 (1956) 298–300.
17) Dröge, W. Free radicals in the physiological control of cell function. Physiol. Rev. 82:47–95; 2002.
18) Kowaltowski AJ, de Souza-Pinto NC, Castilho RF, Vercesi AE. Mitochondria and reactive oxygen species. Free Radic Biol Med. 2009 Aug 15;47(4):333-43.
19) Holmgren, A. Antioxidant function of thioredoxin and glutaredoxin systems. Antioxid. Redox Signaling 2:811–820; 2000.
20) Bokov A, Chaudhuri A, Richardson A. The role of oxidative damage and stress in aging. Mech Ageing Dev. 2004 Oct-Nov;125(10-11):811-26.
21) Orr WC, Sohal RS.Extension of life-span by overexpression of superoxide dismutase and catalase in Drosophila melanogaster. Science. 1994 Feb 25;263(5150):1128-30.
22) Parkes TL, Elia AJ, Dickinson D, Hilliker AJ, Phillips JP, Boulianne GL. Extension of Drosophila lifespan by overexpression of human SOD1 in motorneurons. Nat Genet. 1998 Jun;19(2):171-4.
23) X.J. Chen, R.A. Butow, The organization and inheritance of the mitochondrial genome, Nat. Rev. Genet. 6 (2005) 815–825
24) Krishnan KJ, Greaves LC, Reeve AK, Turnbull DM. Mitochondrial DNA mutations and aging. Ann N Y Acad Sci. 2007 Apr;1100:227-40.
25) Fukui, H. and Moraes, C.T. (2008) The mitochondrial impairment, oxidative stress and neurodegeneration connection: reality or just an attractive hypothesis? Trends Neurosci., 31, 251–256.

26) Khrapko K, Vijg J. Mitochondrial DNA mutations and aging: A case closed? Nat. Genet. 2007 Apr;39(4):445-6
27) Khrapko K, Vijg J. Mitochondrial DNA mutations and aging: devils in the details? Trends Genet. 2009 Feb;25(2):91-8. Review.
28) Hayflick, L. The limited in vitro lifetime of human diploid cell strains. Exp. Cell Res. 37, 614–636 (1965)
29) Crabbe, L., Jauch, A., Naeger, C.M., Holtgreve-Grez, H. and Karlseder, J. Telomere dysfunction as a cause of genomic instability in Werner syndrome. Proc. Natl. Acad. Sci. U.S.A. 104, 2205–2210 (2007)
30) Aubert G, Lansdorp PM. Telomeres and aging. Physiol Rev. 2008 Apr;88(2):557-79. Review.
31) Flanary B.,R The role of microglial cellular senescence in the aging and Alzheimer diseased brain. Rejuvenation Res. 2005 Summer;8(2):82-5.
32) Masoro EJ. Overview of caloric restriction and ageing. Mech Ageing Dev. 2005;126:913-922
33) Rajaram S, Sabaté J. Health benefits of a vegetarian diet. Nutrition. 2000 Jul-Aug;16(7-8):531-3. Review.
34) Key TJ, Appleby PN, Rosell MS. Health effects of vegetarian and vegan diets. Proc Nutr Soc. 2006 Feb;65(1):35-41. Review.
35) Fontana L, Klein S. Aging, adiposity, and calorie restriction. JAMA. 2007 Mar 7;297(9):986-94
36) Fontana L. Excessive adiposity, calorie restriction, and aging. JAMA. 2006 Apr 5;295(13):1577-8.)
37) Kuningas M, Mooijaart SP, van Heemst D, Zwaan BJ, Slagboom PE, Westendorp RG. Genes encoding longevity: from model organisms to humans. Aging Cell. 2008 Mar;7(2):270-80.
38) Browner WS, Kahn AJ, Ziv E, Reiner AP, Oshima J, Cawthon RM, Hsueh WC, Cummings SR. The genetics of human longevity. Am J Med. 2004 Dec 1;117(11):851-60. Review.
39) Kudlow BA, Kennedy BK, Monnat RJ Jr.Werner and Hutchinson-Gilford progeria syndromes: mechanistic basis of human progeroid diseases. Nat Rev Mol Cell Biol. 2007 May;8(5):394-404
40) Epstein, C. J.; Martin, G. M.; Schultz, A. L.; Motulsky, A. G. : Werner's syndrome: a review of its symptomatology, natural history, pathologic features, genetics and relationship to the natural aging process. Medicine 45: 177-222, 1966
41) Yu, C.-E.; Oshima, J.; Fu, Y.-H.; Wijsman, E. M.; Hisama, F.; Alisch, R.; Matthews, S.; Nakura, J.; Miki, T.; Quais, S.; Martin, G. M.; Mulligan, J.; Schellenberg, G. D. : Positional cloning of the Werner's syndrome gene. Science 272: 258-262, 1996.
42) Yu, C.-E.; Oshima, J.; Wijsman, E. M.; Nakura, J.; Miki, T.; Piussan, C.; Matthews, S.; Fu, Y.-H.; Mulligan, J.; Martin, G. M.; Schellenberg, G. D.; Werner's Syndrome Collaborative Group : Mutations in the consensus helicase domains of the Werner syndrome gene. Am. J. Hum. Genet. 60: 330-341, 1997.
43) Bachrati, C. Z. & Hickson, I. D. RecQ helicases: suppressors of tumorigenesis and premature aging. Biochem. J. 374, 577–606 (2003)
44) Prince, P. R., Emond, M. J. & Monnat, R. J. Jr. Loss of Werner syndrome protein function promotes aberrant mitotic recombination. Genes Dev. 15, 933–938 (2001).
45) Chang S, Multani AS, Cabrera NG, Naylor ML, Laud P, Lombard D, Pathak S, Guarente L, DePinho RA. Essential role of limiting telomeres in the pathogenesis of Werner syndrome. Nat Genet. 2004 Aug;36(8):877-82.
46) Hennekam, R. C. Hutchinson–Gilford progeria syndrome: review of the phenotype. Am. J. Med. Genet. A 140, 2603–2624 (2006).
47) Eriksson, M. et al. Recurrent de novo point mutations in lamin A cause Hutchinson–Gilford progeria syndrome. Nature 423, 293–298 (2003).
48) Stuurman, N., Heins, S. & Aebi, U. Nuclear lamins: their structure, assembly, and interactions. J. Struct. Biol. 122, 42–66 (1998).
49) Navarro CL, Cau P, Lévy N. Molecular bases of progeroid syndromes. Hum Mol Genet. 2006 Oct 15;15 Spec No 2:R151-61. Review.
50) Proud VK, Mussell HG, Kaler SG, Young DW, Percy AK. Distinctive Menkes disease variant with occipital horns: delineation of natural history and clinical phenotype. Am J Med Genet. 1996 Oct 2;65(1):44-51.
51) Kodama H, Murata Y. Molecular genetics and pathophysiology of Menkes disease. Pediatr Int. 1999 Aug;41(4):430-5. Review

52) Kaler, S. G.; Gallo, L. K.; Proud, V. K.; Percy, A. K.; Mark, Y.; Segal, N. A.; Goldstein, D. S.; Holmes C. S.; Gahl, W. A. : Occipital horn syndrome and a mild Menkes phenotype associated with splice site mutations at the MNK locus. Nature Genet. 8: 195-202, 1994.
53) Møller LB, Tu¨mer Z, Lund C, Peterson C, Cole T, Hanusch R, et al. Similar splice-site mutations of the atp7a gene lead to different phenotypes: classical Menkes disease or occipital horn syndrome. Am J Hum Genet 2000; 66:1211-20.
54) Petris, M.J., Mercer, J.F., Culvenor, J.G., Lockhart, P., Gleeson, P.A. and Camakaris, J. Ligand-regulated transport of the Menkes copper P-type ATPase efflux pump from the Golgi apparatus to the plasma membrane: a novel mechanism of regulated trafficking. EMBO J., (1996) 15, 6084–6095.
55) Yamaguchi, Y., Heiny, M.E., Suzuki, M. and Gitlin, J.D. (1996) Biochemical characterization and intracellular localization of the Menkes disease protein. Proc. Natl Acad. Sci. USA, 93, 14030–14035.
56) Dierick, H.A., Adam, A.N., Escara-Wilke, J.F. and Glover, T.W. (1997) Immunocytochemical localization of the Menkes copper transport protein (ATP7A) to the trans-Golgi network. Hum. Mol. Genet., 6, 409–416.
57) Mentzel HJ, Seidel J, Vogt S, Vogt L, Kaiser WA. Vascular complications (splenic and hepatic artery aneurysms) in the occipital horn syndrome: report of a patient and review of the literature. Pediatr Radiol. 1999 Jan;29(1):19-22.
58) Tang J, Robertson S, Lem KE, Godwin SC, Kaler SG. Functional copper transport explains neurologic sparing in occipital horn syndrome Genet Med. 2006 Nov;8(11):711-8.
59) Beighton P. The dominant and recessive forms of cutis laxa.J Med Genet. 1972 Jun;9(2):216-21.
60) Tassabehji M, Metcalfe K, Hurst J, Ashcroft GS, Kielty C, Wilmot C, Donnai D, Read AP, Jones CJ. An elastin gene mutation producing abnormal tropoelastin and abnormal elastic fibres in a patient with autosomal dominant cutis laxa. Hum Mol Genet. 1998 Jun;7(6):1021-8.
61) Corbett E, Glaisyer H, Chan C, Madden B, Khaghani A, Yacoub M. Congenital cutis laxa with a dominant inheritance and early onset emphysema Thorax. 1994 Aug;49(8):836-7.
62) Markova D, Zou Y, Ringpfeil F, Sasaki T, Kostka G, Timpl R, Uitto J, Chu ML. Genetic heterogeneity of cutis laxa: a heterozygous tandem duplication within the fibulin-5 (FBLN5) gene. Am J Hum Genet. 2003 Apr;72(4):998-1004.
63) Urban Z, Gao J, Pope FM, Davis EC. Autosomal dominant cutis laxa with severe lung disease: synthesis and matrix deposition of mutant tropoelastin. J Invest Dermatol. 2005 Jun;124(6):1193-9.
64) Mégarbané H, Florence J, Oliver Sass J, Schwonbeck S, Foglio M, de Cid R, Cure S, Saker S, Mégarbané A, Fischer J.An autosomal-recessive form of cutis laxa is due to homozygous elastin mutations, and the phenotype may be modified by a heterozygous fibulin 5 polymorphism. J Invest Dermatol. 2009 Jul;129(7):1650-5.
65) Graul-Neumann LM, Hausser I, Essayie M, Rauch A, Kraus C., Am. J. Med. Genet. 146A: 977-983, 2008
66) Morava E, Guillard M, Lefeber DJ, Wevers RA. Autosomal recessive cutis laxa syndrome revisited. Eur J Hum Genet. 2009 Sep;17(9):1099-110.
67) Boente MC, Winik BC, Asial RA. Wrinkly skin syndrome: ultrastructural alterations of the elastic fibers Pediatr Dermatol. 1999 Mar-Apr;16(2):113-7.
68) Boente Mdel C, Asial RA, Winik BC.Geroderma osteodysplastica. Report of a new family. Pediatr Dermatol. 2006 Sep-Oct;23(5):467-72.
69) Pontz BF, Zepp F, Stöss H. Biochemical, morphological and immunological findings in a patient with a cutis laxa-associated inborn disorder (De Barsy syndrome). Eur J Pediatr. 1986 Oct;145(5):428-34.
70) Loeys, B.; van Maldergem, L.; Mortier, G.; Coucke, P.; Gerniers, S.; Naeyaert, J.-M.; de Paepe, A. : Homozygosity for a missense mutation in fibulin-5 (FBLN5) results in a severe form of cutis laxa. Hum. Molec. Genet. 11: 2113-2118, 2002.
71) Hucthagowder, V.; Sausgruber, N.; Kim, K. H.; Angle, B.; Marmorstein, L. Y.; Urban, Z.Fibulin-4: a novel gene for an autosomal recessive cutis laxa syndrome. Am. J. Hum. Genet. 78: 1075-1080, 2006.
72) Hu Q, Loeys BL, Coucke PJ, De Paepe A, Mecham RP, Choi J, Davis EC, Urban Z. Fibulin-5 mutations: mechanisms of impaired elastic fiber formation in recessive cutis laxa. Hum Mol Genet. 2006 Dec 1;15(23):3379-86.
73) Dasouki M, Markova D, Garola R, Sasaki T, Charbonneau NL, Sakai LY, Chu ML. Am J Med Genet A. 2007 Nov 15;143A(22):2635-41

74) Hoyer J, Kraus C, Hammersen G, Geppert JP, Rauch A. Lethal cutis laxa with contractural arachnodactyly, overgrowth and soft tissue bleeding due to a novel homozygous fibulin-4 gene mutation. Clin Genet. 2009 Sep;76(3):276-81.
75) Debre, R.; Marie, J.; Seringe, P. : 'Cutis laxa' avec dystrophies osseuses. Bull. Mem. Soc. Med. Hop. Paris 53: 1038-1039, 1937.
76) Gazit, E.; Goodman, R. M.; Katznelson, M. B.; Rotem, Y. : The wrinkly skin syndrome: a new heritable disorder of connective tissue. Clin. Genet. 4: 186-192, 1973.
77) Zlotogora, J. : Wrinkly skin syndrome and the syndrome of cutis laxa with growth and developmental delay represent the same disorder. (Letter) Am. J. Med. Genet. 85: 194 only, 1999.
78) Van Maldergem L, Yuksel-Apak M, Kayserili H et al: Cobblestonelike brain dysgenesis and altered glycosylation in congenital cutis laxa, Debre type. Neurology 2008; 71: 1602– 1608.
79) Kornak U, Reynders E, Dimopoulou A, van Reeuwijk J, Fischer B, Rajab A, Budde B, Nürnberg P, Foulquier F; ARCL Debré-type Study Group, Lefeber D, Urban Z, Gruenewald S, Annaert W, Brunner HG, van Bokhoven H, Wevers R, Morava E, Matthijs G, Van Maldergem L, Mundlos S. Impaired glycosylation and cutis laxa caused by mutations in the vesicular H+-ATPase subunit ATP6V0A2. Nat Genet. 2008 Jan;40(1):32-4.
80) Rajab A, Kornak U, Budde BS, Hoffmann K, Jaeken J, Nürnberg P, Mundlos S. Geroderma osteodysplasticum hereditaria and wrinkly skin syndrome in 22 patients from Oman.Am J Med Genet A. 2008 Apr 15;146A(8):965-76.
81) Jefferies KC, Cipriano DJ, Forgac M. Function, structure and regulation of the vacuolar (H+)-ATPases. Arch Biochem Biophys. 2008 Aug 1;476(1):33-42. Review.
82) Qi J, Wang Y, Forgac M. The vacuolar (H+)-ATPase: subunit arrangement and in vivo regulation J Bioenerg Biomembr. 2007 Dec;39(5-6):423-6. Review.
83) Guillard M, Dimopoulou A, Fischer B, Morava E, Lefeber DJ, Kornak U, Wevers RA. Vacuolar H+-ATPase meets glycosylation in patients with cutis laxa. Biochim Biophys Acta. 2009 Sep;1792(9):903-14
84) Kunze, J.; Majewski, F.; Montgomery, P.; Hockey, A.; Karkut, I.; Riebel, T. : De Barsy syndrome--an autosomal recessive, progeroid syndrome. Europ. J. Pediat. 144: 348-354, 1985.
85) Kivuva, E. C.; Parker, M. J.; Cohen, M. C.; Wagner, B. E.; Sobey, G. : De Barsy syndrome: a review of the phenotype. Clin. Dysmorph. 17: 99-107, 2008.
86) De Barsy, A. M.; Moens, E.; Dierckx, L. : Dwarfism, oligophrenia and degeneration of the elastic tissue in skin and cornea. A new syndrome? Helv. Paediat. Acta 23: 305-313, 1968.
87) Hennies HC, Kornak U, Zhang H, Egerer J, Zhang X, Seifert W, Kühnisch J, Budde B, Nätebus M, Brancati F, Wilcox WR, Müller D, Kaplan PB, Rajab A, Zampino G, Fodale V, Dallapiccola B, Newman W, Metcalfe K, Clayton-Smith J, Tassabehji M, Steinmann B, Barr FA, Nürnberg P, Wieacker P, Mundlos S. Gerodermia osteodysplastica is caused by mutations in SCYL1BP1, a Rab-6 interacting golgin. Nat Genet. 2008 Dec;40(12):1410-2.
88) Bamatter, F.; Franceschetti, A.; Klein, D.; Sierro, A. : Gerodermie osteodysplastique hereditaire. Ann. Pediat. 174: 126-127, 1950.
89) Meng Z, Lou Z, Liu Z, Li M, Zhao X, Bartlam M, Rao Z. Crystal structure of human pyrroline-5-carboxylate reductase. J Mol Biol. 2006 Jun 23;359(5):1364-77.
90) Hamamy H, Masri A, Ajlouni K. Wrinkly skin syndrome. Clin Exp Dermatol. 2005 Sep;30(5):590-2.
91) Nanda A, Alsaleh QA, Al-Sabah H, Marzouk EE, Salam AM, Nanda M, Anim JT. Gerodermia osteodysplastica/wrinkly skin syndrome: report of three patients and brief review of the literature. Pediatr Dermatol. 2008 Jan-Feb;25(1):66-71. Review
92) Sommer A. Photo essay--geroderma osteodysplastica. Am J Med Genet C Semin Med Genet. 2007 Aug 15;145C(3):291-2.
93) Al-Gazali LI, Sztriha L, Skaff F, Haas D. Gerodermia osteodysplastica and wrinkly skin syndrome: are they the same? Am J Med Genet. 2001 Jul 1;101(3):213-20.
94) Guerra D, Fornieri C, Bacchelli B, Lugli L, Torelli P, Balli F, Ferrari P. The De Barsy syndrome. J Cutan Pathol. 2004 Oct;31(9):616-24.
95) Watford M. Glutamine metabolism and function in relation to proline synthesis and the safety of glutamine and proline supplementation. J Nutr. 2008;138:2003–7.
96) Mitsubuchi H, Nakamura K, Matsumoto S, Endo F. Inborn errors of proline metabolism. J Nutr. 2008 Oct;138(10):2016S-2020S.

97) Phang, J.M., Pandhare, J. & Liu, Y. The metabolism of proline as microenvironmental stress substrate. J. Nutr. 138, 2008S–2015S (2008).
98) Alberts, Bruce; Johnson, Alexander; Lewis, Julian; Raff, Martin; Roberts, Keith; Walter, Peter. Molecular Biology of the Cell New York and London: Garland Science; c2002
99) Gieffers C, Korioth F, Heimann P, Ungermann C, Frey J. Mitofilin is a transmembrane protein of the inner mitochondrial membrane expressed as two isoforms. Exp Cell Res. 1997 May 1;232(2):395-9.
100) Hagedorn, C.H. & Phang, J.M. Transfer of reducing equivalents into mitochondria by the interconversions of proline and delta 1-pyrroline-5-carboxylate. Arch. Biochem. Biophys. 225, 95–101 (1983).
101) Lodish, Harvey; Berk, Arnold; Zipursky, S. Lawrence; Matsudaira, Paul; Baltimore, David; Darnell, James E. New York: Molecular Cell Biology W. H. Freeman & Co.; c1999
102) Chen, C. & Dickman, M. B., Proline suppresses apoptosis in the fungal pathogen Colletotrichum trifolii. Proc. Natl Acad. Sci. USA, 2005,102, 3459–3464
103) Teramoto S, Tomita T, Matsui H, Ohga E, Matsuse T, Ouchi Y. Hydrogen peroxide-induced apoptosis and necrosis in human lung fibroblasts: protective roles of glutathione. Jpn J Pharmacol. 1999 Jan;79(1):33-40.
104) de Paula Rodrigues, G. H.; das Eiras Tamega, I.; Duque, G.; Spinola Dias Neto, V. : Severe bone changes in a case of Hutchinson-Gilford syndrome. Ann. Genet. 45: 151-155, 2002.
105) Vanhoof G, Goossens F, De Meester I, Hendriks D, Scharpé S. Proline motifs in peptides and their biological processing. FASEB J. 1995 Jun;9(9):736-44. Review.
106) Hu CA, Bart Williams D, Zhaorigetu S, Khalil S, Wan G, Valle D. Functional genomics and SNP analysis of human genes encoding proline metabolic enzymes. Amino Acids. 2008 Nov;35(4):655-64.
107) Kalidas Shetty. Role of proline-linked pentose phosphate pathway in biosynthesis of plant phenolics for functional food and environmental applications: a review Process Biochemistry 39 (2004) 789–803
108) Merrill MJ, Yeh GC, Phang JM Purified human erythrocyte pyrroline-5-carboxylate reductase. Preferential oxidation of NADPH. J Biol Chem 1989, 264:9352–9358
109) Potter JL, Waickman FJ. Hyperprolinemia. I. A study of a large family.J Pediatr. 1973;83:635–8.
110) Raux G, Bumsel E, Hecketsweiler B, Amelsvoort T, Zinkstok J, Manouvrier-Hanu S, Fantini C, Bre´vie`re GM, Di Rosa G, et al. Involvement of hyperprolinemia in cognitive and psychiatric features of the 22q11 deletion syndrome. Hum Mol Genet. 2007;16:83–91.
111) Flynn MP, Martin MC, Moore PT, Stafford JA, Fleming GA, Phang JM. Type II hyperprolinaemia in a pedigree of Irish travellers (nomads). Arch Dis Child. 1989;64:1699–707.
112) Baumgartner, M. R.; Hu, C. A.; Almashanu, S.; Steel, G.; Obie, C.; Aral, B.; Rabier, D.; Kamoun, P.; Saudubray, J.-M.; Valle, D. Hyperammonemia with reduced ornithine, citrulline, arginine and proline: a new inborn error caused by a mutation in the gene encoding delta-1-pyrroline-5-carboxylate synthase. Hum. Molec. Genet. 9: 2853-2858, 2000.
113) Bicknell, L. S.; Pitt, J.; Aftimos, S.; Ramadas, R.; Maw, M. A.; Robertson, S. P. : A missense mutation in ALDH18A1, encoding delta-1-pyrroline-5-carboxylate synthase (P5CS), causes an autosomal recessive neurocutaneous syndrome. Europ. J. Hum. Genet. 16: 1176-1186, 2008.
114) Delwing D, Delwing D, Chiarani F, Kurek AG, Wyse AT. Proline reduces brain cytochrome c oxidase: prevention by antioxidants. Int J Dev Neurosci. 2007 Feb;25(1):17-22.
115) Delwing D, Delwing D, Sanna RJ, Wofchuk S, Wyse AT. Proline promotes decrease in glutamate uptake in slices of cerebral cortex and hippocampus of rats. Life Sci. 2007 Dec 14;81(25-26):1645-50.
116) Krishnan N, Dickman MB, Becker DF. Proline modulates the intracellular redox environment and protects mammalian cells against oxidative stress. Free Radic Biol Med. 2008 Feb 15;44(4):671-81
117) Tadros SF, D'Souza M, Zettel ML, Zhu X, Waxmonsky NC, Frisina RD Glutamate-related gene expression changes with age in the mouse auditory midbrain. Brain Res , 2007,1127: 1-9.
118) Pérez-Arellano I, Carmona-Álvarez F, Martínez AI, Rodríguez-Díaz J, Cervera J. Pyrroline-5-carboxylate synthase and proline biosynthesis: From osmotolerance to rare metabolic disease. Protein Sci. 2010 Jan 20.
119) Knott, A.B., Perkins, G., Schwarzenbacher, R. & Bossy-Wetzel, E. Mitochondrial fragmentation in neurodegeneration. Nat. Rev. Neurosci. 9, 505–518 (2008).

120) Scorrano L. Opening the doors to cytochrome c: changes in mitochondrial shape and apoptosis. Int J Biochem Cell Biol. 2009 Oct;41(10):1875-83.
121) Benard G, Rossignol R. Ultrastructure of the mitochondrion and its bearing on function and bioenergetics. Antioxid Redox Signal. 2008 Aug;10(8):1313-42.
122) Donald, S. P., Sun, X. Y., Hu, C. A., Yu, J., Mei, J. M.,Valle, D. & Phang, J. M. Proline oxidase,encoded by p53-induced gene-6, catalyzes the generation of proline-dependent reactive oxygen species. (2001) Cancer Res. 61, 1810–1815.
123) Maxwell, S. A. & Davis, G. E. (2000). Differential gene expression in p53-mediated apoptosis-resistant vs. apoptosis-sensitive tumor cell lines. Proc. Natl Acad. Sci. USA, 97, 13009–13014.
124) U Zangemeister-Wittke, H-U Simon Apoptosis - Regulation and clinical implications, ECDO Conference report, 8th Euroconference on Apoptosis, Davos, Switzerland, October 14-17, 2000
125) Ma YS, Wu SB, Lee WY, Cheng JS, Wei YH. Response to the increase of oxidative stress and mutation of mitochondrial DNA in aging. Biochim Biophys Acta. 2009 Oct;1790(10):1021-9.
126) Waterhouse NJ, Green DR. Mitochondria and apoptosis: HQ or high-security prison? J Clin Immunol. 1999 Nov;19(6):378-87.
127) Kroemer G, Petit P, Zamzami N, Vayssi`ere JL, Mignotte B. 1995. The biochemistry of programmed cell death. FASEB J. 9:1277–87
128) Zamzami N, Susin SA, Marchetti P, Hirsch T, G´ omez-Monterrey I, 1996. Mitochondrial control of nuclear apoptosis. J. Exp. Med. 183:1533–44
129) Wang C, Youle RJ. The role of mitochondria in apoptosis*.Annu Rev Genet. 2009;43:95-118.
130) Wallace DC. Mitochondrial diseases in man and mouse. Science. 1999; 283: 1482–8.
131) Leonard JV, Schapira AVH. Mitochondrial respiratory chain disorders I: mitochondrial DNA defects. Lancet. 2000a; 355: 299–304.
132) Leonard JV, Schapira AVH. Mitochondrial respiratory chain disorders II: neurodegenerative disorders and nuclear gene defects. Lancet. 2000b; 355: 389–94.
133) van den Ouweland JM, Lemkes H,H, Ruitenbeek W, Sandkuijl LA, de Vijlder MF, Struyvenberg PA, van de Kamp JJ, Maassen JA. Mutation in mitochondrial tRNA(Leu)(UUR) gene in a large pedigree with maternally transmitted type II diabetes mellitus and deafness. Nat Genet. 1992; 1: 368–71.
134) Nelson I, Hanna MG, Alsanjari N, Scaravilli F, Morgan-Hughes JA, Harding AE. A new mitochondrial DNA mutation associated with progressive dementia and chorea: a clinical, pathological, and molecular genetic study. Ann Neurol. 1995; 37: 400–3.
135) Alexander C, Votruba M, Pesch UE, Thiselton DL, Mayer S, Moore A, Rodriguez M, Kellner U, Leo-Kottler B, Auburger G, Bhattacharya SS, Wissinger B. OPA1, encoding a dynamin-related GTPase, is mutated in autosomal dominant optic atrophy linked to chromosome 3q28. Nat Genet. 2000; 26: 211–5.
136) Rotig A, de Lonlay P, Chretien D, Foury F, Koenig M, Sidi D, Munnich A, Rustin P. Aconitase and mitochondrial iron-sulphur protein deficiency in Friedreich ataxia. Nat Genet. 1997; 17: 215–7.
137) Casari G, De Fusco M, Ciarmatori S, Zeviani M, Mora M, Fernandez P, De Michele G, Filla A, Cocozza S, Marconi R, Durr A, Fontaine B, Ballabio A. Spastic paraplegia and OXPHOS impairment caused by mutations in paraplegin, a nuclear-encoded mitochondrial metalloprotease. Cell. 1998; 93: 973–83.
138) Lutsenko S, Cooper MJ. Localization of the Wilson's disease protein product to mitochondria. Proc Natl Acad Sci U S A. 1998; 95: 6004–9.
139) Osakabe T, Hayashi M, Hasegawa K, Okuaki T, Ritty TM, Mecham RP, Wachi H, Seyama Y.. Age- and gender-related changes in ligament components. Ann Clin Biochem. 2001 Sep;38(Pt 5):527-32.
140) Urbán Z, Boyd CD. Elastic-fiber pathologies: primary defects in assembly-and secondary disorders in transport and delivery. Am J Hum Genet. 2000 Jul;67(1):4-7.
141) Milewicz DM, Urbán Z, Boyd C. Genetic disorders of the elastic fiber system. Matrix Biol. 2000 Nov;19(6):471-80.
142) Zhang MC, He L, Giro M, Yong SL, Tiller GE, Davidson JM. Cutis laxa arising from frameshift mutations in exon 30 of the elastin gene (ELN). J Biol Chem. 1999 Jan 8;274(2):981-6.
143) Mizuguchi, T.; Collod-Beroud, G.; Akiyama, T.; Abifadel, M.; Harada, N.; Morisaki, T.; Allard, D.; Varret, M.; Claustres, M.; Morisaki, H.; Ihara, M.; Kinoshita, A.; and 11 others : Heterozygous TGFBR2 mutations in Marfan syndrome. Nature Genet. 36: 855-860, 2004.

144) Loeys, B. L.; Schwarze, U.; Holm, T.; Callewaert, B. L.; Thomas, G. H.; Pannu, H.; De Backer, J. F.; Oswald, G. L.; Symoens, S.; Manouvrier, S.; Roberts, A. E.; Faravelli, F.; and 9 others : Aneurysm syndromes caused by mutations in the TGF-beta receptor. New Eng. J. Med. 355: 788-798, 2006

145) Loeys, B. L.; Chen, J.; Neptune, E. R.; Judge, D. P.; Podowski, M.; Holm, T.; Meyers, J.; Leitch, C. C.; Katsanis, N.; Sharifi, N.; Xu, F. L.; Myers, L. A.; and 12 others : A syndrome of altered cardiovascular, craniofacial, neurocognitive and skeletal development caused by mutations in TGFBR1 or TGFBR2. Nature Genet. 37: 275-281, 2005.

146) K.C. Jefferies, D.J. Cipriano, M. Forgac, Function, structure and regulation of the vacuolar (H(+))-ATPases, Arch. Biochem. Biophys. 476 (1) (2008) 33.

147) Hucthagowder V, Morava E, Kornak U, Lefeber DJ, Fischer B, Dimopoulou A, Aldinger A, Choi J, Davis EC, Abuelo DN, Adamowicz M, Al-Aama J, Basel-Vanagaite L, Fernandez B, Greally MT, Gillessen-Kaesbach G, Kayserili H, Lemyre E, Tekin M, Türkmen S, Tuysuz B, Yüksel-Konuk B, Mundlos S, Van Maldergem L, Wevers RA, Urban Z. Loss-of-function mutations in ATP6V0A2 impair vesicular trafficking, tropoelastin secretion and cell survival. Hum Mol Genet. 2009 Jun 15;18(12):2149-65.

148) Grigoriev I, Splinter D, Keijzer N, Wulf PS, Demmers J, Ohtsuka T, Modesti M, Maly IV, Grosveld F, Hoogenraad CC, Akhmanova A. Rab6 regulates transport and targeting of exocytotic carriers. Dev Cell. 2007 Aug;13(2):305-14.

149) Mallard F, Tang BL, Galli T, Tenza D, Saint-Pol A, Yue X, Antony C, Hong W, Goud B, Johannes L. Early/recycling endosomes-to-TGN transport involves two SNARE complexes and a Rab6 isoform. J Cell Biol. 2002 Feb 18;156(4):653-64.

150) Bruce Alberts, Dennis Bray, Julian Lewis, Martin Raff, Keith Roberts, and James D. Watson. Molecular biology of the cell. 1994, Garland Publishing

151) Dröge, W. Free radicals in the physiological control of cell function. Physiol. Rev. 82:47–95; 2002.

152) Dalton, T. P.; Shertzer, H. G.; Puga, A. Regulation of gene expression by reactiveoxygen. Annu. Rev. Pharmacol. Toxicol. 39:67–101; 1999.

153) Talbot, D. A.; Lambert, A. J.; Brand, M. D. Production of endogenous matrix superoxide from mitochondrial complex I leads to activation of uncoupling protein 3. FEBS Lett. 556:111–115; 2004.

7 Acknowledgements

I would like to thank the Greek Institut for State Scholarships (IKY), which financially supported my work for the last three and a half years. As genetical research has always been an indulging field for me as a physician, I need to thank Prof. Stefan Mundlos for the unique opportunity he offered me to work in the Institut für Medizinische Genetik of Charite University of Berlin and to complete my doctor thesis with a highly intriguing theme. The study was performed in the working team of AG Kornak, with Dr. rer. nat. Uwe Kornak as the leading scientist, who introduced me in the exciting world of genetics and cell biology. I am thankful for his guidance, his support and his trust all these years and also for the fruitful results of our co-operation. My working partner in the project of Cutis Laxa, Mr. Björn Fischer, was the one to guide me in the everyday laboratory work and help me overcome the problems I confronted during this study. All the members of the AG Kornak and the people of the Institute have been very supportive and tolerant against my language difficulties and I want to thank every one of them, Johannes Egerer, Claire Schlack, Sabine Stumpp, Rici Ott, Johannes Grünhagen, Sebastian Köhler, Denise Emmerich, Jirko Kühnisch and Wenke Seifert, for their valuable advice, for the pleasant working environment and for putting up with my constant climatological complaints.

8 Publications

1. Reversade B, Escande-Beillard N, **Dimopoulou A**, Fischer B, Chng SC, Li Y, Shboul M, Tham PY, Kayserili H, Al-Gazali L, Shahwan M, Brancati F, Lee H, O'Connor BD, Schmidt-von Kegler M, Merriman B, Nelson SF, Masri A, Alkazaleh F, Guerra D, Ferrari P, Nanda A, Rajab A, Markie D, Gray M, Nelson J, Grix A, Sommer A, Savarirayan R, Janecke AR, Steichen E, Sillence D, Hausser I, Budde B, Nürnberg G, Nürnberg P, Seemann P, Kunkel D, Zambruno G, Dallapiccola B, Schuelke M, Robertson S, Hamamy H, Wollnik B, Van Maldergem L, Mundlos S, Kornak U. ***Mutations in PYCR1 cause cutis laxa with progeroid features.*** Nat Genet. 2009 Sep;41(9):1016-21.
2. Hucthagowder V, Morava E, Kornak U, Lefeber DJ, Fischer B, **Dimopoulou A**, Aldinger A, Choi J, Davis EC, Abuelo DN, Adamowicz M, Al-Aama J, Basel-Vanagaite L, Fernandez B, Greally MT, Gillessen-Kaesbach G, Kayserili H, Lemyre E, Tekin M, Türkmen S, Tuysuz B, Yüksel-Konuk B, Mundlos S, Van Maldergem L, Wevers RA, Urban Z. ***Loss-of-function mutations in ATP6V0A2 impair vesicular trafficking, tropoelastin secretion and cell survival.*** Hum Mol Genet. 2009 Jun 15;18(12):2149-65.
3. Guillard M, **Dimopoulou A**, Fischer B, Morava E, Lefeber DJ, Kornak U, Wevers RA. ***Vacuolar H+-ATPase meets glycosylation in patients with cutis laxa.*** Biochim Biophys Acta. 2009 Sep;1792(9):903-14. Review
4. Kornak U, Reynders E, **Dimopoulou A**, van Reeuwijk J, Fischer B, Rajab A, Budde B, Nürnberg P, Foulquier F; ARCL Debré-type Study Group, Lefeber D, Urban Z, Gruenewald S, Annaert W, Brunner HG, van Bokhoven H, Wevers R, Morava E, Matthijs G, Van Maldergem L, Mundlos S. ***Impaired glycosylation and cutis laxa caused by mutations in the vesicular H+-ATPase subunit ATP6V0A2***. Nat Genet. 2008 Jan;40(1):32-4.

9 Curriculum Vitae

Mein Lebenslauf wird aus datenschutzrechtlichen Gründen in der elektronischen Version meiner Arbeit nicht veröffentlicht.

10 Summary

Autosomal recessive cutis laxa (ARCL) is a highly heterogeneous group of disorders, which is mainly associated with a progeroid appearance, lax and wrinkled skin, mental retardation and osteopenia and whose pathogenesis is only partially unravelled. After excluding mutations in the human ARCL genes, *GORAB* and *ATP6V0A2*, in the patients of our ARCL cohort without lung involvement, we conducted further genetic analysis in consanguineous families. These families were formerly diagnosed as GO, ARCLII-WSS and de Barsy syndrome. Homozygocity mapping in ten kindreds revealed a candidate region on chromosome 17q25. Sequencing of several genes in the candidate region resulted in the identification of disease-causing mutations in the gene *PYCR1*, encoding for Δ1-pyrroline-5-carboxylate reductase, an enzyme which catalyzes the final step of the de novo synthesis of proline. In total, 22 families of our ARCL cohort were found to bear missense, frameshift and splice site but no nonsense mutations. Apart from the common features of all ARCL forms, intrauterine growth retardation, mental retardation and a typical facies were the constant findings in these patients. Brain and eye abnormalities such as agenesis of corpus callosum and cataract were also evident. Proline levels, measured in serum and cell lysates from patients with mutations in *PYCR1* did not reveal significant changes when compared with control samples. Affected individuals showed a pronounced progeroid appearance, which was not progressive. The detection of mutations in patients diagnosed as de Barsy syndrome implies that *PYCR1* is one of the genes responsible for this genetically heterogeneous phenotype.

All mutations found were associated with a decrease of protein expression in patient fibroblasts. Furthermore, immunofluorescence studies revealed a mitochondrial residence of the protein, as PYCR1 was found to co-localize with specific mitochondrial marker proteins. Immunofluorescence analysis provided evidence for an altered mitochondrial morphology upon loss of PYCR1, which was further confirmed by electron microscopy. The alterations were found to become more severe after transient treatment with H_2O_2 resulting in a five-fold increase in the number of fragmented mitochondria in patient cell lines. Upon oxidative stress the fibroblasts with mutations in *PYCR1* showed higher apoptosis rates compared to control cells.

Our findings suggest that PYCR1 contributes to the maintenance of the normal mitochondrial morphology and protects against oxidative stress, most probably by inhibiting apoptosis. This study postulates a new association between mutations in PYCR1, altered mitochondrial function and progeroid changes in connective tissues.

11 Zusammenfassung

Die autosomal rezessive Cutis laxa (ARCL) ist eine sehr heterogene Gruppe von Erkrankungen, die hauptsächlich durch einen progeroiden Aspekt, laxe und faltige Haut, mentale Retardierung sowie Osteopenie gekennzeichnet sind und deren Pathogenese bisher erst partiell aufgeklärt werden konnte.

In zehn konsanguinen Familien, bei denen im Vorfeld Gerodermia Osteodysplastika (GO), Wrinkly Skin Syndrome oder de Barsy Syndrom diagnostiziert, jedoch keine Mutationen nachgewiesen worden waren, führten wir eine Homozygotie-Kartierung durch. In der resultierenden Kandidatenregion auf Chromosom 17q25 wurden nach Sequenzierung mehrerer Gene pathogene Mutationen im *PYCR1*-Gen entdeckt. *PYCR1* kodiert die Δ1-Pyrollin-5-Karboxylat Reduktase, ein Enzym welches für den letzten Schritt der *de novo* Synthese von Prolin verantwortlich ist. In insgesamt 22 Familien aus unserer Kohorte konnten wir Missense-, Frameshift- und Splicesite-Mutationen, allerdings keine Nonsense-Mutationen in *PYCR1* identifizieren. Zusätzlich zu den typischen Merkmalen aller CL Subtypen, fanden sich bei diesen Patienten eine intrauterine Wachstumsverzögerung, eine schwerere mentale Retardierung und eine typische Facies, sowie eine Agenesie oder Hypoplasie des Corpus callosum und eine Katarakt.

Die betroffenen Individuen wiesen einen deutlich progeroiden, aber nicht progressiven Phänotyp auf. Eine Hypoprolinämie konnte weder im Serum von Patienten mit *PYCR1* Mutationen, noch in Lysaten von betroffenen Hautfibroblasten festgestellt werden. Auch ursprünglich als de Barsy Syndrom diagnostizierte Patienten wiesen Mutationen im *PYCR1*-Gen auf, was für einen hohe genetische Heterogenität dieses Syndroms spricht.

In kultivierten Fibroblasten von Patienten mit einer *PYCR1* Mutation fand sich eine verminderte Expression des PYCR1 Proteins. Immunofluoreszenz-Analysen zeigten, dass das PYCR1 Protein mitochondrial lokalisiert ist, da PYCR1 mit spezifischen mitochondrialen Markerproteinen kolokalisiert war. Außerdem wiesen Zellen mit einer *PYCR1* Mutation eine veränderte mitochondriale Morphologie auf, was mittels elektronmikroskopischer Analyse bestätigt wurde. Nach Behandlung mit H_2O_2 waren die beobachteten Veränderungen deutlich ausgeprägter und es zeigte sich eine fünffach erhöhte Anzahl fragmentierter Mitochondrien in Patienten-Fibroblasten. Nach oxidativem Stress lag in Fibroblasten mit *PYCR1* Mutationen eine höhere Apoptoserate im Vergleich zu Kontrollzellen vor.

Unsere Ergebnisse legen nahe, dass PYCR1 zur Aufrechterhaltung der normalen mitochondrialen Morphologie beiträgt und gleichzeitig eine protektive Funktion gegen oxitativen Stress aus-

übt, möglicherweise durch Inhibition von Apoptose. Unsere Studie demonstriert einen neuartigen Zusammenhang zwischen Mutationen in *PYCR1*, gestörter mitochondrialer Funktion und progeroiden Veränderungen von Bindegewebsstrukturen.